JOURNAL OF ARTHROSCOPY AND JOINT SURGERY

JAJS

Official Journal of the International Society for Knowledge for Surgeons on Arthroscopy and Arthroplasty (ISKSAA)

Indexed in Scopus & Embase

MSK Radiology - Part II

Guest Editors:

Sanjay Patel
Karthikeyan P. Iyengar
Rajesh Botchu

Volume 10 | Issue 3 | July-September 2023

ISSN: 2542-6001

Wolters Kluwer

https://journals.lww.com/jajs

Medknow

ISKSAA International Society for Knowledge for Surgeons on Arthroscopy and Arthroplasty

ISKSAA (**I**nternational **S**ociety for **K**nowledge for **S**urgeons on **A**rthroscopy and **A**rthroplasty) is a society of orthopaedic surgeons from around the world to share and disseminate knowledge, support research and improve patient care in Arthroscopy and Arthroplasty. We are proud to announce that ISKSAA membership is approaching the **2200** mark (India & Overseas) with members from **over 40 countries** making it the fastest growing Orthopaedic Association in the country & region in just 10 years of its inception . With over **475000 hits from over 170 countries** on the website **www.isksaa.com** & more and more interested people joining as members of ISKSAA, we do hope that ISKSAA will stand out as a major body to provide opportunities to our younger colleagues in training, education and fellowships.

Our Goals.....

- To provide health care education opportunities for increasing cognitive and psycho-motor skills in Arthroscopy and Arthroplasty
- To provide CME programs for the ISKSAA members as well as other qualified professionals.
- To provide Clinical Fellowships in Arthroscopy and Arthroplasty
- To provide opportunities to organise and collaborate research projects
- To provide a versatile website for dissemination of knowledge

ISKSAA Life Membership

The membership is open to Orthopaedic Surgeons, Postgraduate Orthopaedic students and Allied medical personal interested in Arthroscopy & Arthroplasty.

Benefits of ISKSAA Life membership include....

- **Free Subscription** of ISKSAA's official , SCOPUS INDEXED , EMBASE INDEXED peer reviewed , online scientific journal **Journal of Arthroscopy and Joint Surgery (JAJS)**.
- Eligibility to apply for **ISKSAA's Prestigious Fellowship Programme**. We have finalised affiliations with ESSKA , ISAKOS , BOA , BASK , BOSTAA , BESS , Edge Hill University at Wrightington and FLINDERS MEDICAL CENTRE , IMRI AUSTRALIA to provide more **ISKSAA Fellowships** in India , UK , USA , Australia and Europe . We have offered over **500 Clinical Fellowships as of date including 54 in ISKSAA 2014 , 40 in ISKSAA 2015 , 63 in ISKSAA 2016 , 55 in ISKSAA 2017 , 20 in ISKSAA 2018 , 100 in ISKSAA 2019 & 130 in ISKSAA 2022and over 50 ISKSAA Wrightington MCh Fellowships from 2014 to 2022 .**
- We have initiated **ISKSAA JOD & ISKSAA WHA paid fellowship programs** from 2017 for 2 months based in Australia .
- **The Last round of 130 ISKSAA fellowships interviews were held in ISKSAA ANNUAL MEET 2022 in November 19-20th 2022 for 2023 at New Delhi along with the ISKSAA Wrightington MCh Fellowships .**
- **The next round of over 100 ISKSAA fellowship interviews will be held during ISKSAA 2023 later this year at New Delhi along with the ISKSAA MCh wrightington fellowships .**
- We had offered **60 1 week ISKSAA certified Fellowships** from 11th – 15th June & 25-29th June 2018 for ISKSAA members registered for ISKSAA LEEDS 2018 on a first come first basis **.**
- Only as a life member , you can enjoy the benefit of **reduced Congress charges** in future ISKSAA Conferences .
- **Member's only section** on the website which has access to the conference proceedings and live surgeries of ISKSAA 2012 , 2013 , 2014 & 2016 along with a host of other educational material .
- Important opportunity for interaction with world leaders in Arthroscopy & Arthroplasty .
- Opportunity to participate in ISKSAA courses and workshops

To enjoy all the benefits & privileges of an ISKSAA member, you are invited to apply for the Life membership of ISKSAA by going to the membership registration section of the website and entering all your details electronically. All details regarding membership application and payment options are available on the website (www.isksaa.com)

Journal of Arthroscopy and Joint Surgery

Editorial Board

Editors in Chief

Dr. Srinivas BS Kambhampati, *Vijayawada*
Prof. Hemant Pandit, *UK*
Mr. Amol Tambe, *UK*

Executive Editors

Dr Ravi Gupta, *Chandigarh*
Mr Sanjeev Anand, *UK*
Prof Lalit Maini, *New Delhi*

Managing Editor

Dr Pushpinder Bajaj, *New Delhi*

Deputy Editor

Mr Kapil Kumar, *UK*

Associate Editors

Dr Manit Arora, *Mohali*
Dr Seow Hui Teo, *Malaysia*
Mr Jeya Palan, *UK*
Dr Mohit Patralekh, *New Delhi*
Dr Srinath Kamineni, *USA*
Mr Kapil Kumar, *UK*
Dr Ranajit Panigrahi, *Bhubaneswar*
Dr Sujit Tripathy, *Bhubaneswar*
Mr Karadi Sunil Kumar, *UK*
Dr Riccardo D'Ambrosi, *Italy*
Dr Vaibhav Bagaria, *Mumbai*
Mr Rajkumar Gangadharan, *UK*
Dr Vivek Pandey, *Manipal*
Mr Rohit Rambani, *UK*
Dr Santosh Sahanand, *Coimbatore*
Dr Yuvarajan Palanisamy, *Coimbatore*
Prof Jagdish Menon, *Puducherry*
Dr Saseendar Shanmugasundaram, *Puducherry*
Mr Dipen Menon, *UK*
Prof Karthik Vishwanathan, *Vadodara*
Dr Senthilvelan Rajagopalan, *Chennai*

Section Editors

Arthroscopy

Dr Anant Joshi, *Mumbai*
Dr Ashish Devgan, *Haryana*
Dr David Rajan, *Coimbatore*
Dr Denny Lie, *Singapore*
Dr Dinesh Patel, *USA*
Dr Dinshaw Pardiwala, *Mumbai*
Dr Gurinder Bedi, *New Delhi*
Dr Sachin Tapasvi, *Pune*
Dr Sripathi Rao, *Manipal*
Dr Sundararajan Silvampatti, *Coimbatore*
Dr Vidyasagar Josyula VS, *Hyderabad*
Prof J E Mendes, *Portugal*

Knee

Dr Ashish Taneja, *New Delhi*
Dr Binu Thomas, *Vellore*
Dr David Martin, *Australia*
Dr Edward T Mah, *Australia*
Dr Mario Penta, *Australia*
Dr Nirbhay Shah, *Gujarat*
Dr Ponky Frier, *South Africa*

Arthroplasty

Dr Asit Shah, *USA*
Dr Rahul Khare, *New Delhi*
Dr Amite Pankaj, *New Delhi*
Dr Ashok Rajagopal, *New Delhi*
Dr Graham Mercer, *Australia*
Dr Parag Sancheti, *Pune*
Dr Peter Campbell, *Australia*
Dr Hiroyuki Sugaya, *Japan*
Dr Hitesh Gopalan, *Kerala*
Dr HK Wong, *Hong Kong*
Dr Huda Basaleem, *Yemen*
Dr Raju Easwaran, *New Delhi*
Dr Rohit Arora, *Austria*
Mr Manoj Sood, *UK*
Mr Ram Venkatesh, *UK*
Mr Robert J Gregory, *UK*
Prof Jegan Krishnan, *Australia*
Prof PP Kotwal, *New Delhi*
Prof Sudhir Kapoor, *New Delhi*

Training and Education

Dr Janak Mehta, *Australia*
Prof S Rajasekaran, *Coimbatore*

Trauma

Dr Andreas Setje, *Germany*
Prof Mandeep S Dillon, *Chandigrah*
Prof Peter Giannoudis, *UK*
Prof S Rajasekaran, *Coimbatore*
Mr Alexander Wood, *UK*
Dr Taofeek Adeyemi, *Nigeria*
Dr Young Lae Moon, *South Korea*
Mr Binod Singh, *UK*
Mr Ved Goswami, *UK*

Foot and Ankle

Mr Maneesh Bhatia, *UK*
Dr. Sundararajan Silvampatti, *Coimbatore*
Prof Mandeep S Dillon, *Chandigrah*

Hip

Dr Ajay Aggarwal, *USA*
Dr Manish Paruthi, *Mumbai*
Dr Parmanand Gupta, *Chandigarh*

Hand & Wrist

Dr Anil Bhat, *Manipal*
Mr Makaram Srinivasan, *UK*
Mr Raj Murali, *UK*
Mr Rakesh Sethi, *UK*
Mr Vijay Bhalaik, *UK*
Prof Amar Rangan, *UK*

Shoulder and Elbow

Dr Sanjay Garude, *Mumbai*
Dr Ashish Babhulkar, *Pune*
Dr Jaap Willems, *Netherlands*
Dr John Ebenezer, *Bengaluru*
Dr Khalid Mohammad, *New Zealand*
Dr Nick Wallwork, *Australia*
Dr Paolo Paladini, *Italy*
Dr Sanjay Desai, *Mumbai*
Dr Sanjay Trivedi, *Gujarat*
Dr Vivek Pandey, *Manipal*
Mr Puneet Monga, *UK*
Mr Radhakanth Pandey, *UK*
Prof Lennard Funk, *UK*

Journal of Arthroscopy and Joint Surgery

General Information

The Journal

Journal of Arthroscopy and Joint Surgery, JAJS is an official, peer reviewed, online scientific journal. The first edition of which rolled out in January 2014. The journal's full text is available online at https://journals.lww.com/jajs and issues are published quarterly in March, June, September, December. The Journal is committed to bring forth scientific manuscripts in the form of original research articles, current concept reviews, meta-analyses, case reports with a clear message and letters to the editor.

Abstracting and Indexing Information

The journal is registered with the following abstracting partners:

Baidu Scholar, CNKI, China National Knowledge Infrastructure, EBSCO Publishing's Electronic Databases, Ex Libris – Primo Central, Google Scholar, Hinari, Infotrieve, National Science Library, ProQuest, TDNet, Wanfang Data.

The journal is indexed with, or included in, the following: EMBASE, SCOPUS.

Information for Authors

There are no page charges for IPCARES submissions. please check https://journals.lww.com/jajs/Pages/iInformationforauthors.aspx for details.

All manuscripts must be submitted online at https://review.jow.medknow.com/jajs.

Subscription Information

A subscription to the Journal of Arthroscopy and Joint Surgery comprises 4 issues. Prices include postage. Annual Subscription Rate for non-members-

- Institutional: INR 12000.00 for India
  USD 200.00 for outside India
- Personal: INR 5000.00 for India
  USD 150 for outside India

For mode of payment and other details, please visit www.medknow.com/subscribe.asp

Claims for missing issues will be serviced at no charge if received within 60 days of the cover date for domestic subscribers, and 3 months for subscribers outside India. Duplicate copies cannot be sent to replace issues not delivered because of failure to notify publisher of change of address.

The journal is published and distributed by Wolters Kluwer India Private Limited. Copies are sent to subscribers directly from the publisher's address. It is illegal to acquire copies from any other source. If a copy is received for personal use as a member of the association/society, one cannot resale or give-away the copy for commercial or library use.

Nonmembers: All change of address information to be sent to WKHLRPMedknow_subscriptions@wolterskluwer.com

Advertising policies

The journal accepts display and classified advertising. Frequency discounts and special positions are available. Inquiries about advertising should be sent to Wolters Kluwer India Private Limited, WKHLRPMedknow_advertise@wolterskluwer.com.

The journal reserves the right to reject any advertisement considered unsuitable according to the set policies of the journal.

The appearance of advertising or product information in the various sections in the journal does not constitute an endorsement or approval by the journal and/or its publisher of the quality or value of the said product or of claims made for it by its manufacturer.

Copyright

The entire contents of the Journal of Arthroscopy and Joint Surgery are protected under Indian and international copyrights. The Journal, however, grants to all users a free, irrevocable, worldwide, perpetual right of access to, and a license to copy, use, distribute, perform and display the work publicly and to make and distribute derivative works in any digital medium for any reasonable non-commercial purpose, subject to proper attribution of authorship and ownership of the rights. The journal also grants the right to make small numbers of printed copies for their personal non-commercial use.

Permissions

For information on how to request permissions to reproduce articles/information from this journal, please visit www.medknow.com.

Disclaimer

The information and opinions presented in the Journal reflect the views of the authors and not of the Journal or its Editorial Board or the Publisher. Publication does not constitute endorsement by the journal. Neither the Journal of Arthroscopy and Joint Surgery nor its publishers nor anyone else involved in creating, producing or delivering the Journal of Arthroscopy and Joint Surgery or the materials contained therein, assumes any liability or responsibility for the accuracy, completeness, or usefulness of any information provided in the Journal of Arthroscopy and Joint Surgery, nor shall they be liable for any direct, indirect, incidental, special, consequential or punitive damages arising out of the use of the Journal of Arthroscopy and Joint Surgery. The Journal of Arthroscopy and Joint Surgery nor its publishers, nor any other party involved in the preparation of material contained in the Journal of Arthroscopy and Joint Surgery represents or warrants that the information contained herein is in every respect accurate or complete, and they are not responsible for any errors or omissions or for the results obtained from the use of such material. Readers are encouraged to confirm the information contained herein with other sources.

Editorial office:

Dr. Pushpinder Singh Bajaj
Managing Editor,
Journal of Arthroscopy and Joint Surgery,
Center for Arthroscopy, Sports Medicine and
Joint Replacement, Bajaj Specialist Clinics, B-7/5 ,G.F.,
Safdarjung Enclave, New Delhi - 110029, India
Email: isksaaeducation@gmail.com

Published by

Wolters Kluwer India Private Limited,
A-202, 2nd Floor, The Qube, C.T.S. No.1498A/2 Village Marol,
Andheri, East, Mumbai - 400 059, India.
Phone: 91-22-66491818
Website: www.medknow.com

Printed at

Nikeda Art Printers Pvt. Ltd.,
Building No. C/3 - 14,15,16,
Shree Balaji Complex, Vehele Road,
Village Bhatale, Taluka Bhiwandi,
District Thane - 421302, India.

Journal of Arthroscopy and Joint Surgery

Volume 10 | Issue 3 | July-September 2023

Contents

MSK Radiology Articles

To IMPROVE your chance of publication in high-quality journals, turn to wkauthorservices.editage.com

The English-language editing and publication support service
trusted by more than 72,000 authors worldwide
is now available from Wolters Kluwer.

Get a quote for your manuscript today!

Wolters Kluwer

editage by CACTUS

Academic Editing · Translation · Plagiarism Check · Artwork Preparation

Second Issue – From the Desk of the Guest Editors

After the success of the first issue of the musculoskeletal (MSK) series, we are pleased to offer the second issue of the MSK-related dedicated articles. We have put together further focused new articles which we think will of interest to the orthopedic surgeons, researchers, and readers of the JAJS.

In this edition of the journal, we have tried to cover the different aspects of the MSK imaging. One of the articles describes the importance of the strength of the magnetic resonance imaging machine and its advantages and disadvantages. The article on the incidental findings of sports imaging is quite interesting as it highlights the importance of knowing and recognizing the subtle findings or "incidentalomas" other than obvious sports injuries, which could change the general management and long-term recovery of the patient.

The article on the ancillary posterior knee edema sign is a new concept and sign that helps to recognize the significance of posterior traumatic knee injuries, as we all know that has a higher impact on the patient's overall outcome.

We have also covered MSK ultrasound in this issue to improve familiarization and to assist the readers, in understanding how the ultrasound images are acquired and their various indications. The article of the ultrasound-guided injections also highlights the "tips and tricks" from the experiences of the authors to improve the ultrasound techniques to assist the operators who are regularly performing ultrasound-guided injections. In addition, we have also covered the novel technique of ultrasound-guided percutaneous release of pulley in the trigger finger management. The article on the approach to bone tumors from the UK's renowned Bone Tumour Centre highlights and guides the readers about the approach to bone tumors and their systematic management pathway. This article explains in detail the different modalities available and how to use them effectively.

Finally, we would like to thank the authors and reviewers for their collaborative effort to create a successful second issue. Once again, we take this opportunity to thank the editorial board for providing us a wonderful opportunity to create these two issues of the journal which are focused on the "faceless" subspecialty of the MSK radiology.

Sanjay Patel, Karthikeyan P. Iyengar[1], Rajesh Botchu[2]

I-MED Radiology Network, Forest Lake Boulevard, Forest Lake, Brisbane, Australia, [1]Department of Orthopedics, Apollo Hospitals Educational and Research Foundation, Southport and Ormskirk NHS Trust, Southport, [2]Department of Musucloskeletal Radiology, Royal Orthopedic Hospital, Birmingham, UK

Address for correspondence: Dr. Sanjay Patel, I-MED Radiology Network, Forest Lake Boulevard, Forest Lake, Brisbane, Australia.
E-mail: sanjaybrisbane@gmail.com

Submitted: 24-May-2023 **Accepted:** 24-May-2023
Published: 19-Jul-2023

This is an open access journal, and articles are distributed under the terms of the Creative Commons Attribution-NonCommercial-ShareAlike 4.0 License, which allows others to remix, tweak, and build upon the work non-commercially, as long as appropriate credit is given and the new creations are licensed under the identical terms.

Access this article online

Quick Response Code:

Website: https://journals.lww.com/jajs

DOI: 10.4103/jajs.jajs_50_23

How to cite this article: Patel S, Iyengar KP, Botchu R. Second issue – From the desk of the guest editors. J Arthrosc Jt Surg 2023;10:91.

Review Article

Settings and Indications of Ultrasound in Imaging of Shoulder, Foot, and Ankle

Yajur Narang, Gabriele Clemente, Hifz Aniq, Rob Campbell, Alpesh Mistry
Department of Radiology, Liverpool University Hospitals NHS Foundation Trust, Liverpool, UK

Abstract

Ultrasonography is a well-established musculoskeletal imaging technique with a multitude of advantages when compared to other modalities. It provides great spatial resolution in the evaluation of superficial articular and peri-articular structures including tendons, ligaments, bursae, and nerves. Given that it is the only modality which allows dynamic assessment, it also plays a crucial role in diagnosing impingement, subluxation/dislocation, and instability. The purpose of this article is to review the settings and indications of US in the imaging of shoulder, foot, and ankle in particular. Relevant literature, predominantly in the form of peer-reviewed journal articles was obtained from the electronic databases such as PubMed and MEDLINE and reviewed in a structured manner. This was combined with background knowledge and expertise in this field.

Keywords: Articular and Peri-articular, dynamic, spatial resolution, ultrasonography

Introduction

Ultrasound (US) is one of the most effective and established imaging techniques, which has been practiced for years. With the ongoing technological advancements, the role of US in musculoskeletal (MSK) imaging is continuing to expand.

MSK US provides great spatial resolution and is an excellent tool for the evaluation of joints, bursae, tendons, ligaments, and other soft-tissue abnormalities.[1] Doppler imaging further provides useful information regarding vascularity which plays an important role in the identification of pathologies such as tumors and synovitis.[2]

US confers great advantages over other modalities. It is safe, cheap, and free of ionizing radiation. Furthermore, it provides quick, real-time imaging with the added benefit of dynamic examination.

This article provides an overview of the settings and indications of US in the imaging of the shoulder, foot, and ankle.

Shoulder

Rotator cuff (RC) and subacromial subdeltoid (SASD) bursal disorders are the most frequent causes of pain in the shoulder. In particular, RC pathology is the most frequent indication for US of the shoulder in patients over 40 years old, most commonly affected by degenerative tears. A common cause of pain between the ages of 17–40 is labral pathology.[3]

Shoulder US allows the evaluation of cuff tear, tendinopathy, calcific tendinitis, and subacromial impingement. Cuff tears and tendinopathy stem from a variety of factors,[4] however, the prevalence of RC tears increases with age and there is a relationship with tendinopathy or tendon degeneration, as well as previous trauma.[5,6]

Tendinopathy is related to overuse, with repetitive stresses leading to the degeneration of collagen fibres.[7] Extrinsic causes related to tendon tears are impingement and traumatic injuries.[8] The changes seen in RC tendinopathy are swelling and enlargement of tendons with areas of hypoechogenicity, loss of fibrillar echotexture, and possible hyperaemia on Doppler related to neovascularity.[9] However,

Access this article online

Quick Response Code:

Website: https://journals.lww.com/jajs

DOI: 10.4103/jajs.jajs_11_23

Address for correspondence: Dr. Yajur Narang, Department of Radiology, Royal Liverpool University Hospitals, Liverpool, UK.
E-mail: yajur.narang@rlbuht.nhs.uk

Submitted: 09-Feb-2023 **Revised:** 28-Feb-2023
Accepted: 01-Mar-2023 **Published:** 19-Jul-2023

This is an open access journal, and articles are distributed under the terms of the Creative Commons Attribution-NonCommercial-ShareAlike 4.0 License, which allows others to remix, tweak, and build upon the work non-commercially, as long as appropriate credit is given and the new creations are licensed under the identical terms.

For reprints contact: WKHLRPMedknow_reprints@wolterskluwer.com

How to cite this article: Narang Y, Clemente G, Aniq H, Campbell R, Mistry A. Settings and indications of ultrasound in imaging of shoulder, foot, and ankle. J Arthrosc Jt Surg 2023;10:92-100.

distinguishing tendinopathy from tears may be challenging. US is an operator-dependent technique, but high sensitivity and specificity similar to those of magnetic resonance imaging (MRI) can be achieved when performed by experienced investigators.[10]

Full-thickness tears

These are tears involving the entirety of tendon substance from its articular to the bursal surface. Complete US evaluation involves examining the short and long axis of the tendon [Figure 1]. The supraspinatus tendon (SST) is most frequently torn, typically 13–17 mm posterior to the long head biceps tendon (LHBT), at the interdigitation with Infraspinatus (IST).[11] The location of the tear and its dimension in the transverse and longitudinal axis are usually defined well with US. The degree of fiber retraction can be assessed with small cuff tears; however, evaluation may be difficult with massive tears as these can retract beneath the bony coracoacromial arch.[12] Focal tears appear anechoic or hypoechoic on US with the defect involving the entire substance of the tendon and cause a depression of the tendon contour. The contour should otherwise parallel the convex contour of the humeral head. Massive tears are those involving two or more tendons of the RC or measuring more than 5 cm in size.

The following are all indirect signs of cuff tears.[13]

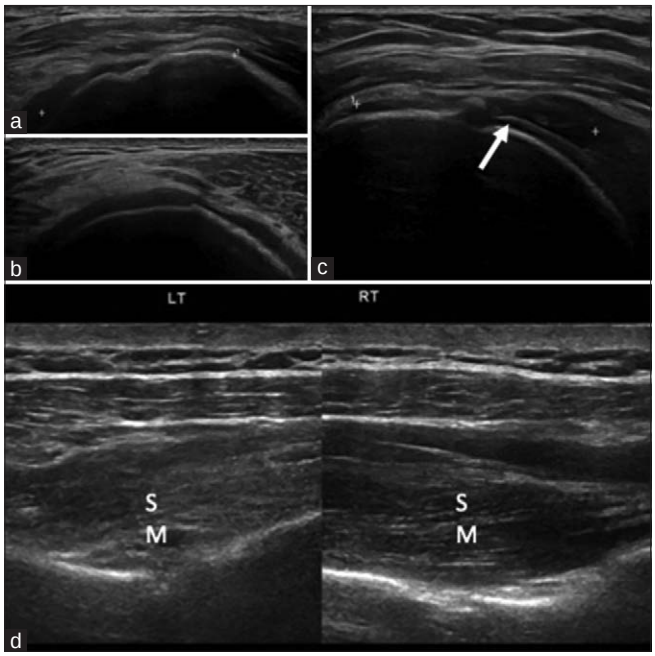

Figure 1: Full-thickness tears. (a) The SST tendon is not seen at its attachment on the greater tuberosity on a longitudinal view as well as (b) on a transverse view. This is compatible with a full-thickness tear with retraction. (c) On this longitudinal view of a complete full-thickness tear of SST, tendon fibres can be seen allowing us to measure the degree of retraction. Note the presence of a cartilage interface sign (arrow). (d) Assessment of the degree of volume loss and fatty infiltration of the left SST muscle, in a Patient with a complete tear, compared to the healthy contralateral side. The left SST muscle appears reduced in volume and hyperechoic, this is compatible with initial fatty infiltration. SM: Supraspinatus muscle, SST: Supraspinatus tendon

- Superior displacement of the humeral head. In large or massive full-thickness cuff tears, the humeral head may be superiorly displaced and in direct contact with the SASD bursa or impinge on the underside of the acromion
- Compression: In smaller minimally retracted full-thickness tears, it may be useful to apply probe pressure over the deltoid as it may herniate into the tear, making them easier to visualise
- Effusion. Acute full-thickness cuff tears are often accompanied by effusion in the bursa and joint or between the cuff tear margins
- Cartilage interface sign. Results from greater US transmission at the level of tear as there is less tendon tissue impeding the US beam. A prominent hyperechoic line of the cartilage is seen.[14,15]

Full-thickness tears in patients younger than 55 years are mostly post-traumatic. In patients over 55 years old, these are usually degenerative.[16] In cases of full-thickness tears, the cuff muscles should be assessed for fatty atrophy and infiltration, as their presence correlates with poor prognosis after repair.[8]

Partial-thickness tears

These are defined as either intrasubstance lesions or limited to the articular or bursal aspect of the tendon [Figure 2].

Intrasubstance tears also include delaminating tears or lesions of the footprint. On imaging, they are seen as focal hypoechoic defects involving part of the tendon fibers.[13,17] In bursal-sided tears, flattening of the convex surface of the bursa is seen. Cortical irregularity at the tendon insertion is seen in articular-sided tears. A rim-rent or partial articular supraspinatus tendon avulsion tear is a subtype of partial tear at the SST footprint that breaches the articular surface of the tendon. Tears of the articular surface (60%) are more frequent than bursal surface tears (40%). Partial tears are seen in patients of all ages, most commonly affecting SST.

It is paramount to appropriately align the orientation of the probe during the US assessment of the RC to eliminate and reduce anisotropy. Anisotropy is a common US artefact which occurs with tendons, muscles, and nerves in which the change in the incident beam angle results in a reduction in the echogenicity of the structure. In RC assessment, it can mimic tendinopathy or tears.

Subacromial impingement and bursal pathology

Neer[18] proposed that subacromial impingement could be related to 95% of cuff tears. Dynamic evaluation with US is useful to demonstrate impingement in real-time. By placing the transducer above the greater tuberosity and distal acromion, during abduction-reduced gliding, bursal thickening, and pooling of fluid can all be appreciated adjacent to the acromion as the SST moves below the coracoacromial arch. Clinically, the patient may present with pain during the maneuver, further reinforcing the suspicion of impingement.[16] However, the absence of signs of impingement on US does not exclude the condition.

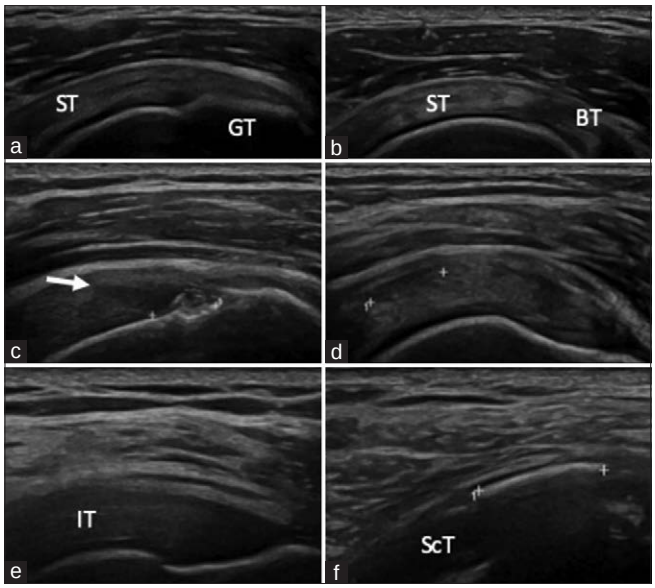

Figure 2: Partial thickness tear and tendinopathy. (a) Longitudinal view of a normal SST tendon, (b) transverse view, the LHBT can be seen in the RI anterior to the tendon. (c) Articular-sided partial tear of the SST tendon, with a hypoechoic defect seen to extend into the tendon fibres (arrow) but not to the bursal surface. Note the cortical irregularity at the tendon attachment in between the markers. (d) Bursal-sided partial tear of the SST tendon, seen with a hypoechoic defect and loss of the normal convexity of the bursal profile. (e) Diffusely tendinopathic IST tendon, the tendon appears markedly thickened and hypoechoic, and its fibres are not well recognisable. (f) Calcific tendinopathy of subscapularis with a large intratendon calcification causing posterior shadowing. ST: Supraspinatus tendon, GT: Greater tuberosity, BT: Biceps tendon, IT: Infraspinatus tendon, ScT: Subscapularis tendon, SST: Supraspinatus tendon, LHBT: Long head biceps tendon

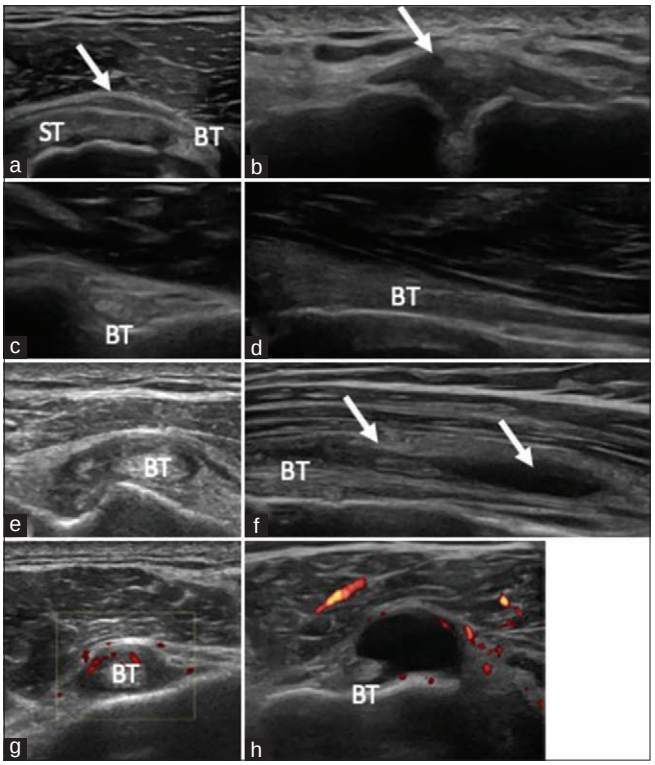

Figure 3: Bursal, ACJ and bicipital pathology. (a) Mild distention of the subacromial bursa (arrow) seen superficially to the SST tendon. (b) Capsular thickening and synovial hypertrophy (arrow) of the ACJ due to osteoarthritis. (c) Normal appearance of the LHBT in the groove on a transverse and (d) longitudinal scan. (e) The LHBT is seen to be dislocated medially from the bicipital groove. (f) Distention of the LHBT tendon sheath with anechoic fluid seen around the tendon (arrows) on this longitudinal view. (g) Mild distention of the LHBT sheath and increased Doppler vascularity compatible with acute tenosynovitis. (h) Marked distention of the LHBT sheath on a transverse image. BT: Biceps Tendon, ST: Supraspinatus tendon, LHBT: Long head biceps tendon, ACJ: Acromioclavicular joint

Besides impingement, the SASD bursa can also be affected by secondary changes related to cuff disease and inflammatory or infective conditions. Bursal distention is classified into communicating and noncommunicating types, with respect to the glenohumeral joint (GHJ). Cuff tears are the most frequent cause of communicating distention, with an association being observed in 90% of cases.[19] This is generally seen with full-thickness tears, and fluid may even extend into the acromioclavicular joint (ACJ).

Noncommunicating distention can be caused by subacromial impingement, intrabursal haemorrhage after trauma, inflammation due to arthropathy, calcific, or septic bursitis.

The abnormal bursa is distended with fluid [Figure 3a]. It can contain echogenic synovial hypertrophy, with evidence of increased Doppler flow in infection or inflammation. However, US cannot accurately distinguish between infection and inflammatory conditions.

Calcific tendinitis

This is caused by the deposition of calcium hydroxyapatite, commonly affecting patients aged 30–50 years.[20]

Involvement of the SST is most common. However, the involvement of any component of the cuff, as well as the LHBT and SASD bursa, is possible [Figure 2f].

US localizes calcifications within tendons and represents a means to guide interventional procedures like barbotage for treatment.[21,22]

Calcifications demonstrate variable appearance on US: Either oval deposits with posterior acoustic shadowing or clumped, amorphous echogenic deposits with no posterior shadowing.[16] In the acute phase, hyperemia can be recognized on Doppler in the surrounding tendon fibers.

Pathology of the long head biceps tendon

Arthroscopy is the gold standard to evaluate the LHBT; however, US can be a useful assessment tool. US allows accurate imaging of the extracapsular tendon for tears, subluxation and dislocation.[23-25]

Tendinosis and tenosynovitis

Pain on the anterior aspect of the shoulder is most commonly observed, exacerbated by palpation at the groove. Tendinosis is often caused by a coexisting abnormality, but primary tendinosis can occur in the extracapsular tendon.

Degenerative or inflammatory tendinosis can be a consequence of overuse, mostly at the distal end of the bicipital groove or at the labral insertion of the tendon.[24,26]

Tendinosis can be seen as thickening and enlargement of LHBT, with possible loss of fibrillar echotexture [Figure 3].[24,27]

Inflammation involving the synovial tendon sheath is often present. Tenosynovitis can be related to repeated stress and tends to involve the bicipital groove.[28] It is also associated with infections or arthropathies as distention of the tendon sheath with fluid in larger quantities than expected compared to joint fluid with or without synovial hypertrophy or vascularity.[24]

Rupture and tears

Tears of the LHBT often happen on a background of existing tendinosis. In patients, over 50 years of age, this can happen with little to no preceding trauma.[29] Rupture clinically causes pain and palpable retraction of the muscle belly with a visible Popeye sign.

On US, fibers are completely torn with a gap filled with fluid or hematoma and/or no tendon visible in the groove as the tendon retracts. Partial tears of the biceps can be difficult to appreciate.[23,24]

Proximal intracapsular tears with lesions of the superior labrum are challenging on US and best appreciated with arthroscopy. Intrasubstance tears can be associated with pain and can be seen as anechoic defects in the substance of the tendon.[30]

Subluxation and dislocation

Subluxation is defined as partial displacement of the tendon from the bicipital groove, whereas dislocation is complete displacement outside the groove. Both are associated with tendinosis or tears.

In the absence of displacement, the LHBT can appear perched medially in the groove. Dynamic imaging with US during internal and external rotation becomes crucial in establishing a diagnosis.

LHBT subluxation is common at the proximal bicipital groove and is often related to destabilising lesions of the rotator interval or subscapularis tendon.[31]

Acromioclavicular joint pathology

Pain related to the ACJ is typically referred to the anterosuperior aspect of the shoulder and can be traumatic, degenerative, infective or inflammatory. US is limited to assessing the joint for capsular hypertrophy and joint distention.[32]

Other indications

Rotator cuff muscle atrophy

Increased echogenicity compared to the nearby trapezius and deltoid muscles can be seen in muscle atrophy allowing for its grading.[33,34]

Glenohumeral joint

Osteoarthritis or synovitis is recognized in the posterior GHJ. However, US is not the preferred modality for imaging; hence, findings should be correlated to radiographic assessment. US can assess for margin osteophytes or effusions in the recesses of the joints. Prominent synovitis may be identified on US.

A para labral cyst caused by labral tears may be identified on US, particularly when large and located posteriorly or extending into the suprascapular notch. As US is limited in the assessment of glenoid labral tears, further imaging with MRI or magnetic resonance angiography would be indicated (ref at the end).

Interventional procedures

The most commonly performed procedures are SASD bursal and ACJ injections in the setting of impingement. However, injection in the GHJ can also be performed, usually with a posterior approach. Suprascapular nerve block which can be effectively administered using US has shown more favorable results compared to SASD bursal injection in people with large cuff tears.

Barbotage is a procedure employed to fragment and encourage the resorption of large calcific deposits related to calcific tendinopathy.

Ankle and Foot

Like the shoulder, there are various indications for which US can be utilized. These include assessment of the ankle ligaments and tendons and review for joint effusions. Added dynamic evaluation with US can provide some functional information. Various specific lesions around the foot and ankle can be easily diagnosed with US. The modality is often used for guided interventions around the foot and ankle.

Ligamentous evaluation

Three ligamentous groups comprise the ankle joint-lateral ligaments, deltoid ligament complex, and syndesmotic ligaments.

Ligaments would appear slightly thickened with minimal alteration of fibrillar structure in mild acute sprains or grade 1 injury. Moderate sprains or grade 2 injury result in partial interruption of the fibrillar pattern. In a severe tear or grade 3 injury, there is a complete disruption of fibers with a gap.[35]

Lateral ligaments

The anterior talofibular ligament (ATFL) is the most commonly injured ligament during inversion strains.[36] To visualize this, the probe is positioned at the distal tip of the lateral malleolus in the longitudinal aspect of the foot.[37] Dynamic maneuvers such as inversion and plantar flexion put tension in the ligament, allowing better visualization. Posterior talofibular ligament is not readily seen on US due to its deep location. The calcaneofibular (CFL) is the second most commonly injured ligament and often occurs together with the ATFL.[38] This structure lies deep to the peroneal tendon and is best visualized with the probe positioned coronally with the upper angle of the probe over the tip of the lateral malleolus and foot in dorsiflexion.[39] Complete CFL tears are often found with fluid in the peroneal tendon sheath.[40]

Deltoid ligaments

Medial deltoid ligaments appear fan-shaped and originate from the apex of the medial malleolus. It comprises of deep anterior and posterior tibio-talar components and superficial tibionavicular, tibio-spring, and tibiocalcaneal ligaments. The superior-medial spring ligament lies between the navicular and sustentaculum tali underneath the tibialis posterior.

The deltoid complex is best visualized in dorsiflexion and eversion.[41] In the acute setting, these tears can be associated with lateral malleolar fractures or distal tibiofibular tears.[35]

Syndesmosis

The weakest of the syndesmotic ligaments is the anterior inferior tibiofibular ligament which is the first to give way during external rotation of the fibula.[42] This is best visualized in an oblique transverse position where the tibia and fibula are in closest contact.[43] The other syndesmotic ligaments are otherwise not adequately assessed on US due to their deep locations between osseous structures.

Tendon evaluation

Because of the superficial nature and amenability to dynamic manoeuvres, visualization of the foot and ankle tendons using high-frequency US is well established. Some of the common pathologies include tenosynovitis, tendinosis, partial and complete tears, subluxation and dislocations.

Tenosynovitis refers to inflammation of the synovial membrane around the tendon [Figure 4b and c]. This can occur with or without tendinosis. The etiology is multifactorial including trauma, infection, localized stress, or arthropathies such as ankylosing spondylitis or rheumatoid arthritis.[44] On US, there is increased fluid content or synovial thickening within the tendon sheath. Color Doppler helps assess the degree of inflammation.[42]

Tendinosis causes tendon thickening with focal or diffuse areas of hypoechogenicity but preservation of fibrillar appearance [Figures 4a and 5a]. A tear on the other hand results in an anechoic/hypoechoic gap with disruption of the fibrillar pattern.[42]

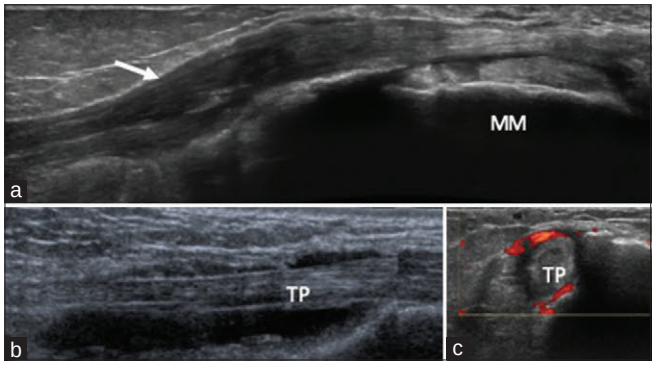

Figure 4: Tibialis Posterior (TP) Pathologies. (a) Tendinopathy-Long view demonstrating fusiform thickening of the mid-tendon substance of TP (arrow). (b) Long and (c) Short axis views demonstrating fluid within the TP tendon sheath with neovascularity in keeping with tenosynovitis. MM: Medial malleolus, TP: Tibialis posterior

Peroneal tendons

US is an excellent tool for identifying peroneal injuries.[45] Trauma or sports injuries are the most common cause of acute peroneal longus tears.[42] One of the most frequent peroneus brevis tears is the longitudinal split, causing the peroneal longus to move into the cleft [Figure 5b]. US demonstrates a central cleft with two hemi-tendons which can often be associated with tenosynovitis.[46]

Intrasheath subluxation results in a reversal in the peroneal tendon positions but with an intact superior peroneal retinaculum (SPR) [Figure 5c].[47] Dislocation on the other hand causes displacement of one or both tendons often associated with SPR injury.[48]

Achilles tendon

The strongest tendon of the body, the Achilles tendon is distinct from other ankle tendons. It is surrounded by a paratenon rather than a synovial sheath.[49] As a result, paratendinopathy occurs instead of tenosynovitis which results in the thickening of paratenon with diffuse edema [Figure 6d].[50]

Achilles tendinopathy otherwise causes tendon thickening with loss of anterior concavity in the transverse plane, with the tendon usually measuring greater than 8 mm. US demonstrates areas of focal or diffuse hypoechogenicity with loss of fibrillar pattern [Figure 6a and b].[51]

Cases of tendinopathy/paratenonitis can often be accompanied by retrocalcaneal bursitis, which results in inflammation of the bursa. Sonographically, there is distension of the bursa by hypo/anechoic fluid.[42] It is also seen as a triad along with insertional tendinopathy and bony prominence of the posterior-superior calcaneum in Haglund's syndrome[Figure 6c].[52]

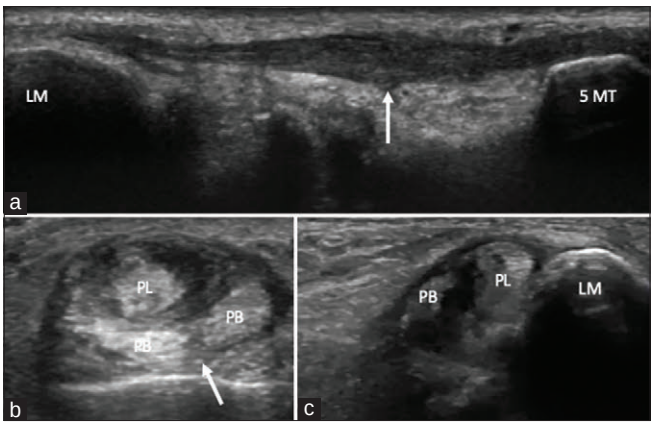

Figure 5: Peroneal Pathologies. (a) Tendinopathy-Short axis US image demonstrating fusiform thickening of peroneal brevis tendon (arrow). (b) Tear of peroneal brevis-Short axis view demonstrating a longitudinal split tear (arrow) of the peroneal brevis tendon wrapping the peroneal longus in a 'boomerang' appearance. (c) Intra-sheath subluxation-Reversed position of peroneal brevis and longus tendons with an intact retinaculum. LM: Lateral Malleolus, 5MT: Base of 5th Metatarsal, PL: Peroneal longus, PB: Peroneal brevis

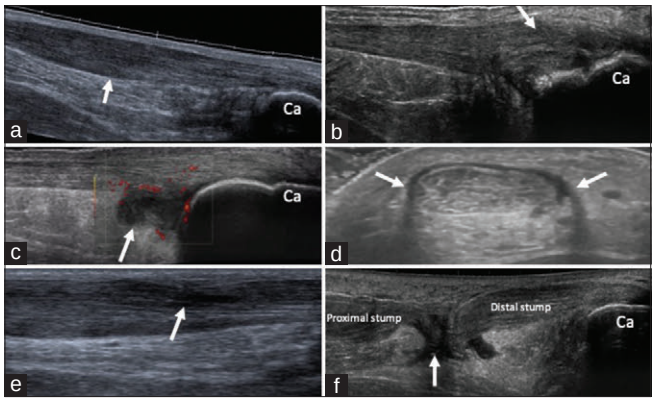

Figure 6: Achilles pathologies. (a) Mid-Achilles tendinopathy-Fusiform thickening of the mid-Achilles fibers (arrow) with maintained fibrillar pattern. (b) Insertional tendinopathy-Tendinous thickening at the insertion with associated cortical irregularity (arrow). (c) Retrocalcaneal bursitis-Thickening of the tendon proximal to the insertion with moderate inflammation and distension of the retrocalcaneal bursal with fluid (arrow). (d) Achilles paratenonitis-Hypoechoic thickening of the surrounding paratenon (arrows). (e) Partial tear-Achilles tendon enlargement with a hypoechoic cleft (arrow) in keeping with a partial tear. (f) Complete tear-Longitudinal view demonstrating a full-thickness complete tear at the critical zone with a tendon gap and associated hematoma (arrow). Ca: Calcaneum

Achilles tears usually happen 2–6 cm from calcaneal insertion, at the critical zone with reduced vascularity. Tears can be divided into partial and complete tears. A complete tear results in complete disruption of the tendon fibers with usually two tendon stumps and hematoma/fluid collection in the tendon gap [Figure 6f]. Partial tears usually result in tendon enlargement with abnormal hypo/anechoic clefts within the substance seen on US [Figure 6e].[42]

Plantar fasciopathy and fibrosis

One of the most common causes of heel pain, plantar fasciitis refers to inflammation of the plantar fascia (PF). Imaging often acts as an important aid in the diagnosis of fasciopathy and in determining concomitant injuries. US is a precise and cheap way to evaluate the bands of PF and attachments on the calcaneum.[53]

Like ligaments, the normal sonographic appearance of PF is a compact fibrillar pattern, best visualized on the long axis and with the probe perpendicular to the fascial plane. Characteristics of PF on US include loss of fibrillar pattern, thickening measuring more than 4 mm and calcification within PF.[54,55] Doppler US can identify hyperemia near its insertion in patients with plantar fasciitis which can also play a role in monitoring treatment response.[53,56]

Another common condition of PF is fibromatosis [Figure 7b], which refers to the benign nodular fibroblastic proliferation of the PF. This most likely involves the distal two-thirds of the fascia, which can be multiple and bilateral. Sonographic findings are of iso to hypoechoic fusiform nodular thickening of PF the majority of which show no doppler flow.[57]

Joint evaluation-arthritis and synovitis

OA is a chronic degenerative phenomenon affecting a large proportion of the population globally. Although more commonly affecting the hips and knees, ankles can also be involved, mainly in post-traumatic cases.[58] US can help in evaluating cortical irregularities, i.e., osteophytosis, loose fragments and chondral lesions to a certain extent.[59] Effusion is usually examined in a neutral position anteriorly and considered abnormal if greater than 4 mm of fluid or if there is evidence of synovial bulging.[58]

US has become an important modality in the assessment of articular and peri-articular pathologies in rheumatic diseases. Power Doppler plays a key role in the differentiation of active inflammation and residual diseases and also helps in differentiating inflammatory versus degenerative disease.[60,61]

Lesions

Intermetatarsal masses

The most common intermetatarsal mass is Morton's Neuroma [Figure 7a], which is localized perineural fibrosis of the plantar digital nerves. It appears as a round or oblong hypoechoic noncompressible mass, most commonly in the 3rd intermetatarsal space. Dynamic maneuvers at the plantar surface with a positive Mulder click can further help in clarifying the diagnosis.[62] Other common intermetatarsal pathologies include bursae which are fluid-filled pockets, visualized as compressible hypoechoic structures. These often occur in combination with Mortons's neuroma, therefore referred to as neuroma-bursal complex. Superficial adventitial bursitis can also occur at frictional sites adjacent to the bony prominences, usually beneath the 1st and 5th metatarsal heads.[63]

Tendon sheath and intratendinous masses

Tenosynovial tumors of the tendon sheaths and giant cell tumors (GCTs**)** occur in close contact with the tendon. These are usually homogenous and hypoechoic to the tendon on US [Figure 7d]. These are often vascular on Doppler imaging and might cause bony erosion. Solid malignant soft-tissue masses can cause confusion and a biopsy is often needed to reach the final diagnosis.[64] Diffuse pigmented villonodular synovitis (PVNS) can mimic inflammatory tenosynovitis and biopsy needs to be considered in such cases [Figure 7c].[65] Achilles tendon xanthomas are painless lumps most commonly at the distal portion of the tendon. They present as hypoechoic foci within the tendon with loss of normal fibrillar appearance, sometimes making it difficult to differentiate from tendinopathy.[42]

Ganglion

A ganglion is one of the most common lesions of the foot and ankle. It is a mass containing gelatinous material and surrounded by a discrete wall. These usually arise from a joint or tendon sheath as a result of mucoid degeneration and partial tendon tears respectively. They can appear as simple cysts or demonstrate loculations and septations.[1]

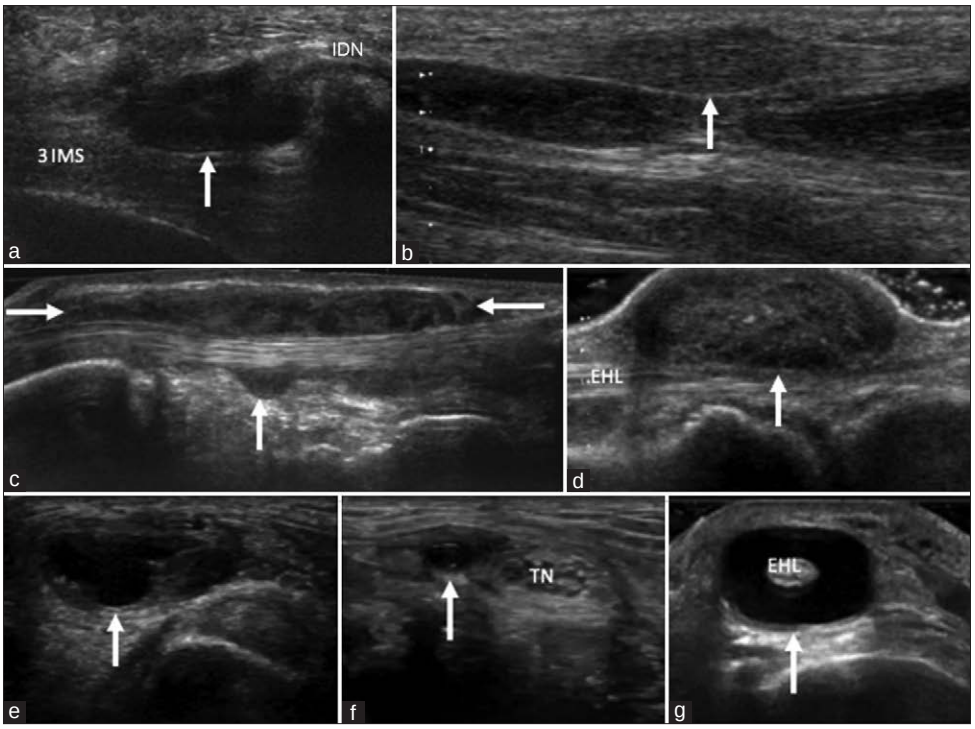

Figure 7: Ankle and foot masses. (a) Morton's Neuroma-Long axis view showing a hypoechoic nodule (arrow) at the second intermetatarsal space in continuation of the IDN. (b) Plantar fibroma-Long axis view demonstrating a discrete hypoechoic fusiform mass of the PF (arrow). (c) PVNS-Lobulated heterogeneous appearances of the TP tendon sheath in keeping with diffuse PVNS (arrow). (d) GCT-Well defined ovoid echogenic focus (arrow) in close relation to the EHL tendon overlying the MTP joint. (e and f) Ganglion cyst (arrows) causing tarsal tunnel syndrome with entrapment of the tibial nerve TN). (g) EHL ganglion (arrow)-Tense fluid-filled ganglion within EHL tendon sheath mimicking tenosynovitis. 3 IMS: 3rd Intermetatarsal space, IDN: Interdigital nerve, EHL: Extensor hallucis longus tendon, TN-Tibial nerve, GCT: Giant cell tumors, TP: Tibialis posterior, PVNS: Pigmented villonodular synovitis, MTP: Metatarsal phalangeal joint

Tendon sheath ganglia in the lower extremity often arise from peroneal tendons presenting as lateral ankle swelling [Figure 7g].[66] Common symptomatic ganglion cysts in the foot involve the sinus tarsi and the tarsal tunnel resulting in compression of the tibial nerve [Figures 7e and f]. Other common causes of tarsal tunnel syndrome include lipomas, nerve sheath tumors, varicosities, talocalcaneal coalitions, tenosynovitis, and scar tissue.[67]

Intervention

One of the most common uses of US in the foot and ankle is for simple injection guidance. The ankle, mid-tarsal, and posterior subtalar joints are some of the most commonly injected joints. Besides joints, US guidance is helpful in peri-tendinous injection for patients with tendinosis and tenosynovitis.[68] Several interventional procedures can be performed under US for Achilles tendinosis. Steroid injections and high-volume stripping are some of the common procedures. Other procedures include dry needling and paratenon stripping.[69] US is the imaging modality of choice for guided treatment of Morton's neuroma. Treatment can include steroid, alcohol, and ablation therapy.[70] US-guided injections of steroids and PRP along with percutaneous fenestration are some treatments for plantar fasciitis.[71]

Conclusions

This review highlights the role of US examination as the primary technique in the initial assessment of shoulder, ankle and foot abnormalities. It is at par or even better than some of the other modalities such as MR. The provision of Doppler imaging, combined with portability and dynamic features makes US an excellent modality to assess shoulder and ankle/foot pathologies. Besides diagnosis, US plays a very important role in the treatment of MSK conditions by aiding precise and effective joint and soft-tissue injections and interventions.

Financial support and sponsorship

Nil.

Conflicts of interest

There are no conflicts of interest.

References

1. Artul S, Habib G. Ultrasound findings of the painful ankle and foot. J Clin Imaging Sci 2014;4:25.
2. Ikeda K, Nakagomi D, Sanayama Y, Yamagata M, Okubo A, Iwamoto T, *et al*. Correlation of radiographic progression with the cumulative activity of synovitis estimated by power Doppler ultrasound in rheumatoid arthritis: Difference between patients treated with methotrexate and those treated with biological agents. J Rheumatol 2013;40:1967-76.

3. Nazarian LN, Jacobson JA, Benson CB, Bancroft LW, Bedi A, McShane JM, *et al.* Imaging algorithms for evaluating suspected rotator cuff disease: Society of Radiologists in Ultrasound consensus conference statement. Radiology 2013;267:589-95.
4. Lewis JS. Rotator cuff tendinopathy. Br J Sports Med 2009;43:236-41.
5. Schaeffeler C, Mueller D, Kirchhoff C, Wolf P, Rummeny EJ, Woertler K. Tears at the rotator cuff footprint: Prevalence and imaging characteristics in 305 MR arthrograms of the shoulder. Eur Radiol 2011;21:1477-84.
6. Dwyer T, Razmjou H, Holtby R. Full-thickness rotator cuff tears in patients younger than 55 years: Clinical outcome of arthroscopic repair in comparison with older patients. Knee Surg Sports Traumatol Arthrosc 2015;23:508-13.
7. Cooper HJ, Milillo R, Klein DA, DiFelice GS. The MRI geyser sign: Acromioclavicular joint cysts in the setting of a chronic rotator cuff tear. Am J Orthop (Belle Mead NJ) 2011;40:E118-21.
8. Gladstone JN, Bishop JY, Lo IK, Flatow EL. Fatty infiltration and atrophy of the rotator cuff do not improve after rotator cuff repair and correlate with poor functional outcome. Am J Sports Med 2007;35:719-28.
9. Goutallier D, Postel JM, Gleyze P, Leguilloux P, Van Driessche S. Influence of cuff muscle fatty degeneration on anatomic and functional outcomes after simple suture of full-thickness tears. J Shoulder Elbow Surg 2003;12:550-4.
10. Slabaugh MA, Friel NA, Karas V, Romeo AA, Verma NN, Cole BJ. Interobserver and intraobserver reliability of the Goutallier classification using magnetic resonance imaging: Proposal of a simplified classification system to increase reliability. Am J Sports Med 2012;40:1728-34.
11. Kim HM, Dahiya N, Teefey SA, Middleton WD, Stobbs G, Steger-May K, *et al.* Location and initiation of degenerative rotator cuff tears: An analysis of three hundred and sixty shoulders. J Bone Joint Surg Am 2010;92:1088-96.
12. Teefey SA, Middleton WD, Payne WT, Yamaguchi K. Detection and measurement of rotator cuff tears with sonography: Analysis of diagnostic errors. AJR Am J Roentgenol 2005;184:1768-73.
13. Wiener SN, Seitz WH Jr. Sonography of the shoulder in patients with tears of the rotator cuff: Accuracy and value for selecting surgical options. AJR Am J Roentgenol 1993;160:103-7.
14. Jacobson JA, Lancaster S, Prasad A, van Holsbeeck MT, Craig JG, Kolowich P. Full-thickness and partial-thickness supraspinatus tendon tears: Value of US signs in diagnosis. Radiology 2004;230:234-42.
15. Hollister MS, Mack LA, Patten RM, Winter TC 3rd, Matsen FA 3rd, Veith RR. Association of sonographically detected subacromial/subdeltoid bursal effusion and intraarticular fluid with rotator cuff tear. AJR Am J Roentgenol 1995;165:605-8.
16. Yablon CM, Jacobson JA. Rotator cuff and subacromial pathology. Semin Musculoskelet Radiol 2015;19:231-42.
17. van Holsbeeck MT, Kolowich PA, Eyler WR, Craig JG, Shirazi KK, Habra GK, *et al.* US depiction of partial-thickness tear of the rotator cuff. Radiology 1995;197:443-6.
18. Neer CS 2nd. Impingement lesions. Clin Orthop Relat Res 1983;(173):70-7.
19. van Holsbeeck M, Strouse PJ. Sonography of the shoulder: Evaluation of the subacromial-subdeltoid bursa. AJR Am J Roentgenol 1993;160:561-4.
20. Greis AC, Derrington SM, McAuliffe M. Evaluation and nonsurgical management of rotator cuff calcific tendinopathy. Orthop Clin North Am 2015;46:293-302.
21. Farin PU, Jaroma H. Sonographic findings of rotator cuff calcifications. J Ultrasound Med 1995;14:7-14.
22. Farin PU, Räsänen H, Jaroma H, Harju A. Rotator cuff calcifications: Treatment with ultrasound-guided percutaneous needle aspiration and lavage. Skeletal Radiol 1996;25:551-4.
23. Armstrong A, Teefey SA, Wu T, Clark AM, Middleton WD, Yamaguchi K, *et al.* The efficacy of ultrasound in the diagnosis of long head of the biceps tendon pathology. J Shoulder Elbow Surg 2006;15:7-11.
24. Skendzel JG, Jacobson JA, Carpenter JE, Miller BS. Long head of biceps brachii tendon evaluation: Accuracy of preoperative ultrasound. AJR Am J Roentgenol 2011;197:942-8.
25. Read JW, Perko M. Shoulder ultrasound: Diagnostic accuracy for impingement syndrome, rotator cuff tear, and biceps tendon pathology. J Shoulder Elbow Surg 1998;7:264-71.
26. Refior HJ, Sowa D. Long tendon of the biceps brachii: Sites of predilection for degenerative lesions. J Shoulder Elbow Surg 1995;4:436-40.
27. Thain LM, Adler RS. Sonography of the rotator cuff and biceps tendon: Technique, normal anatomy, and pathology. J Clin Ultrasound 1999;27:446-58.
28. Ahrens PM, Boileau P. The long head of biceps and associated tendinopathy. J Bone Joint Surg Br 2007;89:1001-9.
29. Carter AN, Erickson SM. Proximal biceps tendon rupture: Primarily an injury of middle age. Phys Sportsmed 1999;27:95-101.
30. Farin PU. Sonography of the biceps tendon of the shoulder: Normal and pathologic findings. J Clin Ultrasound 1996;24:309-16.
31. Bennett WF. Subscapularis, medial, and lateral head coracohumeral ligament insertion anatomy. Arthroscopic appearance and incidence of "hidden" rotator interval lesions. Arthroscopy 2001;17:173-80.
32. Alasaarela E, Tervonen O, Takalo R, Lahde S, Suramo I. Ultrasound evaluation of the acromioclavicular joint. J Rheumatol 1997;24:1959-63.
33. Wall LB, Teefey SA, Middleton WD, Dahiya N, Steger-May K, Kim HM, *et al.* Diagnostic performance and reliability of ultrasonography for fatty degeneration of the rotator cuff muscles. J Bone Joint Surg Am 2012;94:e83.
34. Strobel K, Hodler J, Meyer DC, Pfirrmann CW, Pirkl C, Zanetti M. Fatty atrophy of supraspinatus and infraspinatus muscles: Accuracy of US. Radiology 2005;237:584-9.
35. Morvan G, Mathieu P, Busson J, Wybier M. Ultrasonography of tendons and ligaments of foot and ankle. J Radiol 2000;81:361-80.
36. Kumai T, Takakura Y, Rufai A, Milz S, Benjamin M. The functional anatomy of the human anterior talofibular ligament in relation to ankle sprains. J Anat 2002;200:457-65.
37. De Maeseneer M, Marcelis S, Jager T, Shahabpour M, Van Roy P, Weaver J, *et al.* Sonography of the normal ankle: A target approach using skeletal reference points. AJR Am J Roentgenol 2009;192:487-95.
38. van den Bekerom MP, Oostra RJ, Golanó P, van Dijk CN. The anatomy in relation to injury of the lateral collateral ligaments of the ankle: A current concepts review. Clin Anat 2008;21:619-26.
39. Bianchi S, Martinoli C, Gaignot C, De Gautard R, Meyer JM. Ultrasound of the ankle: Anatomy of the tendons, bursae, and ligaments. Semin Musculoskelet Radiol 2005;9:243-59.
40. Bencardino JT, Rosenberg ZS, Serrano LF. MR imaging features of diseases of the peroneal tendons. Magn Reson Imaging Clin N Am 2001;9:493-505, x.
41. Peetrons P, Creteur V, Bacq C. Sonography of ankle ligaments. J Clin Ultrasound 2004;32:491-9.
42. Park JW, Lee SJ, Choo HJ, Kim SK, Gwak HC, Lee SM. Ultrasonography of the ankle joint. Ultrasonography 2017;36:321-35.
43. Martinoli C. Musculoskeletal ultrasound: technical guidelines. Insights Imaging. 2010 Jul;1:99-141. doi: 10.1007/s13244-010-0032-9.
44. Jacobson JA, van Holsbeeck MT. Musculoskeletal ultrasonography. Orthop Clin North Am 1998;29:135-67.
45. Grant TH, Kelikian AS, Jereb SE, McCarthy RJ. Ultrasound diagnosis of peroneal tendon tears. A surgical correlation. J Bone Joint Surg Am 2005;87:1788-94.
46. Philbin TM, Landis GS, Smith B. Peroneal tendon injuries. J Am Acad Orthop Surg 2009;17:306-17.
47. Lee SJ, Jacobson JA, Kim SM, Fessell D, Jiang Y, Dong Q, *et al.* Ultrasound and MRI of the peroneal tendons and associated pathology. Skeletal Radiol 2013;42:1191-200.
48. Butler BW, Lanthier J, Wertheimer SJ. Subluxing peroneals: A review of the literature and case report. J Foot Ankle Surg 1993;32:134-9.
49. Maffulli N, Sharma P, Luscombe KL. Achilles tendinopathy: Aetiology and management. J R Soc Med 2004;97:472-6.
50. Almekinders LC, Temple JD. Etiology, diagnosis, and treatment of tendonitis: An analysis of the literature. Med Sci Sports Exerc 1998;30:1183-90.
51. Hartgerink P, Fessell DP, Jacobson JA, van Holsbeeck MT. Full- versus partial-thickness Achilles tendon tears: Sonographic accuracy and characterization in 26 cases with surgical correlation. Radiology 2001;220:406-12.
52. Sofka CM, Adler RS, Positano R, Pavlov H, Luchs JS. Haglund's syndrome: Diagnosis and treatment using sonography. HSS J

2006;2:27-9.
53. Draghi F, Gitto S, Bortolotto C, Draghi AG, Ori Belometti G. Imaging of plantar fascia disorders: Findings on plain radiography, ultrasound and magnetic resonance imaging. Insights Imaging 2017;8:69-78.
54. Abul K, Ozer D, Sakizlioglu SS, Buyuk AF, Kaygusuz MA. Detection of normal plantar fascia thickness in adults via the ultrasonographic method. J Am Podiatr Med Assoc 2015;105:8-13.
55. Akfirat M, Sen C, Günes T. Ultrasonographic appearance of the plantar fasciitis. Clin Imaging 2003;27:353-7.
56. McMillan AM, Landorf KB, Gregg JM, De Luca J, Cotchett MP, Menz HB. Hyperemia in plantar fasciitis determined by power Doppler ultrasound. J Orthop Sports Phys Ther 2013;43:875-80.
57. Griffith JF, Wong TY, Wong SM, Wong MW, Metreweli C. Sonography of plantar fibromatosis. AJR Am J Roentgenol 2002;179:1167-72.
58. Nevalainen MT, Pitkänen MM, Saarakkala S. Diagnostic performance of ultrasonography for evaluation of osteoarthritis of ankle joint: Comparison with radiography, cone-beam CT, and symptoms. J Ultrasound Med 2022;41:1139-46.
59. Kok AC, Terra MP, Muller S, Askeland C, van Dijk CN, Kerkhoffs GM, *et al.* Feasibility of ultrasound imaging of osteochondral defects in the ankle: A clinical pilot study. Ultrasound Med Biol 2014;40:2530-6.
60. Brown AK. Using ultrasonography to facilitate best practice in diagnosis and management of RA. Nat Rev Rheumatol 2009;5:698-706.
61. Brown AK, Wakefield RJ, Conaghan PG, Karim Z, O'Connor PJ, Emery P. New approaches to imaging early inflammatory arthritis. Clin Exp Rheumatol 2004;22:S18-25.
62. Park HJ, Kim SS, Rho MH, Hong HP, Lee SY. Sonographic appearances of Morton's neuroma: Differences from other interdigital soft tissue masses. Ultrasound Med Biol 2011;37:1204-9.
63. Adventitious Bursitis | Radiology Reference Article | Radiopaedia.org. Available from: https://radiopaedia.org/articles/adventitious-bursitis?lang=gb. [Last accessed on 2022 Dec 15].
64. Middleton WD, Patel V, Teefey SA, Boyer MI. Giant cell tumors of the tendon sheath: Analysis of sonographic findings. AJR Am J Roentgenol 2004;183:337-9.
65. Saxena A, Perez H. Pigmented villonodular synovitis about the ankle: A review of the literature and presentation in 10 athletic patients. Foot Ankle Int 2004;25:819-26.
66. Kumar D, Sodavarapu P, Salaria AK, Dudekula S, Guduru A. Recurrent ganglion cyst in peroneus longus. Cureus 2020;12:e7972.
67. Nagaoka M, Matsuzaki H. Ultrasonography in tarsal tunnel syndrome. J Ultrasound Med 2005;24:1035-40.
68. Drakonaki EE, Allen GM, Watura R. Ultrasound-guided intervention in the ankle and foot. Br J Radiol 2016;89(1057):20150577.
69. Wijesekera NT, Chew NS, Lee JC, Mitchell AW, Calder JD, Healy JC. Ultrasound-guided treatments for chronic Achilles tendinopathy: An update and current status. Skeletal Radiol 2010;39:425-34.
70. Jain S, Mannan K. The diagnosis and management of Morton's neuroma: A literature review. Foot Ankle Spec 2013;6:307-17.
71. Nair AS, Sahoo RK. Ultrasound-guided injection for plantar fasciitis: A brief review. Saudi J Anaesth 2016;10:440-3.

Review Article

Incidental Findings in Sports Imaging

Jehan Ghany, Kimberly Lam, Abhishek Jain, Andrew Dunn[1], Alpesh Mistry

Department of Radiology, Royal Liverpool and Broadgreen University Hospital, Liverpool University Foundation Trust, Liverpool, [1]OrthTeam Centre, Manchester, UK

Abstract

This narrative review presents a series of cases of less common incidental findings discovered on magnetic resonance imaging of elite athletes, who have presented for investigation of either muscle or joint sports-related injuries or for presigning imaging. The presented incidental findings include anatomical variants of osseous structures and muscles; incidental bone lesions; examples of systemic disease, and nonorthopedic findings found within the imaging field of view. This review will emphasize to the reader about the importance of interrogating the imaging in its entirety and avoiding the common pitfall of "satisfaction of search" within diagnostic radiology.

Keywords: Imaging, incidental, sports

Introduction

This is a narrative review of a selected series of less common incidental findings encountered in our practice of magnetic resonance imaging (MRI) of elite and semi-professional athletes. They have presented for imaging for investigation of muscle or joint sports-related injuries or for presigning imaging.

Incidental findings (also known as 'incidentalomas') are imaging findings serendipitously diagnosed in an asymptomatic patient or in a symptomatic patient undergoing imaging for another reason. Incidentalomas have become a contentious issue in the last decade due to the increasing utilization of medical imaging in clinical care. This has resulted in various guidelines and algorithms for the work up and management of organ-specific incidentalomas which are stratified by clinical risk factors.[1,2] The rates of incidentalomas vary amongst imaging tests, with higher rates reported for chest computed tomography (CT) and cardiac MRI.[3] Rates of malignancy in incidentalomas also vary by organs, with higher rates in renal, thyroid, and ovarian incidentalomas.[3] Incidental findings can be dilemmas for radiologists (who may need to consult often conflicting guidelines) and for referring clinicians, who have to interpret sometimes vague recommendations and communicate findings and relative risks to patients.[4] Incidentalomas may also trigger a cascade of costly investigations (including potential exposure to ionizing radiation) and anxiety for patients.

Access this article online

Quick Response Code:

Website: https://journals.lww.com/jajs

DOI: 10.4103/jajs.jajs_13_23

The incidental findings in this review include both benign and clinically significant entities. They are categorized as follows: Anatomical variants involving osseous structures; anatomical variants involving muscles; and primary bone lesions. Also included are the examples of manifestations of systemic disease and an incidental finding unrelated to the musculoskeletal (MSK) system found within the imaging field of view. There are many more interesting cases that could not be included.

This review will emphasize to the reader about the importance of interrogating the imaging in its entirety and avoiding the common pitfall of "satisfaction of search" within diagnostic radiology. In addition, we hope to prompt the reader to avoid framing bias when investigating or treating professional athletes but also hope to remind readers that not all incidental findings require further workup.

Normal Osseous and Joint Variants

The foot and ankle are frequently imaged joints for suspected injuries in professional soccer players.[5,6] They are also a

Address for correspondence: Dr. Jehan Ghany, Department of Radiology, Royal Liverpool University Hospital, Prescott Street, Liverpool, L7 8XP, UK.
E-mail: ghanyjehan@gmail.com

Submitted: 11-Feb-2023 **Revised:** 20-Feb-2023
Accepted: 26-Feb-2023 **Published:** 19-Jul-2023

This is an open access journal, and articles are distributed under the terms of the Creative Commons Attribution-NonCommercial-ShareAlike 4.0 License, which allows others to remix, tweak, and build upon the work non-commercially, as long as appropriate credit is given and the new creations are licensed under the identical terms.

For reprints contact: WKHLRPMedknow_reprints@wolterskluwer.com

How to cite this article: Ghany J, Lam K, Jain A, Dunn A, Mistry A. Incidental findings in sports imaging. J Arthrosc Jt Surg 2023;10:101-9.

common site for anatomical variants that include coalitions, accessory ossicles, and accessory muscles.[7,8] Awareness of anatomical variants is key to diagnostic interpretation. Some variants are symptomatic in elite athletes. On the other hand, if the reader is unfamiliar with possible variants, this can lead to diagnostic misinterpretation and inaccurate diagnoses of pathology.

Bipartite medial cuneiform

The case in Figure 1a-c is a 28-year-old male professional soccer player who had no specific mechanism of injury but was experiencing deep focal pain around the fifth metatarsal.

Bipartite medial cuneiform is a rare variant, with a described rate of 0.79% in a recently reported series of 751 patients.[9] It was first described in the 1940s and occurs when two primary ossification centers of the cuneiform are formed instead of one. These fail to coalesce, resulting in bipartition. There may be partial or complete bipartition with either cartilaginous or fibrocartilaginous bipartition. Symptomatic bipartite medial cuneiform may result in midfoot pain which is thought to be secondary to instability in the fibrocartilaginous articulation between the dorsal and plantar components. Often, stress changes due to microinstability and/or altered biomechanics can be apparent on MRI with edema-like signal change or diastasis across the bipartition, osteophytes, subchondral cystic change, or cysts.[9] It is important to differentiate between fractures of the medial cuneiform and bipartite cuneiforms. Apart from the usual imaging signs supporting a fracture (e.g. irregular margins and intense edema-like signal), the cuneiform fracture line tends to be orientated with the long axis of the foot, as opposed to the transverse axis as demonstrated by the case, forming an "E sign."[10]

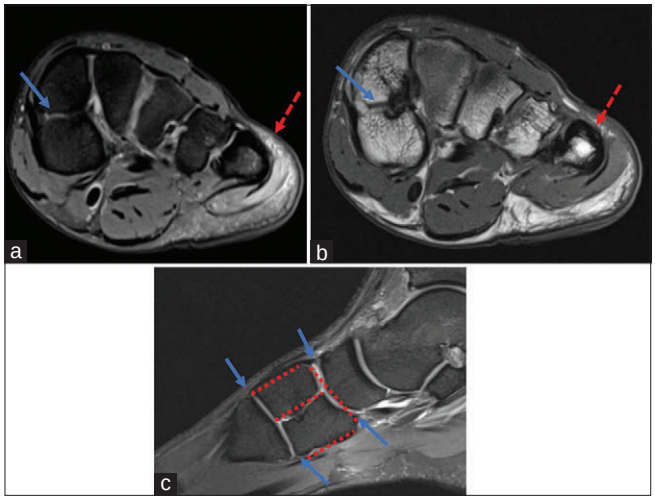

Figure 1: (a) Short axis fluid sensitive sequence demonstrating a T2 hyperintense synchondrosis at the bipartite medial cuneiform without osseous oedema (blue arrow) and Grade 1 contusion at the abductor digiti minimi muscle (red dotted arrow) with overlying mild subcutaneous edema, (b) Short axis T1W sequence also demonstrating the synchondrosis with normal bone marrow pattern at the medial cuneiform. The cortex of the fifth metatarsal is noted as circumferentially thickened with T1 low intensity but with normal marrow signal which may reflect sequalae of prior stress response (red dotted arrow), (c) Fluid sensitive sagittal view of the midfoot demonstrating the dorsal and plantar components articulating with both the navicular and first metatarsal (blue arrows). The "E sign" is also shown (dotted red lines). T1W: T1 weighted

Cubonavicular Coalition

This unusual form of coalition was incidentally observed in a 21-year-old professional male soccer player who sustained an acute ankle injury in a Champions League game with instant swelling and difficulty weightbearing [Figure 2a and b]. MRI revealed an acute partial tear of the superficial tibiospring and tibiocalcaneal components of the deltoid complex [Figure 2a and b]. In addition, an usual form of cubonavicular coalition was found [Figure 2c and d].

Tarsal coalition is a developmental anomaly when there is the failure of mesenchymal separation of tarsal bones, causing an abnormal connection between two or more of the tarsal bones. They tend to be bilateral in 50%–80% of the population and are inherited in an autosomal dominant pattern.[11,12] The quoted incidence of tarsal coalition ranges from 1% to 13%.[13,14] These can be cartilaginous (synchondrosis); fibro-osseous with or without ligamentous attachments (syndesmosis) or osseous (synostosis). The most common form of tarsal coalition are calcaneonavicular and talocalcaneal coalitions which together comprise 90% of all coalitions.[12,13] Rarer types of coalitions include calcaneocuboid, talonavicular, navicular-medial cuneiform, and cuneiform-metatarsal.[15-18] They can be asymptomatic or a cause of midfoot pain, particularly in the athletic adolescent population when ossification is near but not yet complete. Coalitions can lead to disordered biomechanics, hindfoot valgus, loss of the longitudinal arch, and increase in the frequency of ankle sprains.[19]

CN coalition is rare (1%) with only 38 cases described in the literature, 10 of which were osseous coalitions.[16] The case series in the literature describes clinical findings for both osseous and nonosseous coalitions including decreased subtalar motion, pes valgus, and pain in the region of the cuboid and navicular.[20] Other authors have described osteoarthritis in joints adjacent to the CN coalition.[21]

If symptomatic, treatment for CN coalition may range from conservative measures (heel lifts, immobilization in short leg casts, and orthotics); surgical resection of the coalition (usually for the adolescent athlete), and hindfoot (subtalar or triple) arthrodesis.[22,23] The latter technique is usually reserved for older patients with secondary or adjacent osteoarthritis; failed resection or multiple sites of coalitions; with good results reported for both surgical techniques.[12,23,24]

Unfused Sternal Segment

Figure 3 is a case of 25-year-old male professional English Rugby League player who experienced a high impact front-on tackle during a game, resulting in immediate MSK pain to his

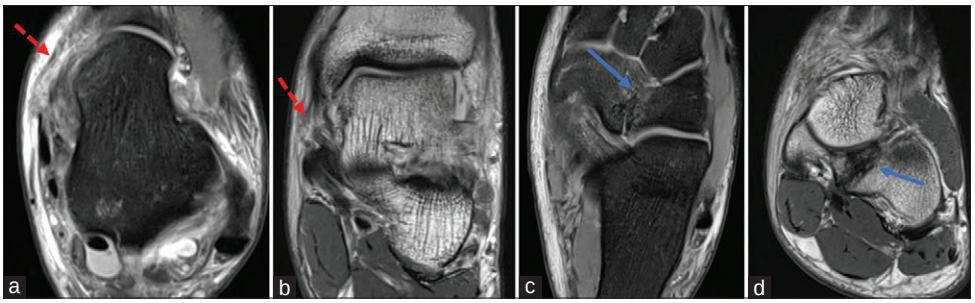

Figure 2: (a) Axial PD FS ankle. The high grade sprain of the tibiospring ligament is indicated by the dotted red arrow with surrounding soft tissue edema, (b) The red arrow indicates high grade sprain of the tibiocalcaneal component of the deltoid complex on PD coronal imaging, (c) The CN coalition is well seen on the fluid sensitive sequence as indicated by the blue arrow, with features of both synchondrosis more proximally and fibroosseous coalition more distally. The navicular articulates with the cuneiforms and the cuboid articulates normally with the lateral cuneiform and calcaneum, (d) Volumetric PD coronal imaging again demonstrates the CN coalition at the blue arrow with features of mixed type of coalition. FS: Fat saturation, PD: Proton density

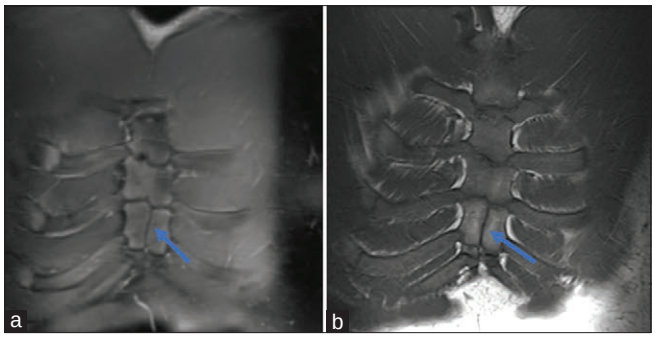

Figure 3: (a and b) Are coronal imaging fluid sensitive and T1 sequences respectively, demonstrating the unfused vertical segmentation of segment 3 with otherwise normal horizontal and vertical segmentation

chest. He underwent MRI to assess the extent of chest wall injury. Marrow signal was normal without features of osseous contusion or fracture of the chest wall. Examination of the sternum revealed an incidental unfused third sternal segment.

The sternum develops from the two bars of mesenchymal tissue on either side of the midline. These bars unify, and then undergo chondrification and ossification sequentially. There are ossification centers at the manubrium, mesosternum, and xiphyoid process. The mesosternum (body of the sternum) usually forms as four individual segments which may have either one or two ossification centers each.[25] The ossification centers of each segment usually fuse in the midline, known as 'horizontal fusion' and then undergo 'vertical fusion' with the subjacent segments (manubrium and xiphoid) to form the mature sternum. The Ashley classification for mesosternum ossification centers is based on the autopsy samples and describes four main patterns of ossification [Table 1].[26]

In a case series of 262 CTs of patients under 30, the oldest male patients with unfused sternal segments were 19 years old and oldest female patients with unfused segments were 8 years old, with more frequent persistent vertical segmentation noted in males (29.7% vs. 15% of females).[27] In our described case, our patient was 25 years old with an unfused segment, which is older than the cases in the described series. Unfused horizontal segments are also referred to as sternal clefts in the literature

Table 1: Ashley classification of mesosternum ossification centers[26]

Type I	Segments 1, 2, 3 have single ossification centers
Type II	Segment 1 has single ossification center, Segment 3 has two ossification centers
Type III	Segments 1, 2, 3 have two ossification centers
Type IV	Segment 1 has two ossification centers and Segment 3 has a single ossification center

and have been associated with congenital heart disease and other defects, such as ectopia cordis.[28,29] In our case, there were no other known birth defects or other medical issues, so his unfused sternal segment 3 was an incidental finding.

At the more severe end of the spectrum, unfused horizontal segmentation of the manubrium or of the more proximal segments of the mesosternum or more complete sternal clefts can expose the mediastinal contents.[30] It is important for the MSK radiologist to be aware of other sternal variants such as pseudoclefts, sternal foramina, sclerotic bands, focal sternal notches, varieties of xiphoid endings, and persistent xiphoid cartilage, so that these are not mistaken for pathology such as fractures.[30]

Normal Muscle Variants

Accessory head of gastrocnemius

A 22-year-old male professional footballer presented with extensive postmatch knee swelling but without any identifiable mechanism of injury. MRI revealed a large volume of intermuscular hemorrhage in the posterior compartment of the knee [Figure 4a]. The dynamic and static stabilizers of the knee were intact and there was no meniscus or chondral injury. The speculated cause was traumatic injury to a posterior geniculate or popliteal branch vessel which may or may not have been related to the incidental finding of an an accessory or third head of the gastrocnemius muscle [Figure 4b].

The third head of gastrocnemius was originally described by several anatomists' case reports in the 1800s.[31,32] Frey

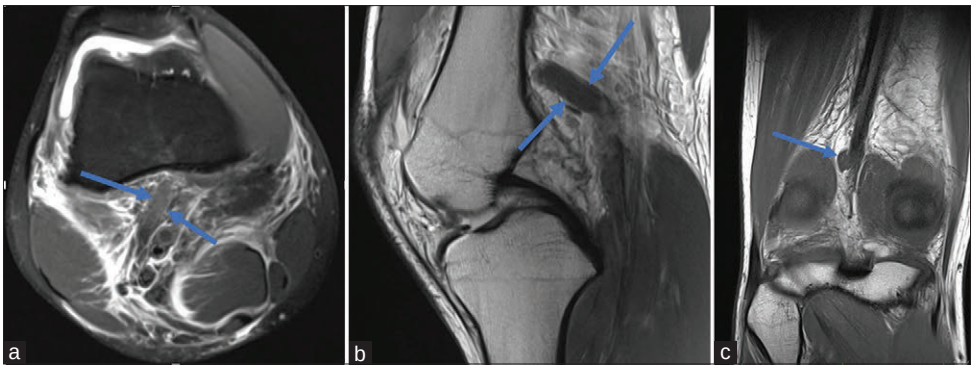

Figure 4: (a) Demonstrating a large volume of hemorrhage within the posterior compartment and the midline-crossing accessory head of gastrocnemius (blue arrows), (b) Sagittal PD imaging of the knee demonstrating the accessory head of gastrocnemius arising at the medial epicondyle of the femur, (c) Coronal PD view demonstrates the accessory head crossing the midline and located lateral to the popliteal neurovascular bundle. This anatomical arrangement has been described as potentially leading to popliteal vessel entrapment syndrome. PD: Proton density

described other variants with the potential to compress the popliteal neurovascular bundle due to the third head crossing the midline to insert onto either the medial or lateral head of gastrocnemius.[33] This is the anatomical arrangement that was seen in our case [Figure 4c]. An ipsilateral third head could also compress the popliteal artery/vein against the ipsilateral head of gastrocnemius prior to its insertion on the posterior ipsilateral femoral condyle; or there may be a bulky belly of the third head of gastrocnemius which could compress the vessels but still insert on the ipsilateral side. These variations emphasize that the third head does not need to cross the midline in order to cause compression or vascular compromise. Koplas *et al*. described a series of 1039 knee MRIs with an overall frequency of 2% of a third head of gastrocnemius.[34] 1.9% of the cases had a third head originating from the lateral head of gastrocnemius and coursing lateral to the popliteal vessels without claudication symptoms.

Since the knee is a commonly injured and imaged joint in the general and athletic populations, it is important for the MSK radiologist to be aware of the accessory head of gastrocnemius, given the possibility of symptomatic findings such as potential popliteal artery or venous entrapment. In our case, we postulated that the significant hemorrhage could potentially be related to a branch of the inferior geniculate artery that may have been compromised by the accessory head crossing the midline. This, however, has not been previously described in the literature. Once the swelling had resolved the player was quickly back to training and competition without any functional deficit and has not had a further similar presentation.

Articularis Genu

Figure 5 is a case of a 24-year-old male professional footballer undergoing bilateral knee imaging as a presigning scan. MRI imaging of both knees revealed bilateral incidental articularis genu (AG) muscles (blue arrows and right knee only shown).

Prior cadaveric studies described it as "flat, wispy and highly variable"[35,36] muscle, but this has been refuted by later cadaveric-MRI correlation studies that describe the AG as having from 3 to 6 muscle bundles with deep (originating from the femur) and superficial layers (originating from the vastus intermedius). They found that the superficial layer originated from the vastus intermedius aponeurosis and that there was no fascia separating the vastus intermedius from the AG. The deep layers were also difficult to separate from vastus intermedius proximally. However, there is ongoing ambiguity in the literature regarding the origin of the AG, with authors traditionally considering only the deep component (i.e. those layers that arise from the femoral shaft and blend with the joint capsule) as being the AG. All cadaveric-MRI studies to date agree that the medial part of vastus intermedius, vastus medialis and AG have shared innervation from the medial deep division of the femoral nerve. Together, the three muscles work synergistically as a functional unit during knee extension to retract the suprapatellar bursa.

Caterson *et al*. performed a further cadaveric and MRI correlation which also found AG to be a separate, substantial component of the anterior compartment that was clearly identified on preoperative MRI and could be used as an adequate anterior soft tissue cover in cases of resection of the distal femur with neoplastic infiltration and may thus offer an option for sparing the bulk of the quadriceps during resection.[37] In the case depicted, the distal AG is clearly seen a separate structure at the level of the quadriceps insertion with three muscle bundle, medial most prominent [Figure 5a] but blends with the vastus medialis on the axial and coronal imaging [Figure 5b and c].

Incidental Osseous Findings

Fibrous cortical defect

A 14-year-old male academy soccer player had MRI performed at 2 weeks after he sustained a direct medial knee injury. His symptoms were not resolving and as he complained of medial instability, there was concern for medial ligamentous injury. MRI showed an unstable osteochondritis dessicans lesions, a discoid lateral meniscus, and a fibrous cortical defect in the proximal tibial metaphysis [Figure 6a-c].

Fibrous cortical defects or nonossifying fibromas are the most common fibrous lesion of bone, predominantly seen in children

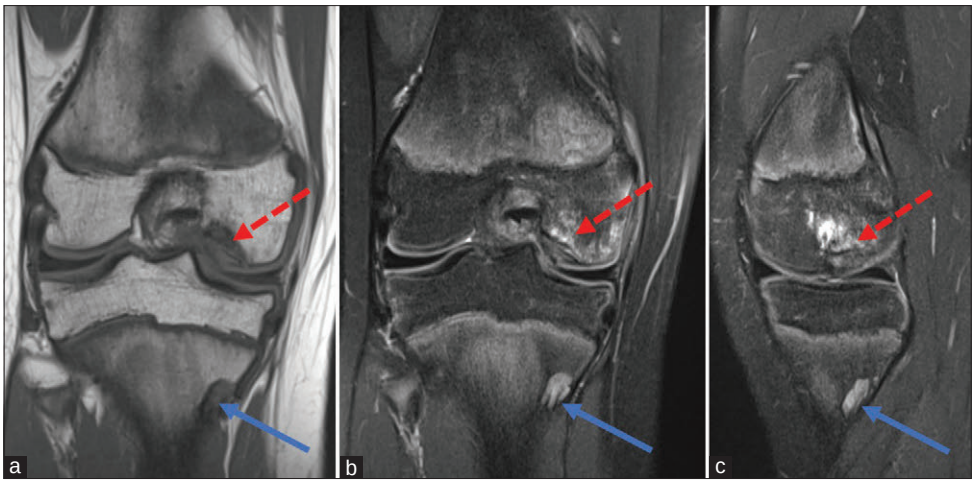

Figure 5: (a and b) T1 and PD FS coronal imaging depicting the focus of osteochondritis dissecans in the medial femoral condyle with features of instability (red dotted arrow) and the incidental fibrous cortical defect (blue arrow), (c) Sagittal PD FS image demonstrating the unstable osteochondritis dissecans (red dotted arrow) and the T2 hyperintense, well defined, fibrous cortical defect adjacent to the posterior cortex of the tibia (blue arrow) without aggressive features or osseous edema. FS: Fat saturation, PD: Proton density

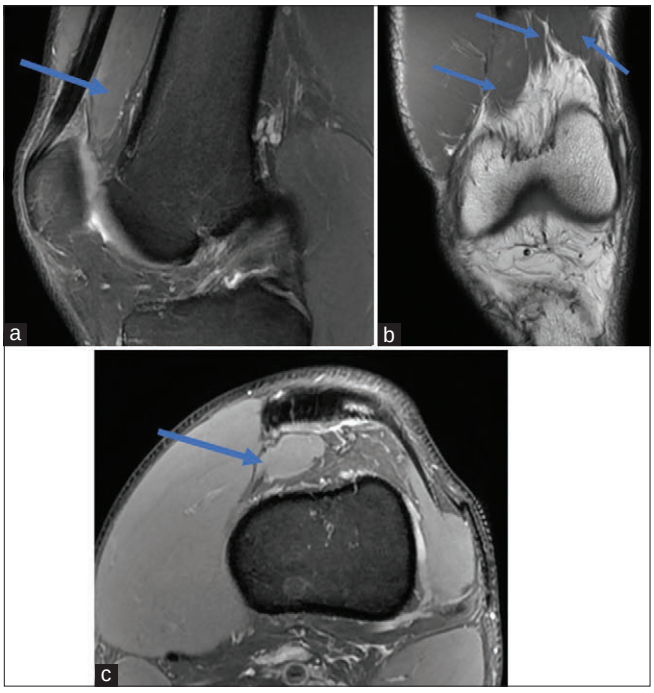

Figure 6: (a) Sagittal PD FS image demonstrating the AG in the suprapatellar fossa abutting the anterior femoral cortex and extending to the suprapatellar bursa (blue arrow).(b) Coronal T1 FSE imaging: Blue arrows depicting the multiple bundles of AG. Lack of intervening fascia can be appreciated between AG and vastus medialis. Figure 5c: Axial PD FS imaging demonstrating suprapatellar and low lying location of AG (blue arrow). AG: articularis genu. FS: Fat saturation PD: Proton density

and adolescents and are usually asymptomatic. On radiographs, these typically appear as an eccentric cortical based lucent focus with thin sclerotic margins. Enlarging lesions can demonstrate scalloping or extend into the medullary region.

When identified incidentally on MRI usually performed for another reason, these lesions can show low to intermediate T1 and intermediate to high T2 signal. There can be enhancement with gadolinium.

Most lesions undergo spontaneous involution and can show sclerosis or remodeling, which can appear as low signal intensity on MRI.[38,39]

Biopsy, intervention, and surgery in small fibrous cortical defects should be avoided and follow-up imaging is not usually necessary unless symptomatic.

Pathological fractures can rarely complicate lesions larger than 3 cm in weight-bearing bones. If the lesion is large involving more than 50% of the medullary cavity, if there is cortical breach or lack of a neocortex on CT, it may be worth considering orthopedic referral for pre-emptive treatment with curettage and grafting.[38,40]

Intraosseous lipoma

A 32-year-old male pro soccer player had MRI done for suspected medial deltoid ligamentous injury following a game. The MRI showed an acute grade 2 partial tear of the deep and superficial portions of the deltoid ligament with surrounding oedema [Figure 7a and b]. An incidental calcaneal intraosseous lipoma with partial cystic degeneration was also demonstrated [Figure 7c and d].

Intraosseous lipomas are frequently found in the lower extremities, the calcaneus is the most commonly reported site. They are usually incidental asymptomatic lesions, and dull pain is the most common symptom if lesions are symptomatic. They may contain thin septa and various amounts of fat, fibrous tissue, cystic degeneration or bone which result in a range of radiographic and MRI appearances.[41]

The Milgram staging system suggests the radiographic findings reflect the sequential histopathologic progression of intraosseous lipomas as:

- Stage 1: Absence of necrosis; well demarcated homogenous fatty lesions;
- Stage 2: Predominantly fatty lesions with partial necrosis and dystrophic calcification
- Stage 3: Heterogenous lesions with necrosis, cystic transformation, calcification or reactive new bone formation.[42]

In some cases the peripheral rim of fatty tissue may appear heterogenous with fibrous elements, or fibrovascular septa within the fat may demonstrate enhancement.

In soft tissue lipomas the heterogenous appearances and enhancement may cause concern, but are acceptable in intraosseous lipomas as they reflect varying fibrous elements, ischaemia or necrosis.[43-45]

Osteoid osteoma

A 22 year old male professional soccer player underwent a pre-signing study. Prior MRI (not available) had shown edema related to the left L2 pars, for which the patient had been treated for pars stress response. CT was then performed to exclude a fracture, which confirms a nidus of an osteoid osteoma (blue arrow) on Figure 8a and b.

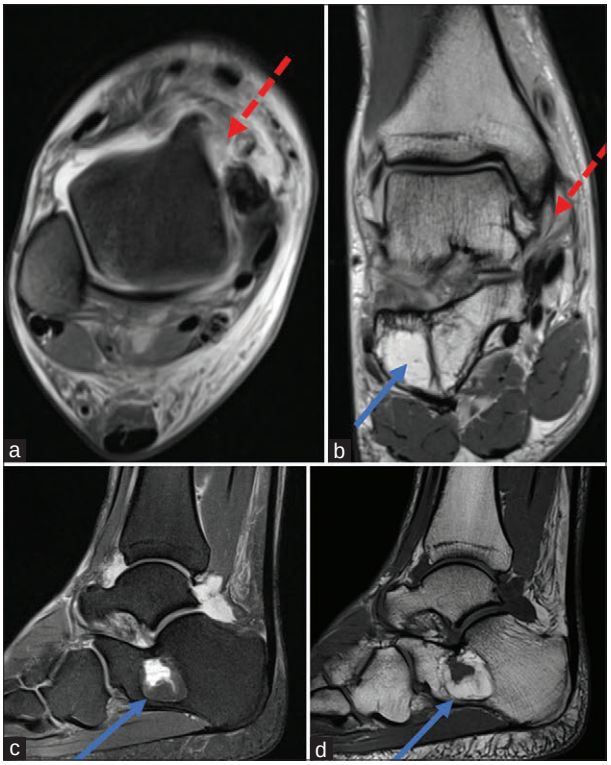

Figure 7: (a and b) PD FS axial and T1 FSE coronal imaging of the ankle demonstrating grade 2 partial tear of the deep and superficial components of the deltoid ligament (red dotted arrows). The blue arrow in Fig 7b denotes the partially visualized intra-osseous lipoma. (c) Sagittal PD FS imaging demonstrates a well defined focus in the body of the calcaneum with heterogenous internal signal (blue arrow). (d) T1 FSE sagittal imaging demonstrates that the fat components are similar intensity in signal to the marrow fat, with partial cystic degeneration appreciated as T2 hyperintense and T1 hypointensity centrally within the lesion. FSE: Fast spin echo; FS: Fat saturation; PD: Proton density

Treatment options for osteoid osteoma include conservative management with NSAIDS, percutaneous ablation, surgical curettage or excision.[46]

Back pain in young athletes can also be caused by spondylolysis which occur as a defect of pars interarticulars usually in the lower lumbar levels.

MRI in both conditions usually show bone marrow oedema and thin slice CT or volumetric T1 vibe MRI sequences are useful to detect the nidus with various degrees of surrounding sclerosis, or to visualise the pars defect.

If the osteoid osteoma nidus is very tiny or if the lytic defects are subtle in early stage spondylolysis, it can be challenging to differentiate between the two conditions if the sclerosis at the pars interarticularis is the only finding.[47,48]

Extra-Musculoskeletal Findings

Duplex kidney

This is a case of a 15 year old female soccer footballer who was experiencing shooting pain from her left SI joint to her left gluteal region to hip. MRI imaging of her lumbar spine and pelvis demonstrated grade 2 incomplete pars fractures of both L5 [Figure 9a] and osseous stress response in the left ischial tuberosity apophysis (apophysitis) [Figure 9b]. Scout imaging from those exams also demonstrated an enlarged left duplex kidney [Figure 9c].

Congenital upper renal tract anomalies account for 50% of all congenital abnormalities; with duplex kidney having an incidence of 12%–15% in the general population with two thirds being associated with anomalies of other major organ systems.[49] Ureteropelvic duplications are defined as the presence of two separate pelvicalyceal systems within one kidney and may be discovered during the neonatal period or are usually incidentally discovered (as in this case) and are asymptomatic. Occasionally they are discovered due to a complication. Duplex kidneys, along with other abnormalities

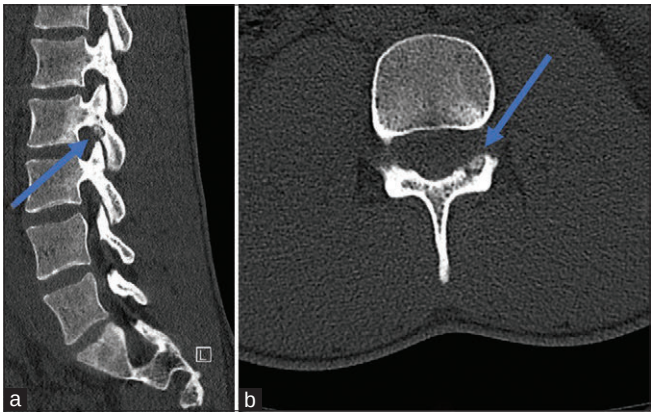

Figure 8: (a) Sagittal CT of the lumbar spine shows the nidus of the osteoid osteoma within the L2 pars, (b) Axial CT of the L2 vertebral body at its inferior aspect demonstrates the osteoid osteoma. CT: Computed tomography

Figure 9: (a) Coronal STIR imaging. Incomplete bilateral grade 2 pars fractures of L5 (red dotted arrows), (b) Axial PD FS imaging of the pelvis demonstrates osseous stress response and apophysitis at the left ischial tuberosity (red dotted arrow), (c) Coronal Scout imaging demonstrating a duplex left pelvicalyceal system (blue arrow). FS: Fat saturation

of the developing urinary collection system (such as pyelocaliceal diverticulum, megacalycosis, megaureter, ectopic ureter amongst others) are related to defects in the embryological development of the ureteric bud starting during the 5th week of gestation.[50] Pelvicalyceal duplication may be either complete or incomplete. Complete systems each have their own ureter, whereas incomplete systems refer to fusion of the ureters proximal to the level of the ureteropelvic junction.[51]

Investigations for duplex kidney include CT and/or MR Urography to confirm complete or incomplete duplication and ureteric trajectory. Voiding cystoureterogram and/or functional nuclear medicine imaging is used to look for differential functioning, reflux, or scarring.

Treatment will depend on the presence of complications and extent of anomalies; and include ureteric reimplantation or resection.

Manifestations of Systemic Conditions

Crohn's disease

A 36-year-old male professional soccer player with a history of Crohn's disease had presigning imaging of the hips, knees, and hamstrings. He was completely asymptomatic at the time of imaging. MRI imaging demonstrated moderate insertional quadriceps tendinosis and prepatellar bursitis [Figure 10a]. The pelvic MRI scan shows a perianal fistula [Figure 10b and c], best seen on the fluid sensitive sequences. No previous scans were available for comparison at the time of reporting. There was no involvement of the sacroiliac joints.

Perianal fistulas occur in 30% of individuals diagnosed with luminal Crohn's disease and can be difficult to treat, with significant associated morbidity compared to patients without perianal disease including effects on the quality of life.[52,53] Treatment is usually a combination of systemic anti-tumor necrosis factor agents and surgical therapy.[54] Recent advances include the use of allogenic bone marrow-derived mesenchymal stem cell therapy.[55] MRI pelvis with a dedicated small field of view and specialized planes provides the most detailed overview including complexity, size and number of tracts; associated abscesses; and disease involving the levator ani musculature, rectum, and lymphadenopathy.[56]

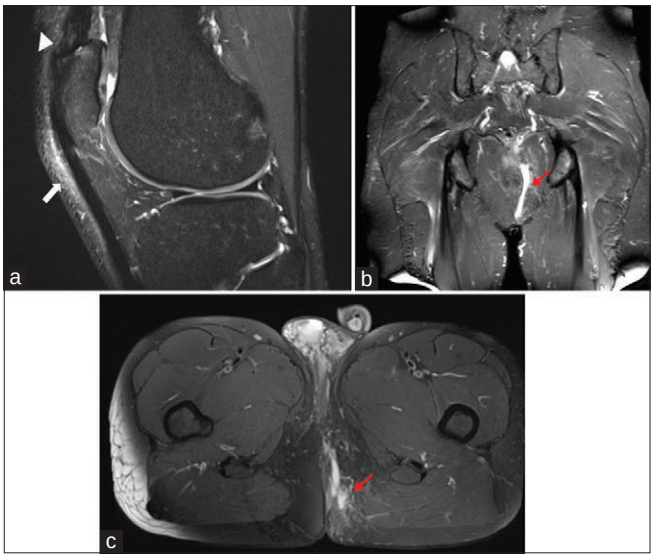

Figure 10: (a) PD FS sagittal imaging demonstrating moderate insertional quadriceps tendinosis (white arrowhead) and minimal prepatellar bursitis (white block arrow). (b) Coronal STIR imaging demonstrating the perianal fistula extending to the level of the ischial tuberosity (red arrow). (c) Axial PD FS axial imaging demonstrating the T2 hyperintense fistula within the left ischiorectal fossa (red arrow). FS: Fat saturation

It is also used to evaluate the success of posttreatment tract closure and persistent internal tracts which are not always clinically appreciable.[57] It is important to bear in mind that MRI parameters (such as contrast enhancement) do not always consistently correlate with clinical remission.[58] In this case, the quadriceps tendinosis may have been related to his Crohn's disease; a result of his professional athletic career or a combination of both.

Psoriatic Arthropathy

A 19-year-old male professional soccer player had insidious onset of symptoms and was thought to have a stress injury. Initial foot MRI performed showed capsulitis and joint effusion [Figure 11a] which was thought to be related to an injury however was an atypical location for an isolated finding. He responded in the short term to an image-guided corticosteroid injection. Four months following the initial presentation, he developed persistent pain and repeat MRI

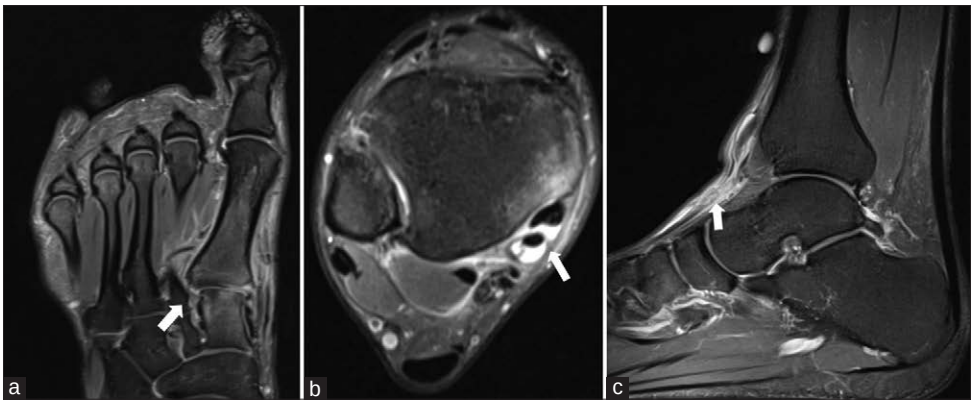

Figure 11: (a) Coronal PD FS image depicting the capsulitis and joint effusion centered at the first tarsometatarsal joint of the left foot (white block arrow). (b) Axial PD FS imaging performed 4 months later demonstrating subenthesial osseous edema in the posteromedial tibia and tenosynovitis of the posterior tibialis tendon and flexor digitorum longus tendon (white block arrow). (c) Sagittal PD FS performed 9 months after initial presentation demonstrating an acute rupture of the anterior tibialis tendon (white block arrow). FS: Fat saturation

showed tenosynovitis of tibialis posterior and subenthesial osseous edema at the level of the posterior tibia [Figure 11b].

He was then reviewed by a rheumatologist who made a diagnosis of psoriatic arthritis. Methotrexate systemic treatment was commenced. Five months following the commencement of therapy, he developed a tear of tibialis anterior tendon [Figure 11c].

Whenever the imaging findings in athletes do not correspond to the clinical working diagnosis, other differentials should be considered such as underlying systemic disease; inflammatory arthropathies; or infectious causes.[59]

Conclusion

This narrative review has demonstrated a multitude of various findings that might be encountered when imaging the professional athletic population for acute injury or for presigning imaging. Other examples in our collection which have not been pictorially depicted in this review include chronic pelvoureteric junction obstruction on a pre-signing scan, spermatic cord lipoma and inguinal hernia in a football player with acute myosseous avulsion of the adductor magnus; incidental gallstone in a case of acute 9th rib costochondral cartilage fracture; calcaneal cyst in a soccer player with metatarsal stress fracture, amongst many others.

These case examples stress the importance of reviewing all of the relevant sequences acquired during imaging, including scout imaging and avoiding the commonly cited error of "satisfaction of search" in diagnostic radiology. The cases also highlight the utility of the experienced MSK radiologist, who, although specialized in sports imaging, is well versed with other pathologies and findings encountered outside of the MSK system and can thus aid in directing appropriate onward management for these athletes.

Financial support and sponsorship

Nil.

Conflicts of interest

There are no conflicts of interest.

References

1. Berland LL. Overview of white papers of the ACR Incidental Findings Committee II on adnexal, vascular, splenic, nodal, gallbladder, and biliary findings. J Am Coll Radiol 2013;10:672-4.
2. Hitzeman N, Cotton E. Incidentalomas: Initial management. Am Fam Physician 2014;90:784-9.
3. O'Sullivan JW, Muntinga T, Grigg S, Ioannidis JP. Prevalence and outcomes of incidental imaging findings: Umbrella review. BMJ 2018;361:k2387.
4. Sexton SM. How should we manage incidentalomas? Am Fam Physician 2014;90:758-9.
5. Forsythe B, Knapik DM, Crawford MD, Diaz CC, Hardin D, Gallucci J, Silvers-Granelli HJ, Mandelbaum BR, Lemak L, Putukian M, Giza E. Incidence of Injury for Professional Soccer Players in the United States: A 6-Year Prospective Study of Major League Soccer. Orthop J Sports Med. 2022;10:23259671211055136. doi: 10.1177/23259671211055136.
6. Walls RJ, Ross KA, Fraser EJ, Hodgkins CW, Smyth NA, Egan CJ, *et al*. Football injuries of the ankle: A review of injury mechanisms, diagnosis and management. World J Orthop 2016;7:8-19.
7. Shortt CP. Magnetic resonance imaging of the midfoot and forefoot: Normal variants and pitfalls. Magn Reson Imaging Clin N Am 2010;18:707-15.
8. Gyftopoulos S, Bencardino JT. Normal variants and pitfalls in MR imaging of the ankle and foot. Magn Reson Imaging Clin N Am 2010;18:691-705.
9. Serfaty A, Pessoa A, Antunes E, Malheiro E, Canella C, Marchiori E. Bipartite medial cuneiform: Magnetic resonance imaging findings and prevalence of this rare anatomical variant. Skeletal Radiol 2020;49:691-8.
10. Elias I, Dheer S, Zoga AC, Raikin SM, Morrison WB. Magnetic resonance imaging findings in bipartite medial cuneiform – A potential pitfall in diagnosis of midfoot injuries: A case series. J Med Case Rep 2008;2:272.
11. Leonard MA. The inheritance of tarsal coalition and its relationship to spastic flat foot. J Bone Joint Surg Br 1974;56B: 520-6.
12. Jackson TJ, Mathew SE, Larson AN, Stans AA, Milbrandt TA. Characteristics and reoperation rates of paediatric tarsal coalitions: A population-based study. J Child Orthop 2020;14:537-43.
13. Stormont DM, Peterson HA. The relative incidence of tarsal coalition. Clin Orthop Relat Res. 1983;(181):28-36.
14. Park JJ, Seok HG, Woo IH, Park CH. Racial differences in prevalence and anatomical distribution of tarsal coalition. Sci Rep

2022;12:21567.
15. Craig CL, Goldberg MJ. Calcaneocuboid coalition in Crouzon's syndrome (craniofacial dysostosis): Report of a case and review of the literature. J Bone Joint Surg Am 1977;59:826-7.
16. Macera A, Teodonno F, Carulli C, Frances Borrego A, Innocenti M. Talonavicular coalition as a cause of foot pain. Joints 2017;5:246-8.
17. Malone JB, Raney EM. Bilateral navicular-medial cuneiform synostosis manifesting as medial foot pain: A case report and review of the literature. J Pediatr Orthop B 2016;25:138-41.
18. Stevens BW, Kolodziej P. Non-osseous tarsal coalition of the lateral cuneiform-third metatarsal joint. Foot Ankle Int 2008;29:867-70.
19. Bohne WH. Tarsal coalition. Curr Opin Pediatr 2001;13:29-35.
20. Kummer A, Dugert E, Jammal M. Complete cubonavicular coalition associated with midfoot osteoarthritis. Case Rep Orthop 2020;2020:8850768. [doi: 10.1155/2020/8850768].
21. Ehredt DJ Jr., Zulauf EE, Kim HM, Connors J. Cryopreserved amniotic membrane and autogenous adipose tissue as an interpositional spacer after resection of a cubonavicular coalition: A case report and review of the literature. J Foot Ankle Surg 2020;59:173-7.
22. Vincent KA. Tarsal coalition and painful flatfoot. J Am Acad Orthop Surg 1998;6:274-81.
23. Sarage AL, Gambardella GV, Fullem B, Saxena A, Caminear DS. Cuboid-navicular tarsal coalition: Report of a small case series with description of a surgical approach for resection. J Foot Ankle Surg 2012;51:783-6.
24. Saxena A, Allen R, Wright A, Migliorini F, Maffulli N. Tarsal coalition resections: A long-term retrospective analysis of 97 resections in 78 patients. J Orthop Surg Res 2022;17:458.
25. Delgado J, Jaimes C, Gwal K, Jaramillo D, Ho-Fung V. Sternal development in the pediatric population: Evaluation using computed tomography. Pediatr Radiol 2014;44:425-33.
26. Ashley GT. The relationship between the pattern of ossification and the definitive shape of the mesosternum in man. J Anat 1956;90:87-105.
27. Gumeler E, Akpinar E, Ariyurek OM. MDCT evaluation of sternal development. Surg Radiol Anat 2019;41:281-6.
28. Restrepo CS, Martinez S, Lemos DF, Washington L, McAdams HP, Vargas D, *et al*. Imaging appearances of the sternum and sternoclavicular joints. Radiographics 2009;29:839-59.
29. Abel RM, Robinson M, Gibbons P, Parikh DH. Cleft sternum: Case report and literature review. Pediatr Pulmonol 2004;37:375-7.
30. Yekeler E, Tunaci M, Tunaci A, Dursun M, Acunas G. Frequency of sternal variations and anomalies evaluated by MDCT. AJR Am J Roentgenol 2006;186:956-60.
31. Bryce TH. Notes on the myology of a Negro. J Anat Physiol 1897;31:607-18.
32. Turner W. Notes on the dissection of a third Negro. J Anat Physiol 1897;31:624-6.
33. Frey H. Musculus gastrocnemius tertius. Gegenbaurs Morphol Jahrb 1919;50:517-30.
34. Koplas MC, Grooff P, Piraino D, Recht M. Third head of the gastrocnemius: An MR imaging study based on 1,039 consecutive knee examinations. Skeletal Radiol 2009;38:349-54.
35. Kimura K, Takahashi Y. M. articularis genus. Observations on arrangement and consideration of function. Surg Radiol Anat 1987;9:231-9.
36. Reider B, Marshall JL, Koslin B, Ring B, Girgis FG. The anterior aspect of the knee joint. J Bone Joint Surg Am 1981;63:351-6.
37. Caterson J, Williams MA, McCarthy C, Athanasou N, Temple HT, Cosker T, *et al*. The articularis genu muscle and its relevance in oncological surgical margins. Bone Jt Open 2020;1:585-93.
38. Betsy M, Kupersmith LM, Springfield DS. Metaphyseal fibrous defects. J Am Acad Orthop Surg 2004;12:89-95.
39. Błaż M, Palczewski P, Swiątkowski J, Gołębiowski M. Cortical fibrous defects and non-ossifying fibromas in children and young adults: The analysis of radiological features in 28 cases and a review of literature. Pol J Radiol 2011;76:32-9.
40. Goldin AN, Muzykewicz DA, Mubarak SJ. Nonossifying fibromas: A computed tomography-based criteria to predict fracture risk. J Pediatr Orthop 2020;40:e149-54.
41. Elias I, Zoga AC, Raikin SM, Schweitzer ME, Morrison WB. Incidence and morphologic characteristics of benign calcaneal cystic lesions on MRI. Foot Ankle Int 2007;28:707-14.
42. Levy DM, Gross CE, Garras DN. Treatment of unicameral bone cysts of the calcaneus: A systematic review. J Foot Ankle Surg 2015;54:652-6.
43. Campbell RS, Grainger AJ, Mangham DC, Beggs I, Teh J, Davies AM. Intraosseous lipoma: Report of 35 new cases and a review of the literature. Skeletal Radiol 2003;32:209-22.
44. Milgram JW. Intraosseous lipomas: Radiologic and pathologic manifestations. Radiology 1988;167:155-60.
45. Murphey MD, Carroll JF, Flemming DJ, Pope TL, Gannon FH, Kransdorf MJ. From the archives of the AFIP: Benign musculoskeletal lipomatous lesions. Radiographics 2004;24:1433-66.
46. Beyer T, van Rijswijk CS, Villagrán JM, Rehnitz C, Muto M, von Falck C, *et al*. European multicentre study on technical success and long-term clinical outcome of radiofrequency ablation for the treatment of spinal osteoid osteomas and osteoblastomas. Neuroradiology 2019;61:935-42.
47. Tawfik S, Phan K, Mobbs RJ, Rao PJ. The incidence of pars interarticularis defects in athletes. Global Spine J 2020;10:89-101.
48. Viana SL, Viana MA, de Alencar EL. Atypical, unusual, and misleading imaging presentations of spondylolysis. Skeletal Radiol 2015;44:1253-62.
49. Barakat AJ, Drougas JG. Occurrence of congenital abnormalities of kidney and urinary tract in 13,775 autopsies. Urology 1991;38:347-50.
50. Fernbach SK, Feinstein KA, Spencer K, Lindstrom CA. Ureteral duplication and its complications. Radiographics 1997;17:109-27.
51. Campo I, Sertorio F, Wong M, Anfigeno L, Bertolotto M, Mattioli G, *et al*. Magnetic resonance urography of congenital abnormalities – What the radiologist needs to know. Pediatr Radiol 2022;52:985-97.
52. Brochard C, Rabilloud ML, Hamonic S, Bajeux E, Pagenault M, Dabadie A, *et al*. Natural history of perianal Crohn's disease: Long-term follow-up of a population-based cohort. Clin Gastroenterol Hepatol 2022;20:e102-10.
53. Mak WY, Mak OS, Lee CK, Tang W, Leung WK, Wong MT, *et al*. Significant medical and surgical morbidity in perianal Crohn's disease: Results from a territory-wide study. J Crohns Colitis 2018;12:1392-8.
54. Present DH, Rutgeerts P, Targan S, Hanauer SB, Mayer L, van Hogezand RA, *et al*. Infliximab for the treatment of fistulas in patients with Crohn's disease. N Engl J Med 1999;340:1398-405.
55. Barnhoorn MC, Wasser MN, Roelofs H, Maljaars PW, Molendijk I, Bonsing BA, *et al*. Long-term evaluation of allogeneic bone marrow-derived mesenchymal stromal cell therapy for Crohn's disease perianal fistulas. J Crohns Colitis 2020;14:64-70.
56. Vasudevan A, Bruining DH, Loftus EV Jr., Faubion W, Ehman EC, Raffals L. Approach to medical therapy in perianal Crohn's disease. World J Gastroenterol 2021;27:3693-704.
57. Bell SJ, Halligan S, Windsor AC, Williams AB, Wiesel P, Kamm MA. Response of fistulating Crohn's disease to infliximab treatment assessed by magnetic resonance imaging. Aliment Pharmacol Ther 2003;17:387-93.
58. Lee T, Yong E, Ding NS. Radiological outcomes in perianal fistulizing Crohn's disease: A systematic review and meta-analysis. JGH Open 2020;4:340-4.
59. Kin-Hoo Koo K, Chinoy H, Creaney L, Hayton M. Inflammatory arthropathy in the elite sports athlete. Curr Sports Med Rep 2021;20:577-83.

Review Article

Musculoskeletal Magnetic Resonance Imaging Revisited – Does Tesla of Magnetic Resonance Imaging Machines Matter?

Simranjeet Kaur, Bernhard J. Tins, Naomi Winn, Kartik P. Ganga[1]

Department of Radiology, Robert Jones and Agnes Hunt Orthopaedic Hospital NHS, Oswestry, [1]Department of Radiology, Hull University Teaching Hospital NHS Trust, Hull, UK

Abstract

The field of modern medical science has been revolutionized by magnetic resonance imaging (MRI) which is the preferred modality for the investigation of a whole spectrum of musculoskeletal (MSK) conditions. MRI is a careful interplay between the temporal, spatial, and contrast resolution which forms the foundation for its improved diagnostic performance and value. There are a lot of aspects that improve the image quality and diagnostic performance, however, a higher magnet strength of 3-Tesla has the biggest impact within the current diagnostic range. However various advancements in the hardware and software parameters such as multichannel multi-phased array coils, advanced gradient systems and better post processing techniques have significantly improved image quality at 1.5T scanners as well. All the leading manufacturers offer MRI systems with a higher field strength of 3T which are increasingly being used in recent clinical settings. Scanning at 3T has the advantage of a better signal-to-noise ratio which translates into better spatial and temporal resolution with the added advantage of faster acquisition. Challenges of 3T scanning include higher magnetic susceptibility, chemical shift, and higher radiofrequency energy deposition. This is particularly important in the presence of orthopedic implants because of the two-fold increase in susceptibility artifacts resulting in significant periprosthetic signal loss, signal displacements with voids and pileups, and failed spectral fat suppression. Various modifications are needed to minimize the artifacts at 3T scanners to better utilize the improved spatial and contrast resolution achieved as a result of scanning at a higher field strength. This review discusses the technical features of scanning at 1.5 and 3T scanners along with their clinical implications and diagnostic usefulness in MSK imaging.

Keywords: 1.5T, 3T, magnetic resonance imaging, musculoskeletal imaging, musculoskeletal magnetic resonance imaging

Introduction

Ever since its inception in mid-1970s, magnetic resonance imaging (MRI) has revolutionized the field of medical practice. It is the imaging modality of choice for the investigation of a whole gamut of musculoskeletal (MSK) conditions and diseases. It has evolved into the cornerstone imaging technique for sports and orthopedics by providing highly accurate information for detection, characterization, surveillance, and monitoring of a huge spectrum of MSK conditions.[1,2] One of the attributes that sets MSK MRI apart from other radiological investigations including radiography, ultrasound, and computed tomography (CT), is the ability for multiplanar imaging and excellent soft tissue and contrast resolution which permits the differential display of submillimeter MSK structures.[3,4]

MSK MRI is all about a fine interplay between the spatial, temporal, and contrast resolution which translates into better image quality and is the foundation for its improved diagnostic value and performance.[5] Conventionally, most MRI imaging was done at 1.5 Tesla, but higher field strength imaging at 3T has become increasingly common in the recent clinical settings. There have been many advancements in the software and hardware aspects of MRI to improve diagnostic efficiency, however, a 3T magnet strength has the maximum impact within the present diagnostic range. A higher field strength of 3T, when coupled with the advent of high-end surface coils, advanced multichannel receiver coils, high-performance radiofrequency (RF) pulse transmission, and gradient systems

Access this article online

Quick Response Code:

Website: https://journals.lww.com/jajs

DOI: 10.4103/jajs.jajs_15_23

Address for correspondence: Dr. Simranjeet Kaur, Department of Radiology, Robert Jones and Agnes Hunt Orthopaedic Hospital NHS, Oswestry, SY10 7AG, UK.
E-mail: simranjeet.kaur5@nhs.net

Submitted: 16-Feb-2023 **Revised:** 16-Mar-2023
Accepted: 17-Mar-2023 **Published:** 19-Jul-2023

This is an open access journal, and articles are distributed under the terms of the Creative Commons Attribution-NonCommercial-ShareAlike 4.0 License, which allows others to remix, tweak, and build upon the work non-commercially, as long as appropriate credit is given and the new creations are licensed under the identical terms.

For reprints contact: WKHLRPMedknow_reprints@wolterskluwer.com

How to cite this article: Kaur S, Tins BJ, Winn N, Ganga KP. Musculoskeletal magnetic resonance imaging revisited – Does tesla of magnetic resonance imaging machines matter? J Arthrosc Jt Surg 2023;10:110-7.

yields additional gains. Scanning at a high field strength however comes with its own set of problems such as chemical shift, magnetic susceptibility, and increased RF deposition. Most of the improvements in MRI are extremely beneficial clinically, improving the image quality and diagnostic confidence, but often need certain modifications depending on different clinical situations to make the best use of the advanced technology.

A Basic Primer of Magnetic Resonance Physics for Musculoskeletal Magnetic Resonance Imaging

Signal-to-noise ratio

The signal-to-noise ratio (SNR) is the value-defining currency of MSK MRI.[5] It is a complex interplay between the magnetic strength, volume of tissue, and RF coil being used.[6] However, the predominant determinant for SNR is the strength of the static magnetic field (B0), which indirectly then determines the spatial, temporal, and contrast resolution. Theoretically, speaking doubling, the static field strength should double the SNR, but because of the variation in T1 relaxation times and the complexities of the RF coils, the increase in SNR is slightly less than double.[7]

SNR is directly proportional to the voxel volume and square root of phase encoding steps and number of averages. Increasing the number of phase steps and averages increases the SNR but at the same time increases the time of acquisition. Scanning at 3T enables four times faster acquisition as compared to 1.5T, thereby reducing scan times, and allowing for a high SNR without increasing the scan time. Faster acquisition and reduced scan times are particularly beneficial in claustrophobic, pediatric, and seriously ill patients whom stay still for longer durations in a problem. Faster scanning at 3T results in lesser artifacts as patients' motion is minimized, resulting in fewer recalls. It increases the patient's throughput with faster and efficient workflow without sacrificing diagnostic confidence.

The SNR also depends on the number of excitations and is proportional to the square root of number of excitations. Therefore, doubling the SNR at 3T enables quadrupling the number of excitations allowing for an effective utilization of the acceleration techniques and parallel imaging acquisitions for faster two-dimensional (2D) and three-dimensional (3D) pulse sequences.[8,9] The two-fold increase in SNR on a 3T scanner also allows for doubling the matrix size to achieve the same SNR as 1.5-T keeping other parameters constant. The increase in SNR can then be translated into thinner slice acquisitions at 3.0T.[5] The contrast resolution is often higher on a 3T scanner because the modulation of the T1 and T2 constants results in a larger gap between the T2 decay and T1 recovery maps, translating into better contrast between various tissues.

In order to make the maximum use of the increased SNR on a 3T scanner, the field-dependent changes in the tissue relaxation times should be considered. The T1 relaxation times are prolonged at 3T as compared to 1.5T and for most tissue types this increase is approximately 10%–30%.[6,10,11] The T1 of cartilage is 1060 milliseconds (ms) at 1.5T and increases by 14.5% to 1240 milliseconds (ms) at 3T. The T1 relaxation times of subcutaneous fat increase by more than 20% from 288 msonds to 371 msonds at 1.5 and 3T, respectively. There is a tendency for shortening of T2 times by approximately 10% to 15% when scanning at 3T versus 1.5 T.,[6,12] The change in these values affects the choice of time to repeat (TR) and time to echo (TE) on a 3T scanner and influences the range of the contrast difference needed to image the underlying tissues. In order to optimize the signal gain and tissue contrast at 3T, the pulse sequences on a 3T scanner need a longer TR to allow for the longitudinal magnetization to adequately recover and a shorter TE as the T2 constants are shorter. The increased time incurred because of longer TR can be offset by using longer echo trains and acceleration techniques such as parallel imaging, partial phase Fourier sampling, and simultaneous multi-slice acquisition.[8,9]

Resonance frequency

The Larmor frequency depends on and is proportional to the static magnetic field and the gyromagnetic ratio (which is a constant for H proton in water). Thereby, by doubling the magnetic field strength from 1.5T to 3T, the Larmor frequency also doubles increasing from 63.9 MHz to 127.7 MHz. In order to selectively excite the H protons in water, the RF pulse applied should have a frequency equivalent to the Larmor frequency. At 3T the frequency of the RF pulse is doubled which in turn quadruples the energy deposited as compared to 1.5T. The Food and Drug Administration has set a legal limit for the whole body for a time period of 15 min to 4W/kg and 12W/kg for extremities over a period of 5 min.[13,14] These limits can often be reached when fast multi-slice spin echo sequences are used, therefore caution must be exercised while using these sequences.

Chemical shift effects

Type I chemical shift artifacts refer to the frequency displacement in the frequency encoding direction because of the differing precession frequencies of the H proton in water and fat molecule. The difference in the precession frequency is directly proportional to the magnetic field strength, thereby doubling at 3T. This is problematic in spin echo sequences which are most used in MSK applications. Doubling the bandwidth is one way of resolving this problem. It not only solves the problem of chemical shift but also allows for an increased number of slices, shortens the TE, and reduces echo spacing.[7] However, increasing the bandwidth shortens the window length for signal readout, thereby reducing the SNR by square root of two.

Susceptibility artifacts

There is a microscopic variation in the magnetic field that occurs at the interfaces between materials of different magnetic susceptibility. These artifacts are proportional to the magnetic field strength and therefore are higher at 3T as compared to 1.5T. Different materials have different susceptibilities to become magnetized which produces a secondary magnetic field which in turn causes local derangements in the main magnetic field-these derangements to determine the extent of

the susceptibility artifact. During routine MSK imaging, such interfaces with different magnetic susceptibility are much less common (except when orthopedic implants are present) and B0 shimming can be effectively performed for small MSK parts like the peripheral joints. Furthermore, the traditional Spin Echo sequences that are used routinely in MSK imaging are less affected by susceptibility. However, the situation becomes complicated in the presence of orthopedic implants. There is a huge difference in the susceptibility between the native tissue and the implanted material resulting in significant artifacts which are further increased in 3T scanners. Iron, cobalt, and nickel are ferromagnetic materials which cause a greater disturbance in the magnetic field as compared to newer implants made of titanium and other paramagnetic substances. With an increasing aging population, there is an increasing utilization of orthopedic implants, which further increases the need for imaging of patients with these implants. Novel materials such as carbon-fiber-reinforced-polymers have been developed which have been shown to cause a further reduction in the susceptibility artifacts.[15]

1.5T versus 3T – Applications

Large joints imaging

The increased SNR, spatial and temporal resolution at 3T translates into a better depiction of ligaments, tendons, fascicles, and cartilage.[16] However, despite this theoretical benefit, 2 out of 3 MRI scanners that are sold currently are still 1.5T.[17]

There is an ongoing debate regarding the image quality for MSK imaging as 3T MRI is not without limitations as compared to 1.5T. This is likely because the same advancements that have helped 3T to revolutionize MSK imaging have also led to significant improvements in image quality at 1.5T as well.

Few studies suggest that for diagnosing various ligamentous and meniscal pathologies 1.5T is as accurate as a 3T scanner. A meta-analysis for assessing lesions of the knee found the specificity of 70% and sensitivity of 85% for 3.0T MRI detection of articular cartilage lesions and a greater diagnostic accuracy.[18] Another study compared a 5-min knee MRI acquisition using simultaneous multi-slice and parallel imaging acceleration on both 1.5T and 3T magnetic strength which found no difference in the detection rate of meniscal and ligamentous tears. However, there was a higher detection rate for partial thickness cartilage defects at 3T.[19]

Other studies have similarly shown that 3T MRI is superior for acetabular cartilage defects, whereas there is no difference in the diagnostic accuracy of 3T MRI versus 1.5T MR arthrography (MRA) for the for acetabular labral tears.[20,21] Another meta-analysis showed that the high-field MRA had the highest accuracy for diagnosing rotator cuff tears followed by low-field MRA, high-field conventional MRI, high-frequency ultrasound, low-field MRI, and finally low frequency ultrasound.[22] Another meta-analysis showed 3T MRA has increased sensitivity and specificity as compared to 3T MRI for the detection of labral pathology in the shoulder [Figure 1].[23] Thus, there is no clear evidence regarding the advantage of one field strength over the other.

Small joints

There is no difference in the detection rate of fractures, osteomyelitis, and bone marrow edema in small extremity joints between a 1.5T and a 3T scanner. There is however a definite advantage of increased spatial and contrast resolution and a high SNR in 3T magnets for the evaluation of thin articular cartilage and delicate ligamentous structures.[24] 3T is also more beneficial in evaluating small anatomic structures such as annular pulleys of the finger, triangular fibrocartilage complex, and the intrinsic and extrinsic ligaments of the wrist [Figure 2].

Spine

MRI is pivotal for evaluating the causes of back pain and is performed using both 1.5T and 3T scanners. The increased SNR at 3T renders it ideal for evaluating the neuroanatomic structures of the spine [Figure 3].[17] The conventional T1-weighted images in a 3T scan usually reveal suboptimal hypointensity of the cerebrospinal fluid (CSF). This is due to the incomplete suppression of CSF at 3T caused by the longer T1 relaxation times and can be solved by adding a fluid-attenuated inversion recovery pulse.[25]

3D volumetric MRI plays a significant role in MSK imaging with the advantage of increasing through-plane resolution and generating high-quality multiplanar reformations from the original dataset. Volume interpolated breath-hold examination (VIBE) uses fast 3D gradient echo sequences producing T1 images with high-quality multiplanar reconstruction. VIBE sequence at 3T is beneficial in spine as it provides a high-resolution isotropic data set which can be used for multiplanar reconstruction with the added benefit of reduced susceptibility to magnetic field inhomogeneities and pulsation artifacts because of shorter echo times [Figure 4]. A study concluded that thin slice 3D T1 VIBE is 100% accurate in detecting complete pars stress fractures and a high diagnostic accuracy in diagnosing and characterizing incomplete pars stress fractures as compared to CT. It also had the added benefit of depicting bone marrow edema and is of particular interest in the younger population as it does not use ionizing radiation.[26]

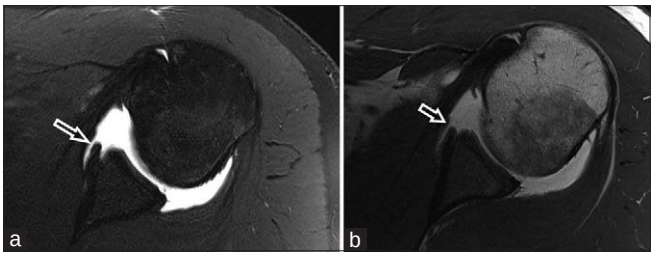

Figure 1: (a) Axial FS T1 and (b) Axial T1 image on a 3T scanner after intra-articular contrast injection depicts tear of the anteroinferior labrum along with the periosteal stripping and avulsion (white arrow) FS: Fat-saturated

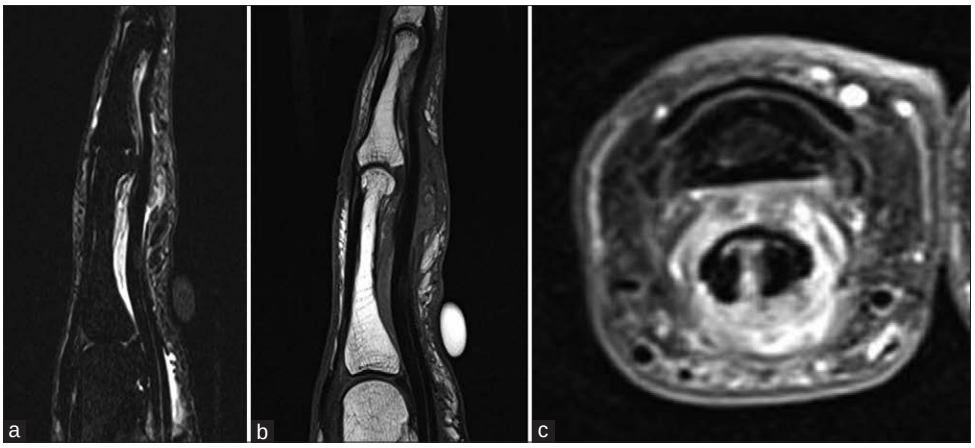

Figure 2: (a) Sagittal PD FS, (b) Sagittal T1 and (c) Axial PD FS image of left index finger at a 3T scanner demonstrating flexor tenosynovitis. There is improved spatial and contrast resolution at 3T scanner, and it is superior in depicting smaller delicate structures like the finger pulleys, intrinsic and extrinsic wrist ligaments, and the thin articular cartilage in small joints. PD: Proton density, FS: Fat-saturated

Figure 3: (a) Sagittal T1 and (b) Sagittal T2 weighted image of lumbosacral spine acquired at a 3T magnet shows good evaluation of the neuroanatomic structures of the spine

Whole body magnetic resonance imaging

Whole-body MRI is used for screening and surveillance of patients with Li Fraumeni syndrome,[27] neurofibromatosis and schwannomatosis,[28,29] multiple myeloma,[30] chronic recurrent multifocal osteomyelitis[31] and detection of metastasis in patients with liposarcoma. 1.5T scanners were preferred for whole-body MRIs because of their lower dielectric and susceptibility artifacts. However, the new 3T scanners allow for a high-resolution multiparametric acquisition of a whole-body MRI in 30–40 min.[28,29]

Magnetic resonance imaging neurography

Imaging protocols for MR neurography include 2D and 3D T1 or intermediate weighted sequences, T2-weighted sequences with fat suppression, and diffusion-weighted pulse sequences. Studies have shown that high-quality imaging of the brachial plexus is possible using a 3T scanner resulting in higher SNR and contrast-to-noise ratio (CNR) as compared to 1.5T scanner [Figure 5]. But it does not translate into improved diagnostic performance as pathological findings were seen equally well with both field strengths.[32] However, in the presence of orthopedic implants such as hip arthroplasty, cervical spine instrumentation, neurography done at 1.5T is beneficial because of the decrease in magnetic susceptibility and field heterogeneity.

Orthopedic hardware imaging

One of the most challenging tasks while using a 3T scanner is imaging in the presence of metallic orthopedic implants. Implants lead to a twofold increase in susceptibility resulting in local field distortions causing periprosthetic signal loss, signal displacements with areas of signal voids, pile-ups, and failed spectral fat suppression.

Gradient echo imaging of soft tissues in these cases is virtually impossible since the magnetic field inhomogeneity results in rapid spin dephasing resulting in more severe signal voids. Spin echo sequences are preferred because of the refocussing pulse results in rephasing of spins reducing areas of signal voids, although the spatially dependent artifacts will still be present. Fat saturation is another problem with hardware imaging as the magnetic field inhomogeneity almost always results in failure of fat suppression. Novel/newer sequences such as iterative decomposition of water and fat with echo asymmetry and least-squares estimation is more reliable than fat saturation, as field inhomogeneities can be corrected to a certain degree during reconstruction.

Compressed sensing acceleration refers to under-sampling of sparse k regions and using dedicated reconstruction algorithms to recover the missing data. This results in faster acquisition and retains more SNR as compared to other techniques like parallel imaging while scanning metal implants.[33] The compressed sensing space encoding metal artifact correction (SEMAC) developed by Siemens is a turbo spin echo sequence (TSE) that allows for an eight-fold reduction of metal artifacts of MRI hip.[34,35] It combines the view angle tilting (VAT) principle with additional phase encoding steps in the slice encoding direction to reduce the slice selective distortions. In VAT a gradient is

applied on the slice during readout of an equal magnitude to the slice select gradient. This results in re-registration of the spins thereby reducing the in-plane distortion artifacts. Using high bandwidth RF pulses in the range of 4000 Hz as compared to conventional 850 Hz can also help in reducing thought plane artifacts allowing for fewer SEMAC-encoding steps [Figure 6].[36] This allows all relevant contrasts to be obtained at a level of artifact comparable to 1.5T with the added benefit of improved image quality at 3T scanner.

Multi-acquisition variable-resonance image combination is another novel technique developed by GE to minimize artifacts around metallic prosthesis which uses multiple different overlapping volumes at different frequency offsets.

Quantitative magnetic resonance imaging imaging

There is a lot of ongoing research on the quantitative compositional analysis of the cartilage, and it is now known that early physiological changes in the cartilage matrix occur in asymptomatic osteoarthritis (OA). As the cartilage undergoes degeneration there is increased permeability which increases the intrinsic water content and motion. The hydrodynamic pressure builds up and increased stress is generated through the cartilage matrix resulting in degeneration of the proteoglycan-collagen matrix and cartilage loss.

The T2 relaxation time depends on the water content and the proteoglycan-collagen matrix. T2 and T2*(T2* is only used in this quantitative MRI section) mapping are quantitative MRI biomarkers which can detect early cartilage degeneration, by detecting areas of increased water content and collagen network disruption [Figure 7]. A multi-spin echo sequence is used most frequently to reduce scan times and signal levels are matched to one or more decaying exponentials, depending on the number of T2 distributions thought to be in the sample.[7] The long acquisition times often result in low resolution in conventional T2 mapping. The modern T2 mapping techniques available at 3.0T help in faster, more accurate, and high resolution which is specific absorption rate (SAR)-compliant.[37-39]

Miscellaneous

3T scanning allows for the multiparametric assessment of bone and soft tissue tumors using fast 3D sequences. The 3D spoiled gradient echo sequence such as VIBE for delayed post-contrast T1 imaging is advantageous over 2D conventional TSE sequences because of faster acquisition, high SNR, and high isotropic resolution allowing for multiplanar reformats.[40]

The chemical shift MRI with its "in" and "opposed" phase imaging is especially valuable in spine imaging to differentiate between neoplastic marrow replacing infiltration and benign conditions such as edema or hematopoietic marrow. A signal drop of <20% on 1.5T and <25% on 3T is suggestive of a neoplastic marrow-replacing lesion.[41,42]

At 3T, the opposed-phase images should be acquired before the in-phase images because of the enhanced susceptibility artifacts on subsequently acquired opposed-phase images. This can result in over-exaggeration of the signal drop.[43]

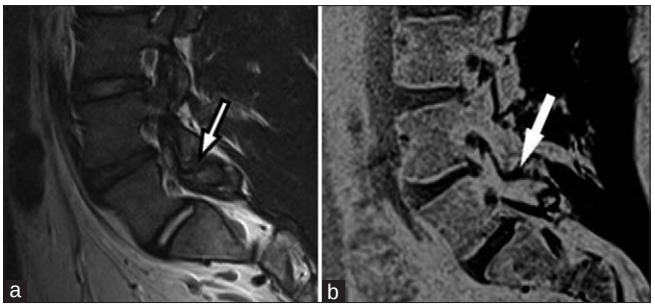

Figure 4: (a) Sagittal T2 weighted image in a young boy with back pain raised the suspicion of a pars defect (black lined arrow) in L5. (b) Sagittal T1 VIBE sequence on a 3T MRI demonstrates normal cortical anatomy (white arrow) with no evidence of any fracture, thus obviating the need for a CT. VIBE: Volume interpolated breath hold examination, MRI: Magnetic resonance imaging, CT: Computed tomography

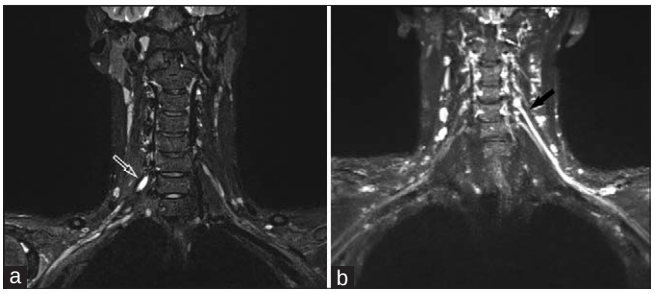

Figure 5: (a) Coronal T2 STIR sequence on a 3T scanner for brachial plexus imaging depicting the pseudo-meningocele formation (white lined arrow) in relation to the right C7 nerve root. (b) Coronal T2 STIR MIP image in another patient depicts the increased signal intensity with mild thickening of the left C5 nerve root(black arrow) in a patient with traction injury of the brachial plexus. STIR : Short tau inversion recovery, MIP: Maximum intensity projection

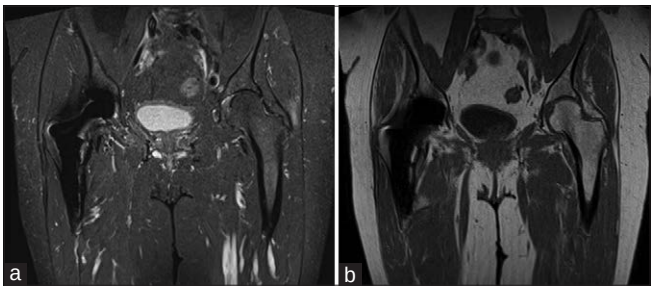

Figure 6: (a) Coronal STIR and (b) Coronal T1 weighted image with high bandwidth and metal artefact reduction techniques depict excellent anatomy with significant reduction of the artifacts

As discussed previously, T1 values increase in the order of approximately 20% when using a 3T MRI scanner. The T1 shortening effect of the gadolinium is however not affected by the field strength.[18,44] As a result, there is an increased contrast between the enhanced and the unenhanced tissue on 3T scanner.[45] This can be used to reduce the dose of the gadolinium-based contrast agents while maintaining the same CNR.

There is no straight answer to which scanner (1.5T or 3T) is better and one size does not fit all. The choice of scanner depends on a lot of factors as to which body part is being

imaged, presence or absence of any metallic implant, safety of the implant, clinical indication, advanced and quantitative imaging, and cost pressures. Table 1 summarizes the differences between the two scanners including the respective advantages and disadvantages.

Higher Field Strengths

In 2017, the first 7T MRI machine was given regulatory approval for clinical use for neuro and MSK applications.[46,47] Ultrahigh field scanners provide the advantage of further improvements in resolution, faster acquisition times, and significant improvement in signal gain. However, increased RF deposition and magnetic field inhomogeneity pose a considerable problem for ultrahigh field scanning. Neuro and MSK imaging are the two areas of interest for ultra-high field scanning. With the increase in burden of OA and the significant morbidity associated with the disease, there is a strong demand for identifying early changes in the cartilage that would later progress to OA, allowing early intervention.

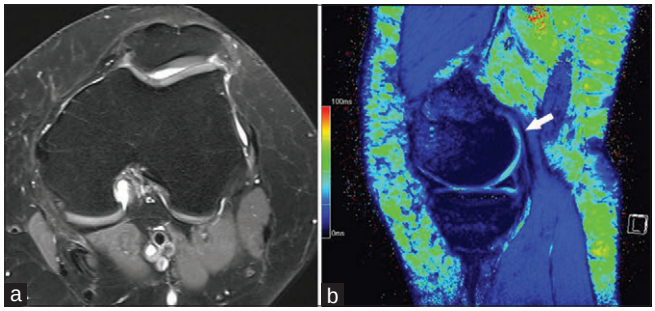

Figure 7: (a) Axial PD FS on a 3 T scanner show normal signal characteristic and thickness of the cartilage overlying the dorsal femoral condyles. (b) Sagittal T2 mapping depict focal area of increased water content (white arrow) in the cartilage overlying the dorsal medial femoral condyle. PD: Proton density, FS: Fat-saturated

Ultrahigh field scanners allow for qualitative MRI imaging like T2, T2*, T1rho mapping, sodium imaging, chemical exchange saturation transfer, and spectroscopy.[48] These techniques along with high SNR allow for the biochemical and metabolic tissue characterization. The clinically approved 7T scanners will revolutionize the future of medical imaging.

Magnetic strengths of more than 7 Tesla have been used to conduct studies on diffusion MRI with improved SNR, spatial resolution, and contrast-to-noise ratio. Most of these studies have been conducted on small mammals and *ex vivo* tissues and are relevant to neurosciences for visualization of white matter pathways and structural connectivity.[49]

The University of Minnesota, in 2018 became the first university in the world to conduct MRI of human body at 10.5T.[50] It is a 110-magnet which can produce images with sub-millimeter resolution, finer detail and can be pivotal for new discoveries. Its focus is on the imaging of the brain to conduct research into its working for better understanding and treatment of neurological diseases such as Alzheimer's and Parkinson's.

Low Field Magnetic Resonance Imaging

Imaging at low (<0.5T) and medium (0.5–1T) strength scanners is characterized by an expected reduction in SNR.[51] There is no doubt that the high-field scanners produce better-quality images, but this does not necessarily translate into better

Table 1: Differences between 1.5T and 3T MRI scanner

Attribute	1.5T scanner	3T scanner
Image quality	Lower SNR	Higher SNR
Artifacts	Fewer artifacts	Comparatively more artifacts especially susceptibility and chemical shift artifacts
Specific absorption rate	Less	More. Legal limits can sometimes be reached while using multi-slice spin echo sequences on a 3T scanner
Speed of scanning/throughput	Slower as compared to 3T scanner. Scan times can be shortened but at the expense of SNR/image quality	Overall shorter scanning times with increased patient throughput
Cost	Lower as compared to 3T	Significantly expensive
MSK specific differences		
Large joints	Although lower SNR, but the recent advancements have significantly improved image quality on a 1.5T scanner with comparable diagnostic accuracy	Theoretically speaking better definition of cartilage, labrum and ligaments
Small joints	No difference in detection rate of fractures, osteomyelitis and bone marrow oedema as compared to 3T	Definite advantage in evaluating small anatomic structures like annular pulleys of fingers, triangular fibrocartilage complex and intrinsic and extrinsic wrist ligaments
Whole body MRI	Long acquisition time	Faster with high resolution multiparametric acquisition
MRI neurography	In presence of cervical instrumentation or hip arthroplasty, neurography at 1.5T is beneficial because of the magnetic susceptibility and field heterogeneity	Better quality images, but does not translate into better diagnostic performance
Orthopaedic hardware imaging	More implants are safer to scan	Not all implants are compatible or safe at 3T
Quantitative imaging	1.5 T aren't the preferred scanners for quantitative imaging	Faster and more accurate

SNR: Signal to noise ratio, MSK: Musculoskeletal, MRI: Magnetic resonance imaging

diagnostic power. The tremendous advancements and improvements in RF systems, gradients, and application of artificial intelligence (AI) allow the acquisition of diagnostically adequate MRI using low-field scanners without compromising efficiency and patient throughput. These scanners are beneficial in MSK radiology for scanning of extremities. These extremity scanners are smaller with lower purchase and maintenance costs. They are also easy to install in a limited space and help in faster patient diagnosis. This is particularly important in patients with occult bony injuries on plain radiographs in which a delayed diagnosis can cause a detrimental delay in treatment.[51] These scanners are also better tolerated by children and patients with claustrophobia. It is helpful in imaging metallic implants and for interventional procedures as many of the devices can be used on the low-field scanners without the need for costly modifications.[52] Low-field MRI combined with the AI-based postprocessing has the potential to open up new fields of application in a cost-effective manner.

Upright Magnetic Resonance Imaging

A conventional MRI is a static examination which is not able to diagnose dynamic pathologies which are often masked in a static position. This is of particular importance in case of imaging of spine. The spine is a complex dynamic structure whose loading characteristics change with the position of the patient and the direction and type of force applied.[53] The conventional MRI is unable to provide any information on the biomechanical causes of pain. This can be offset using upright MRI or weight-bearing MRI. Although the magnet is of low field strength, the advantages of scanning the patient in upright weight-bearing position far outweigh the disadvantages of a lower field strength. This can detect dynamic problems like anterolisthesis which can become more apparent on sitting and even more exaggerated in flexion, dynamic spinal stenosis, and symptomatic synovial cyst fluctuating between flexion and extension.[54] Idiopathic juvenile scoliosis is another condition that can be assessed using weight-bearing MRI. Supine MRI does not show the full extent of scoliosis and proper radiological assessment is made with the patient standing. Standing MRI can be helpful in these patients as it can be performed quickly with the patient standing and without the use of ionizing radiation.

Conclusion

Good quality MSK MRI imaging involves a careful interplay and negotiation between temporal, spatial, and contrast resolution. 3T magnets excel in producing images with a high SNR, but magnet strength is only one of the parameters that improve image quality in MSK imaging. There are various other hardware and software advancements that work in unison to increase image quality and diagnostic accuracy. Hardware and software parameters such as dedicated multichannel, multielement transmit-receive extremity coils, coils with integrated analog-digital signal, sophisticated sequence design and built-in AI influence spatial resolution and image quality at all field strengths. It is worthwhile to note that a newer well-equipped 1.5T MRI with a dedicated coil and advanced sequence technology can outperform an old 3T scanner. Another debate which remains unresolved is whether the improved diagnostic accuracy at 3T in-fact translates into clinical relevance for the orthopedic and trauma surgeons.

The biggest strength of a 3T scanner is its speed of acquisition with the increased SNR. It can acquire high-quality images in a short duration of time allowing for an improved throughput and efficient workflow. It also allows for advanced imaging such as diffusion-weighted imaging, diffusion tensor imaging, Quantitative MRI to be acquired in realistic time frames. There is a continuous need for further advancements and developments in both hardware and software to improve the field of imaging. The 3T MRI scanner is beneficial for improved image quality and diagnostic accuracy but often requires certain modifications to optimize and better utilize the advantages of a high field scanning.

Financial support and sponsorship

Nil.

Conflicts of interest

There are no conflicts of interest.

References

1. Ahlawat S, Fritz J, Morris CD, Fayad LM. Magnetic resonance imaging biomarkers in musculoskeletal soft tissue tumors: Review of conventional features and focus on nonmorphologic imaging. J Magn Reson Imaging 2019;50:11-27.
2. Fritz B, Parkar AP, Cerezal L, Storgaard M, Boesen M, Åström G, *et al.* Sports imaging of team handball injuries. Semin Musculoskelet Radiol 2020;24:227-45.
3. Coris EE, Zwygart K, Fletcher M, Pescasio M. Imaging in sports medicine: An overview. Sports Med Arthrosc Rev 2009;17:2-12.
4. Hynes JP, Walsh J, Farrell TP, Murray AS, Eustace SJ. Role of musculoskeletal radiology in modern sports medicine. Semin Musculoskelet Radiol 2018;22:582-91.
5. Khodarahmi I, Fritz J. The value of 3 tesla field strength for musculoskeletal magnetic resonance imaging. Invest Radiol 2021;56:749-63.
6. Gold GE, Han E, Stainsby J, Wright G, Brittain J, Beaulieu C. Musculoskeletal MRI at 3.0 T: Relaxation times and image contrast. AJR Am J Roentgenol 2004;183:343-51.
7. Shapiro L, Harish M, Hargreaves B, Staroswiecki E, Gold G. Advances in musculoskeletal MRI: Technical considerations. J Magn Reson Imaging 2012;36:775-87.
8. Fritz J, Guggenberger R, Del Grande F. Rapid musculoskeletal MRI in 2021: Clinical application of advanced accelerated techniques. AJR Am J Roentgenol 2021;216:718-33.
9. Del Grande F, Guggenberger R, Fritz J. Rapid musculoskeletal MRI in 2021: Value and optimized use of widely accessible techniques. AJR Am J Roentgenol 2021;216:704-17.
10. Wright PJ, Mougin OE, Totman JJ, Peters AM, Brookes MJ, Coxon R, *et al.* Water proton T1 measurements in brain tissue at 7, 3, and 1.5 T using IR-EPI, IR-TSE, and MPRAGE: Results and optimization. MAGMA 2008;21:121-30.
11. Gilligan LA, Dillman JR, Tkach JA, Xanthakos SA, Gill JK, Trout AT. Magnetic resonance imaging T1 relaxation times for the liver, pancreas and spleen in healthy children at 1.5 and 3 tesla. Pediatr Radiol 2019;49:1018-24.
12. Schick F, Pieper CC, Kupczyk P, Almansour H, Keller G, Springer F, *et al.* 1.5 versus 3 tesla magnetic resonance imaging: A review of favorite clinical applications For Both Field Strengths-Part 1. Invest Radiol 2021;56:680-91.
13. Shellock FG, Spinazzi A. MRI safety update 2008: part 2, screening

patients for MRI. AJR Am J Roentgenol 2008;191:1140-9.
14. Shellock FG, Crues JV. MR procedures: Biologic effects, safety, and patient care. Radiology 2004;232:635-52.
15. Zimel MN, Hwang S, Riedel ER, Healey JH. Carbon fiber intramedullary nails reduce artifact in postoperative advanced imaging. Skeletal Radiol 2015;44:1317-25.
16. Zhao J, Krug R, Xu D, Lu Y, Link TM. MRI of the spine: Image quality and normal-neoplastic bone marrow contrast at 3 T versus 1.5 T. AJR Am J Roentgenol 2009;192:873-80.
17. Runge VM, Heverhagen JT. Advocating the development of next-generation high-relaxivity gadolinium chelates for clinical magnetic resonance. Invest Radiol 2018;53:381-9.
18. Cheng Q, Zhao FC. Comparison of 1.5- and 3.0-T magnetic resonance imaging for evaluating lesions of the knee: A systematic review and meta-analysis (PRISMA-compliant article). Medicine (Baltimore) 2018;97:e12401.
19. Del Grande F, Rashidi A, Luna R, Delcogliano M, Stern SE, Dalili D, *et al*. Five-minute five-sequence knee MRI using combined simultaneous multislice and parallel imaging acceleration: Comparison with 10-minute parallel imaging knee MRI. Radiology 2021;299:635-46.
20. Chopra A, Grainger AJ, Dube B, Evans R, Hodgson R, Conroy J, *et al*. Comparative reliability and diagnostic performance of conventional 3T magnetic resonance imaging and 1.5T magnetic resonance arthrography for the evaluation of internal derangement of the hip. Eur Radiol 2018;28:963-71.
21. Magee T. Comparison of 3.0-T MR versus 3.0-T MR arthrography of the hip for detection of acetabular labral tears and chondral defects in the same patient population. Br J Radiol 2015;88:20140817.
22. Liu F, Dong J, Shen WJ, Kang Q, Zhou D, Xiong F. Detecting rotator cuff tears: A network meta-analysis of 144 diagnostic studies. Orthop J Sports Med 2020;8:2325967119900356.
23. Liu F, Cheng X, Dong J, Zhou D, Sun Q, Bai X, *et al*. Imaging modality for measuring the presence and extent of the labral lesions of the shoulder: A systematic review and meta-analysis. BMC Musculoskelet Disord 2019;20:487.
24. Rashidi A, Haj-Mirzaian A, Dalili D, Fritz B, Fritz J. Evidence-based use of clinical examination, ultrasonography, and MRI for diagnosing ulnar collateral ligament tears of the metacarpophalangeal joint of the thumb: Systematic review and meta-analysis. Eur Radiol 2021;31:5699-712.
25. Ganesan K, Bydder GM. A prospective comparison study of fast T1 weighted fluid attenuation inversion recovery and T1 weighted turbo spin echo sequence at 3 T in degenerative disease of the cervical spine. Br J Radiol 2014;87:20140091.
26. Ang EC, Robertson AF, Malara FA, O'Shea T, Roebert JK, Schneider ME, *et al*. Diagnostic accuracy of 3-T magnetic resonance imaging with 3D T1 VIBE versus computer tomography in pars stress fracture of the lumbar spine. Skeletal Radiol 2016;45:1533-40.
27. Consul N, Amini B, Ibarra-Rovira JJ, Blair KJ, Moseley TW, Taher A, *et al*. Li-fraumeni syndrome and whole-body MRI screening: Screening guidelines, imaging features, and impact on patient management. AJR Am J Roentgenol 2021;216:252-63.
28. Ahlawat S, Fayad LM, Khan MS, Bredella MA, Harris GJ, Evans DG, *et al*. Current whole-body MRI applications in the neurofibromatoses: NF1, NF2, and schwannomatosis. Neurology 2016;87:S31-9.
29. Ahlawat S, Blakeley JO, Langmead S, Belzberg AJ, Fayad LM. Current status and recommendations for imaging in neurofibromatosis type 1, neurofibromatosis type 2, and schwannomatosis. Skeletal Radiol 2020;49:199-219.
30. Hillengass J, Usmani S, Rajkumar SV, Durie BG, Mateos MV, Lonial S, *et al*. International myeloma working group consensus recommendations on imaging in monoclonal plasma cell disorders. Lancet Oncol 2019;20:e302-12.
31. Fritz J, Tzaribatchev N, Claussen CD, Carrino JA, Horger MS. Chronic recurrent multifocal osteomyelitis: Comparison of whole-body MR imaging with radiography and correlation with clinical and laboratory data. Radiology 2009;252:842-51.
32. Tagliafico A, Succio G, Emanuele Neumaier C, Serafini G, Ghidara M, Calabrese M, *et al*. MR imaging of the brachial plexus: Comparison between 1.5-T and 3-T MR imaging: Preliminary experience. Skeletal Radiol 2011;40:717-24.
33. Khodarahmi I, Fritz J. Advanced MR imaging after total hip arthroplasty: The clinical impact. Semin Musculoskelet Radiol 2017;21:616-29.
34. Jungmann PM, Bensler S, Zingg P, Fritz B, Pfirrmann CW, Sutter R. Improved visualization of juxtaprosthetic tissue using metal artifact reduction magnetic resonance imaging: experimental and clinical optimization of compressed sensing SEMAC. Invest Radiol 2019;54:23-31.
35. Fritz J, Fritz B, Thawait GK, Raithel E, Gilson WD, Nittka M, *et al*. Advanced metal artifact reduction MRI of metal-on-metal hip resurfacing arthroplasty implants: Compressed sensing acceleration enables the time-neutral use of SEMAC. Skeletal Radiol 2016;45:1345-56.
36. Bachschmidt TJ, Sutter R, Jakob PM, Pfirrmann CW, Nittka M. Knee implant imaging at 3 Tesla using high-bandwidth radiofrequency pulses. J Magn Reson Imaging 2015;41:1570-80.
37. Fritz J. T2 mapping without additional scan time using synthetic knee MRI. Radiology 2019;293:631-2.
38. Hilbert T, Sumpf TJ, Weiland E, Frahm J, Thiran JP, Meuli R, *et al*. Accelerated T (2) mapping combining parallel MRI and model-based reconstruction: GRAPPATINI. J Magn Reson Imaging 2018;48:359-68.
39. Hilbert T, Schulz J, Marques JP, Thiran JP, Krueger G, Norris DG, *et al*. Fast model-based T (2) mapping using SAR-reduced simultaneous multislice excitation. Magn Reson Med 2019;82:2090-103.
40. Ahlawat S, Morris C, Fayad LM. Three-dimensional volumetric MRI with isotropic resolution: Improved speed of acquisition, spatial resolution and assessment of lesion conspicuity in patients with recurrent soft tissue sarcoma. Skeletal Radiol 2016;45:645-52.
41. Disler DG, McCauley TR, Ratner LM, Kesack CD, Cooper JA. In-phase and out-of-phase MR imaging of bone marrow: Prediction of neoplasia based on the detection of coexistent fat and water. AJR Am J Roentgenol 1997;169:1439-47.
42. Kumar NM, Ahlawat S, Fayad LM. Chemical shift imaging with in-phase and opposed-phase sequences at 3 T: what is the optimal threshold, measurement method, and diagnostic accuracy for characterizing marrow signal abnormalities? Skeletal Radiol 2018;47:1661-71.
43. Del Grande F, Subhawong T, Flammang A, Fayad LM. Chemical shift imaging at 3 Tesla: Effect of echo time on assessing bone marrow abnormalities. Skeletal Radiol 2014;43:1139-47.
44. Pietsch H. Current and future MR contrast agents: Seeking a better chemical stability and relaxivity for optimal safety and efficacy. Invest Radiol 2020;55:589-91.
45. Del Grande F, Santini F, Herzka DA, Aro MR, Dean CW, Gold GE, *et al*. Fat-suppression techniques for 3-T MR imaging of the musculoskeletal system. Radiographics 2014;34:217-33.
46. EU Gives First Approval for Ultra-High-Field MRI Scanner, the Siemens Magnetom Terra | Medgadget. Available from: https://www.medgadget.com/2017/08/eu-gives-first-approval-ultra-high-field-mri-scanner-siemens-magnetom-terra.html. [Last accessed on 2023 Feb 06].
47. FDA Gives First Clearance to Siemens High-Field 7 Tesla MRI Scanner | Medgadget. Available from: https://www.medgadget.com/2017/10/fda-gives-first-clearance-high-field-7-tesla-mri-scanner.html. [Last accessed on 2023 Feb 06].
48. Juras V, Mlynarik V, Szomolanyi P, Valkovič L, Trattnig S. Magnetic resonance imaging of the musculoskeletal system at 7T: Morphological imaging and beyond. Top Magn Reson Imaging 2019;28:125-35.
49. Grier MD, Yacoub E, Adriany G, Lagore RL, Harel N, Zhang RY, *et al*. Ultra-high field (10.5T) diffusion-weighted MRI of the macaque brain. Neuroimage 2022;255:119200.
50. U Scientists Scan World's First 10.5-Tesla Human MRI Image. Available from: https://research.umn.edu/inquiry/post/u-scientists-scan-worlds-first-105-tesla-human-mri-image. [Last accessed on 2023 Mar 07].
51. Ghazinoor S, Crues JV 3rd, Crowley C. Low-field musculoskeletal MRI. J Magn Reson Imaging 2007;25:234-44.
52. Hennig J. Low-field magnetic resonance imaging: Just less expensive or completely different? Radiologe 2022;62:385-93.
53. Faruqi T, Padget W, Patel N. Utility of weight-bearing MRI in the lumbar spine: A novel indication. Cureus 2022;14:e23930.
54. Upright MRI-the Modern Way to Image the Spine. Available from: www.hse.gov.uk/press/2006/e06107.htm. [Last accessed 2023 Mar 07].

Review Article

Ultrasound-Guided Joint Injections: Tips and Tricks

Pablo Longhi Lorenzzoni, Sanjay Patel[1]

Med SBCR FRANZCR, I-MED Network, Brisbane, [1]MBBS, MRCR FRCR, FRANZCR, I-MED Network, Brisbane, Australia

Abstract

Joint injections have emerged as a crucial aspect of a radiologist's role, regularly employed for both diagnostic and therapeutic purposes. Ultrasound guidance is an invaluable tool in this regard, due to its accessibility, low cost, and absence of radiation. Pain relief through the use of corticosteroids, local anesthetics, or viscosupplements, joint aspiration in cases of suspected infection, and contrast injection for arthrography are all common indications for these procedures. In this article, we aim to provide guidance for common joint procedures (as well as one nonjoint but frequently performed procedure) while also revealing some valuable trade secrets and tips.

Keywords: Hyaluronic acid, joint injections, MSK procedures, pain treatment, steroid, ultrasound guided

Introduction

One of the most honorable objectives of the medical profession is to alleviate human suffering and pain, which is considered a fundamental duty of physicians, even in cases where all available treatment options have been exhausted. In contemporary medicine, a variety of drugs are readily available to facilitate this goal, and their delivery methods have become increasingly precise. As radiologists, one of the most gratifying aspects of our job is utilizing our knowledge of pathology and anatomy, as well as our technical expertise, to achieve this noble goal. Ultrasound remains the most commonly used modality due to its real-time, radiation-free guidance.

While some of the more formal aspects have been treated in other reviews,[1] it can be a vexing experience to find a concise and comprehensive repository of practical advice for ultrasound-guided injections and the few readily available are often not as broad.[2,3] Moreover, many little tips and tricks have been passed down through generations in an informal manner without being adequately documented. With this review, we endeavor to provide a comprehensive yet succinct guide that includes the most current techniques and drugs, as well as divulging some of these invaluable secrets.

Little Tips

Consent

There is little benefit to expounding on this topic, as it should already be common practice. Taking the time to fully explain the procedure and its intended outcomes, while securing the patient's written consent, is a prudent and time-saving measure.

Planning

Once an individual has become accustomed to a particular procedure, they may tend to disregard the planning phase, particularly when the procedure involves a rapid and seemingly uncomplicated injection. However, this oversight can result in a simple injection becoming a significantly prolonged procedure. Planning is a crucial phase during which factors such as the injection's required depth, the needle's length, the appropriate dosage of the drug to be administered, and the probability of the proposed procedure achieving its intended outcome are established. For a patient who has been experiencing pain and is seeking a successful outcome, experiencing a failure due to inadequate planning can be highly frustrating. Additionally, planning offers an additional opportunity to communicate the details of the procedure and reconfirm the patient's consent. Failure to adequately plan often necessitates starting over, leading to unpleasant explanations. Effective planning mitigates unnecessary difficulties for all parties involved.

Access this article online

Quick Response Code:

Website: https://journals.lww.com/jajs

DOI: 10.4103/jajs.jajs_20_23

Address for correspondence: Dr. Pablo Longhi Lorenzzoni, 1/25 Ferguson Street, Albany Creek Qld 4035 Australia.
E-mail: pablo@lorenzzoni.org

Submitted: 02-Mar-2023 **Revised:** 17-Mar-2023
Accepted:18-Mar-2023 **Published:** 19-Jul-2023

This is an open access journal, and articles are distributed under the terms of the Creative Commons Attribution-NonCommercial-ShareAlike 4.0 License, which allows others to remix, tweak, and build upon the work non-commercially, as long as appropriate credit is given and the new creations are licensed under the identical terms.

For reprints contact: WKHLRPMedknow_reprints@wolterskluwer.com

How to cite this article: Lorenzzoni PL, Patel S. Ultrasound-guided joint injections: Tips and tricks. J Arthrosc Jt Surg 2023;10:118-24.

Needle size

One of the most prevalent errors made by registrars is selecting a needle that is too short for the intended task. This may arise from an over-reliance on the measurements recorded by machines. However, in the real world, the situation is often more intricate. Despite having a well-conceived plan, the needle's placement may deviate slightly upon reaching the skin. Consequently, the angle may require adjustment, or the measurements could be distorted by excessive pressure on the ultrasound probe. Even a minor alteration can render an otherwise suitable needle too short for the procedure. While planning is critical, it is also essential to leave room for contingencies. Choosing a needle that is too short may preclude any opportunity for recovery without changing the needle.

Another common issue that arises is selecting the appropriate needle thickness. While a 25-gauge needle is commonly used for injections, administering a large volume of fluid can be time-consuming and stressful for the patient. In such instances, a 22-gauge needle may be more appropriate, as it reduces injection pressure and saves time. When aspirating fluids, thicker needles may be required, such as an 18-gauge or even 16-gauge needle for ganglions, unless the fluid has low viscosity, such as simple cysts. However, it should be noted that needles thicker than 22-gauge may necessitate the use of local anesthetic on the skin, whereas thinner needles may not require it except for extremely anxious patients.

Needle bevel

A little-known trade secret is the significance of the direction of the bevel, which refers to the slanted surface at the tip of the needle. The longest part of the bevel determines the direction in which the needle is introduced, causing the needle to turn slightly toward this side. Many registrars have found relief when struggling to pass through a narrow structure by simply rotating the bevel 180° the opposite way. Additionally, during deep and challenging injections, especially when the position is suboptimal, success may hinge on turning the short part of the bevel toward the target structure. This is because the injectate exits the needle at a slight angle toward the shortest part of the bevel. Furthermore, in situations where it may appear that the joint has been reached but contrast is not flowing freely, rotating the bevel 360° may allow the needle to cut through the thick capsule, thereby facilitating the free flow of contrast into the joint.

Local anesthetic

An additional undisclosed technique, particularly when using ultrasound for guidance, involves using local anesthetic as a means of smoothing out the skin when it is challenging to achieve good contact with the probe. It can also be used to create more space for maneuvering by pushing away other structures from the intended target area.

It is important to note that lignocaine with epinephrine should be avoided. This combination has little to no practical application in daily practice and may be better suited for other professions. Furthermore, it limits the amount of local anesthetic that can be used, reducing the ability to employ the aforementioned techniques.

Moreover, when choosing a local anesthetic for combined joint injections (not the skin and needle tract), it is essential to remember that all local anesthetics are chondrotoxic. While a single joint injection is unlikely to cause significant harm, ropivacaine has proven to be less damaging *in vitro*[4] and is a wise option to consider.

What to inject?

In a 2009 review, MacMahon *et al*.[5] published some corticosteroid dose suggestions that the authors adapted based on their own experience in Table 1.

The use of corticosteroids in combination with local anesthetics in a 1:1 dilution is a common practice in radiology. However, there is much debate regarding the optimal combination of drugs, with varying preferences observed among different radiologist groups. The selection of drugs is often influenced by factors such as current trends and past experiences, rather than standardized guidelines. Nevertheless, some recommendations can be made to ensure optimal outcomes:

- The larger the corticosteroid particle, the more potent (and longer) the effect, but also greater the dermal and subcutaneous tissue atrophy
- Triamcinolone acetonide particles range from 15 to 60 μm and are therefore one of the most potent available. Betamethasone particles range from 10 to 20 μm. Methylprednisolone, from 0.5 to 26 μm. Dexamethasone particles are about 0.5 μm. For comparison, an erythrocyte measures between 2.5 and 7.5 μm[1,6]
- Some combinations cause precipitation or aggregation of the particles; especially important are the combinations of triamcinolone and bupivacaine (particle aggregate of more than 100 μm)[1] and dexamethasone and ropivacaine (previously thought as essentially nonparticulate, this combination often produce aggregates larger than 20 μm).[7,8]
- There is still controversy[9] whether joint injections can cause cartilage damage and, if so, at least part of that damage may be attributable to the analgesic effect.[10] Caution in the use of corticosteroids and good consent is essential. The pressure for ever longer effects has to be balanced against the real benefits from the injection and the likelihood of speeding up the need for a joint replacement. As a rule of thumb, lower doses and effect durations have less deleterious effects than higher doses and durations[11]
- On the other hand, newer agents that aim to "replenish" synovial fluid, such as hyaluronic acid (known as viscosupplements), have a more favorable profile[9] and mixing them with corticosteroids seems to be safe.[12-14]

What to aspirate and why?

Septic arthritis is the obvious indication for aspiration, but in the context of osteoarthritis, inflammatory, or crystalline arthropathy, patients may present with joint effusion for pain

Table 1: Doses of corticosteroid according to joints (adapted from MacMahon *et al*., 2009)[5]

Joint	Methylprednisolone acetate (mg)	Triamcinolone acetate (mg)	Betamethasone* (mL)	Dexamethasone sodium phosphate (mg)
Large (hip, knee, shoulder, ankle)	20–80	20–40	2–3	2–4
Medium (elbow, wrist)	10–40	10–20	1–2	1.5–3
Small (STT, CMC, ACJ, SCJ, DRUJ)	4–10	Not used†	0.5–1	0.7–1.2

*Betamethasone-combination of acetate and sodium phosphate equivalent to 5.7 mg/mL, †The authors prefer not to use large particulate agents in small joints. STT: Scaphotrapeziotrapezoidal, SCJ: Sternoclavicular joint, ACJ: Acromioclavicular joint, DRUJ: Distal radioulnar joint, CMC: Carpometacarpal joint

relief injection. Although one may know the most likely cause of the effusion, several reasons exist for aspirating before injecting the joint. The primary reason is to obtain confirmation that the effusion is not caused by septic arthritis. Additionally, if macroscopic evidence of infection is retrieved from the joint, a local anesthetic-only injection may be administered for brief pain relief after the joint is fully drained, pending analysis of the aspirate.[15] Therefore, it is crucial to aspirate before injecting any joint to avoid complications and ensure the safety of the patient. Besides, different approaches can be envisioned if we are talking about a crystal-deposition disease or just degenerative osteoarthritis. Finally, the injectate concentration may be at least as important as the dose and injecting any medicine in the presence of a joint effusion will decrease the final concentration and may be responsible for a lower strength or even a failed injection.

There are multiple methods for aspiration and injection, but to completely protect against iatrogenic infection, the authors recommend the double syringe sterile system[16] which consists of a three-way tap, a large syringe for the aspiration, and a second syringe with the injectate; to that, the authors add a short extension tube to improve the mobility and decrease the needle movement during the procedure [Figure 1].

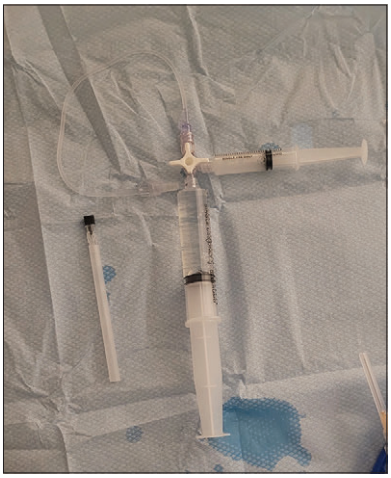

Figure 1: Double-syringe sterile injection/aspiration system

Upper Extremity

Subacromial subdeltoid bursa

Probably the most frequent of the shoulder girdle injections, approaching the subacromial subdeltoid bursa can only rarely be difficult. What to inject and how much have seen no short of controversy,[17,18] but it seems to have coalesced around the high-volume injections.[19] The authors prefer an anterior approach with the patient in supine position [Figure 2a and b] using a combination of triamcinolone 40 mg, xylocaine 1% 2 ml, and bupivacaine 0.25% 7 mL.

Glenohumeral joint

Glenohumeral joint (GHJ) injections can be used for pain relief in osteoarthritis and for adhesive capsulitis. For osteoarthritis, viscosupplements such as hyaluronic acid can be used and several combinations of local anesthetic and corticosteroids have been commonly applied.[2] According to Table 1, the authors prefer 2 mL of betamethasone and 2 mL of bupivacaine 0.25% for low-volume injections.

The same combinations have been used for adhesive capsulitis, sometimes associated with volume distention by saline 0.9% (a procedure called hydrodilatation[20]). There is at least one randomized trial that showed no significant difference between the simple injection and the hydrodilatation[21] and maybe things are more complex than previously thought with regard to this poorly understood disease. If hydrodilatation is to be performed, the authors prefer a variation of the double-syringe technique replacing the aspiration syringe with one filled with 20 mL of saline, to be injected last according to patient's tolerance.[22]

There are two commonly used approaches for the GHJ, one anterior, via the rotator interval [Figure 2c and 2d], and the other posterior, adjacent or under the posterior labrum [Figure 2e and 2f]. For treatment of adhesive capsulitis, it seems that the rotator interval approach is more effective both for low and large volumes.[23,24]

Acromioclavicular joint

Acromioclavicular joint (ACJ) injections are commonly used for pain relief in degenerative conditions.[2] The small volume of this joint space allows for the injection of only a small amount of the commonly combined steroid and local anesthetic and the authors prefer 0.5 mL betamethasone and 0.5 mL of lignocaine 2%.[25] In-plane approaches are possible in all but the most irregular joints and the off-plane approach is usually achievable in any condition [Figure 2g and h].

Sternoclavicular joint

Sternoclavicular (SC) joint injections are also commonly used for pain relief in degenerative conditions. One must

remember that the SC joint usually has an articular disc that divides the joint into two compartments: the sternal and the clavicular compartment. In degenerated joints, there is usually communication between the compartments and approach of just one of them is usually enough.[26]

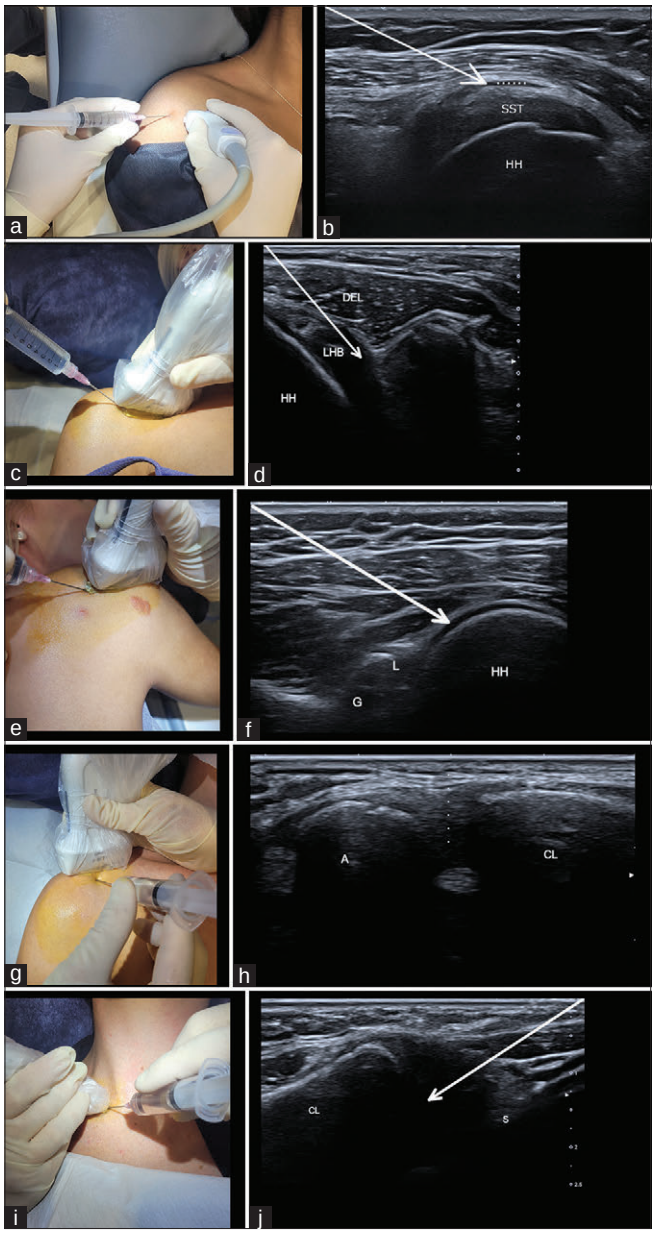

Figure 2: Shoulder girdle injections. (a) Probe and needle position for subacromial subdeltoid bursa injection; (b) SSP; HH; white arrow: Needle path; white dotted line: Subacromial subdeltoid bursa; (c) Probe and needle position for GHJ injection, rotator interval approach; (d) HH; LHB; DEL; (e) Probe and needle position for GHJ injection, posterior approach; (f) HH; G; L; white arrow: Needle path; (g) Probe and needle position for ACJ injection, off-plane anterior approach; (h) A; CL; white dotted line: Off-plane needle path; (i) Probe and needle position for SCJ injection, quasi-coronal approach; (j) S; CL; white arrow: Needle path. SSP: Supraspinatus, HH: Humeral head, LHB: Long head of the biceps tendon, DEL: Deltoid muscle, G: Glenoid, L: Labrum, A: Acromion, CL: Clavicle, S: Sternum, GHJ: Glenohumeral joint, ACJ: Acromioclavicular joint

In-plane techniques are preferred by the authors due to better localization of the needle at all times (considering the upper mediastinum and its large vessels lie just deep to the joint) and can be achieved in a quasi-coronal plane or a sagittal plane [Figure 2i and j]. The mixture can be the same as what is used for ACJs.

Elbow

The elbow is made up of three joints with a single capsule. While this means that multiple approaches are possible, it also means that any approach affects all of them and that the volume to be used is slightly larger than one would expect.

The easiest approach is probably the radiocapitellar joint in an off-plane fashion [Figure 3a and b], but the posterior approach in-plane is not hard at all and has the benefit of maintaining the vision of the needle at all times [Figure 3c and d], but by no means, these are the only possible approaches.[3]

As to the injectate, a volume of 2–3 mL is possibly needed. That can be viscosupplements or a 1:1 combination of steroid and local anesthetic for the other joints.

Radiocarpal joint

The radiocarpal joint is a single compartment, medially containing a fibrous structure known as the triangular fibrocartilage complex (TFCC). Requests for injecting the RCJ are common, but requests for injecting the ulnocarpal joint are common either, despite the fact that there is only one joint compartment there.

We advocate the dorsal approach with a cushion underneath the wrist to provide a good angle and an in-plane, distal to proximal needle between the scaphoid and the radius as this is easier to achieve [Figure 4a and b]. This is a variation of the landmark-driven technique (and if you want you can still use the Lister tubercle as a guide). A volume of 2 mL is possible

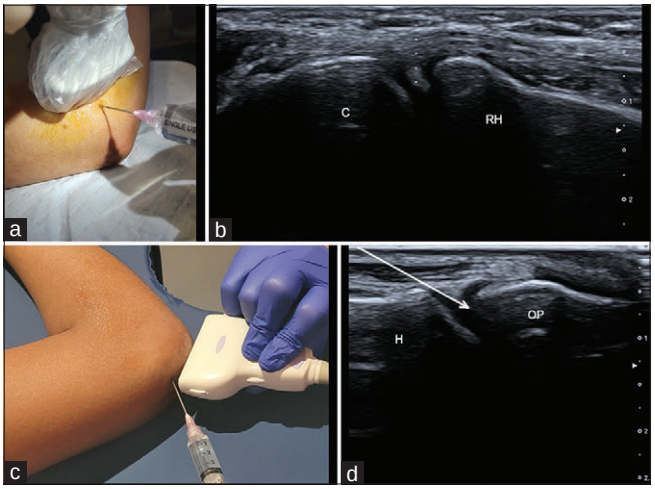

Figure 3: Elbow. (a) Probe and needle position for elbow injection, off-plane radiocapitellar approach; (b) RH; C; white dotted line: Off-plane needle path; (c) Probe and needle position for elbow injection, in-plane posterior approach; (d) H; OP; white arrow: Needle path.) RH: Radial head, C: Capitellum, H: Humerus, OP: Olecranon process

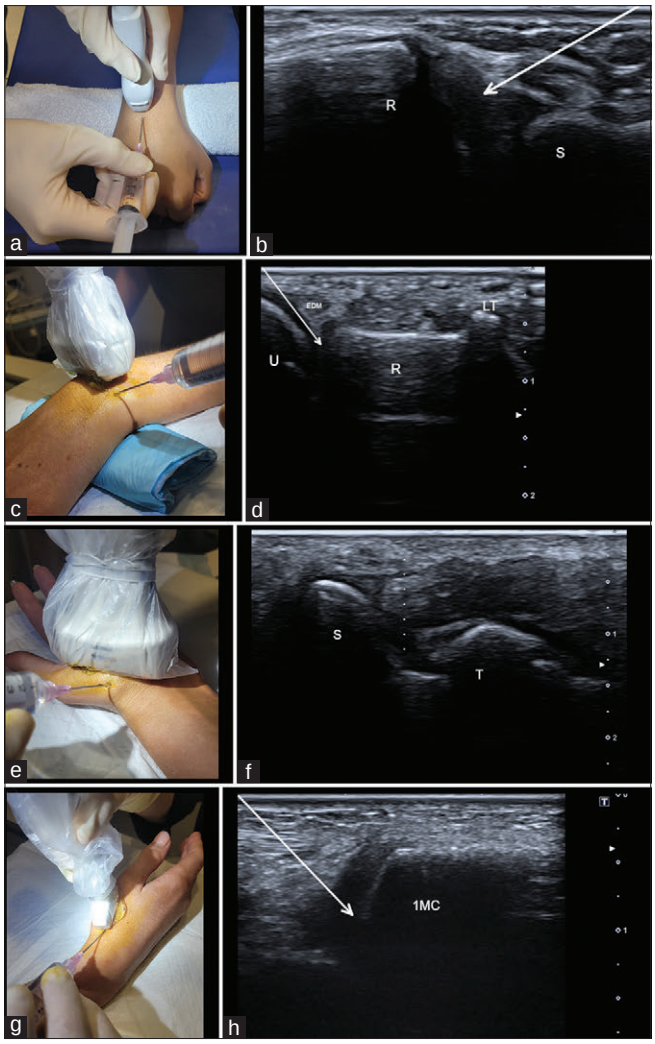

Figure 4: Wrist. (a) Probe and needle position for radiocarpal joint injection; (b) R; S; white arrow: Needle path; (c) Probe and needle position for DRUJ injection; (d) R; U; LT; EDM; white arrow: Needle path; (e) Probe and needle position for STT joint injection, off-plane volar approach; (f) S; T; white dotted line: Off-plane needle path; (g) Probe and needle position for 1CMC joint injection; (h) 1MC; white arrow: Needle path. R: Radius, S: Scaphoid, DRUJ: distal radial-ulnar joint, R: Radius, U: Ulna, LT: Lister tubercle, EDM: Extensor digiti minimi, Scaphoid, T: Trapezium, 1CMC: First carpometacarpal joint, 1MC: first metacarpal

without discomfort and the same injectate 1:1 mixture is suggested.[27]

Distal radial-ulnar joint

The distal radial-ulnar joint (DRUJ) is an L-shaped joint separate from the RCJ and stabilized by the TFCC. It is formed by the sigmoid notch of the distal epiphysis of the radius and the head of the ulna and allows pronation and supination of the hand. Damages to the TFCC create instability of this joint and ulnar-sided wrist pain can sometimes be attributed to the DRUJ rather than the RCJ.

The authors prefer to approach the DRUJ dorsally, in a transverse plane with the needle in-plane from the ulnar side.[28] The needle passes below the extensor digiti minimi aiming at the radius [Figure 4c and d]. Only a small volume is possible, adding up to 1 mL.

Scaphotrapeziotrapezoidal joint

The STT joint is located in the radial side of the wrist and is primarily involved in movements of the thumb. It is the second most common site of osteoarthritis in the wrist and is a common site for pain-relief treatment. Again, only a small volume is possible, sometimes not reaching 1 mL. It can be approached in the dorsal or volar aspects, and it is a difficult injection for the less experienced since an off-plane technique is needed most of the time. Despite being slightly more uncomfortable, volar approaches[29] are preferred [Figure 4e and f].

First carpometacarpal joint

One of the most common sites for osteoarthritis and importantly associated with thumb movement is the 1 carpometacarpal joint. Patients usually complain of pain when gripping or holding objects, and on visual inspection, osteoarthritis of this joint produces a "squared" base of the thumb, hard to miss. Only volumes sometimes adding up to 1 mL are possible. An in-plane approach using a small "hockey-stick" probe is preferred [Figure 4g and h] and is usually achievable aiming toward the metacarpal base.[30]

Lower Extremity

Hip

The hip is a ball-and-socket joint with a thick capsule formed by various ligaments. It can be safely approached by ultrasound provided that one uses long spinal needles and, in some overweight patients, the convex probe. It is vital to stay away from the femoral vessels.

The authors prefer an in-plane injection targeting the anterior synovial recess underneath the joint capsule at the femoral head-neck junction,[31] approaching from the distal aspect of the probe and aligning the probe with the femoral neck as shown in Figure 5a and b. It is important to keep in mind that the capsule can be very thick and a good technique is to actually "feel" the bevel of the needle touching bone. Volumes of 4 mL are achievable with ease. This joint is also commonly treated with viscosupplements.[32]

Knee

Several approaches are possible to aspirate or inject the knee joint, and this is one of the easiest joints to approach with a needle when an effusion (even a minimal one) is present. The suprapatellar pouch is almost painless to inject and does not require touching the patella as in the landmark-guided injection.

For the easy injection, an in-plane approach with the probe in transverse plane is effective [Figure 5c and d]. Volumes of 4 mL are easily achieved and viscosupplements are also commonly used.

The real trouble comes when there is hardly any fluid in the joint. Here, the authors advocate two different approaches:

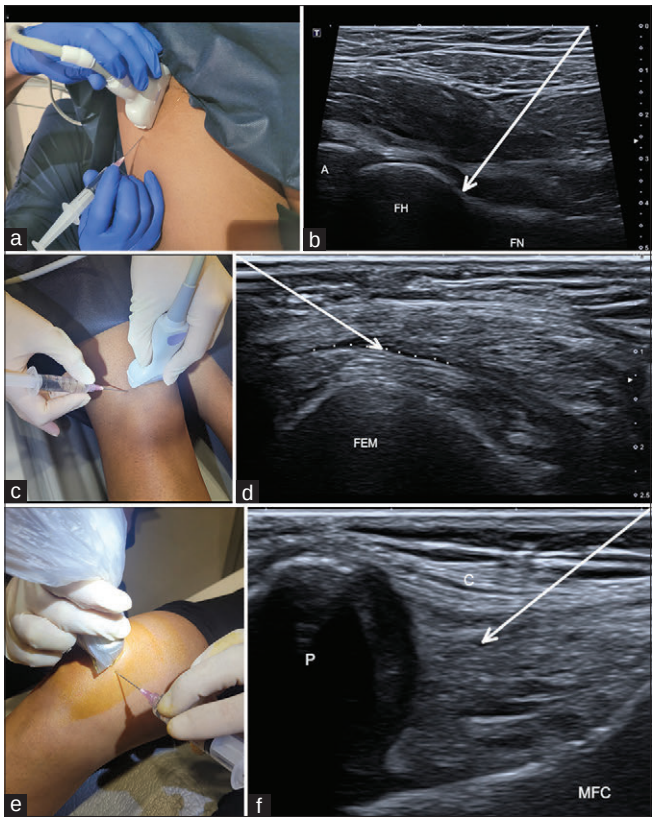

Figure 5: Hip and knee. (a) Probe and needle position for Hip joint injection; (b) A; FH; FN; white arrow: Needle path; (c) Probe and needle position for knee joint injection, suprapatellar pouch approach; (d) FEM; white dotted line: Suprapatellar pouch; white arrow: Needle path; (e) Probe and needle position for Knee joint injection, mid-medial subpatellar approach; (f) P; MFC; C; white arrow: Needle path.A: Acetabulum, FH: Femoral head, FN: Femoral neck, FEM: Femur, P: Patella, MFC: Medial femoral condyle, C: Capsule

First is a variation of the suprapatellar pouch approach using a double-syringe technique. The second syringe is filled with saline and is used to confirm the correct placement of the needle in the articular space rather than in the fat pad. Once a good position is achieved, small amounts of saline can be injected and observed to move away from the needle bevel. That's when the three-way tap is switched to the injectate position and the payload (steroid-anesthetic mixture or viscosupplement) is delivered.

The second is the more traditional mid-medial subpatellar approach that is also commonplace in landmark-based injections.[33] The probe is positioned transversely in the medial compartment, imaging the patella and the medial femoral condyle, and the needle penetrates the skin medially aiming toward the patella [Figure 5e and f]. This requires a bit more of experience and is often more uncomfortable than the first technique.

Tibiotalar joint

This is usually not a difficult joint to approach and the anterior recess is a good target[34] for an in-plane injection with the probe in a sagittal plane [Figure 6a and b]. Volumes of 4 mL are easily achievable but often not needed.

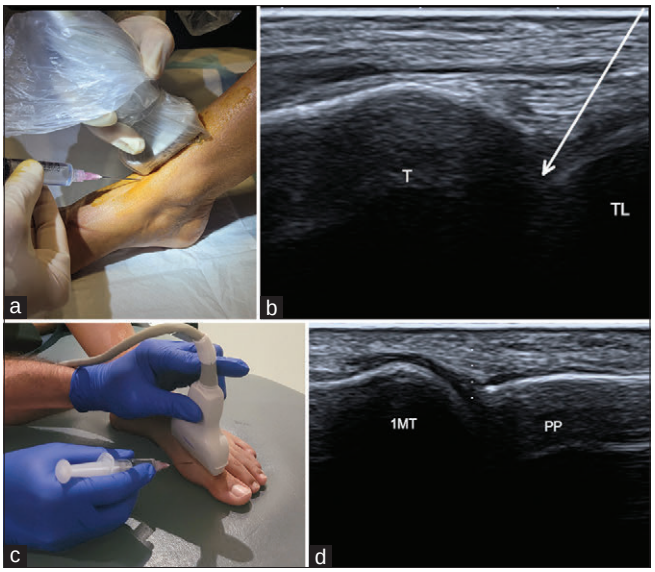

Figure 6: Ankle and Foot. (a) Probe and needle position for Tibiotalar joint injection; (b) T: Tibia; TL: Talus; white arrow: needle path; (c) Probe and needle position for 1MTP joint injection, off-plane approach; (d) 1MT: first metatarsal; PP: Proximal phalanx; white dotted line: off-plane needle path

First metatarsal-phalangeal joint

The first metatarsal-phalangeal joint (MTP) is a common site for degenerative change and for inflammatory arthritis. In the latter, it often presents with joint effusion that needs aspiration for microscopy analysis,[35] and while several approaches can be used, an off-plane technique from the medial aspect of the joint is accurate and not difficult to achieve [Figure 6c and d].

Conclusion

There is much more that can be written about joint injections and there are uncountable ways to approach them. In this article, we summarized some of the most common injections we have in our daily practice and how we approach them while sharing some tricks of the trade and words of caution, which even the most seasoned practitioners among us may find useful.

Acknowledgments

We'd like to acknowledge I-MED Network for allowing us to produce the pictures used in this article, especially in the person of Sonographers Julie Brunning and Min-Chu Wei (Karen), Radiographers Amy Christine Walton and Emma Thomson, and Radiographer Students Isabella Quan and Jananie Nanayakkara (Tara).

Financial support and sponsorship

Nil.

Conflicts of interest

There are no conflicts of interest.

References

1. Shah A, Mak D, Davies AM, James SL, Botchu R. Musculoskeletal corticosteroid administration: Current concepts. Can Assoc Radiol J 2019;70:29-36.
2. Messina C, Banfi G, Orlandi D, Lacelli F, Serafini G, Mauri G, *et al.* Ultrasound-guided interventional procedures around the shoulder. Br J Radiol 2016;89:1057.
3. Patel RP, McGill K, Motamedi D, Morgan T. Ultrasound-guided interventions of the upper extremity joints. Skeletal Radiol 2022;52:897-909.
4. Grishko V, Xu M, Wilson G, Pearsall AW 4th. Apoptosis and mitochondrial dysfunction in human chondrocytes following exposure to lidocaine, bupivacaine, and ropivacaine. J Bone Joint Surg Am 2010;92:609-18.
5. MacMahon PJ, Eustace SJ, Kavanagh EC. Injectable corticosteroid and local anesthetic preparations: A review for radiologists. Radiology 2009;252:647-61.
6. Derby R, Lee SH, Date ES, Lee JH, Lee CH. Size and aggregation of corticosteroids used for epidural injections. Pain Med 2008;9:227-34.
7. Watkins TW, Dupre S, Coucher JR. Ropivacaine and dexamethasone: A potentially dangerous combination for therapeutic pain injections. J Med Imaging Radiat Oncol 2015;59:571-7.
8. Choi EJ, Kim DH, Han WK, Lee HJ, Kang I, Nahm FS, *et al.* Non-particulate steroids (Betamethasone Sodium Phosphate, Dexamethasone Sodium Phosphate, and Dexamethasone Palmitate) combined with local anesthetics (Ropivacaine, Levobupivacaine, Bupivacaine, and Lidocaine): A potentially unsafe mixture. J Pain Res 2021;14:1495-504.
9. Raynauld JP, Buckland-Wright C, Ward R, Choquette D, Haraoui B, Martel-Pelletier J, *et al.* Safety and efficacy of long-term intraarticular steroid injections in osteoarthritis of the knee: A randomized, double-blind, placebo-controlled trial. Arthritis Rheum 2003;48:370-7.
10. Mulherin D, Fitzgerald O, Bresnihan B. Clinical improvement and radiological deterioration in rheumatoid arthritis: Evidence that the pathogenesis of synovial inflammation and articular erosion may differ. Br J Rheumatol 1996;35:1263-8.
11. Navarro-Sarabia F, Coronel P, Collantes E, Navarro FJ, de la Serna AR, Naranjo A, *et al*. A 40-month multicentre, randomised placebo-controlled study to assess the efficacy and carry-over effect of repeated intra-articular injections of hyaluronic acid in knee osteoarthritis: The AMELIA project. Ann Rheum Dis 2011;70:1957-62.
12. Ozturk C, Atamaz F, Hepguler S, Argin M, Arkun R. The safety and efficacy of intraarticular hyaluronan with/without corticosteroid in knee osteoarthritis: 1-year, single-blind, randomized study. Rheumatol Int 2006;26:314-9.
13. Smith C, Patel R, Vannabouathong C, Sales B, Rabinovich A, McCormack R, *et al.* Combined intra-articular injection of corticosteroid and hyaluronic acid reduces pain compared to hyaluronic acid alone in the treatment of knee osteoarthritis. Knee Surg Sports Traumatol Arthrosc 2019;27:1974-83.
14. He WW, Kuang MJ, Zhao J, Sun L, Lu B, Wang Y, *et al.* Efficacy and safety of intraarticular hyaluronic acid and corticosteroid for knee osteoarthritis: A meta-analysis. Int J Surg 2017;39:95-103.
15. Courtney P, Doherty M. Joint aspiration and injection and synovial fluid analysis. Best Pract Res Clin Rheumatol 2009;23:161-92.
16. Lazarescu AE, Hogea BG, Andor BC, Totorean A, Cojocaru DG, Negru M, *et al.* Using a double syringe sterile system for MSK aspiration/injection procedures eliminates risk of iatrogenic infection. Ther Clin Risk Manag 2022;18:1029-36.
17. Hong JY, Yoon SH, Moon DJ, Kwack KS, Joen B, Lee HY. Comparison of high- and low-dose corticosteroid in subacromial injection for periarticular shoulder disorder: A randomized, triple-blind, placebo-controlled trial. Arch Phys Med Rehabil 2011;92:1951-60.
18. Boonard M, Sumanont S, Arirachakaran A, Apiwatanakul P, Boonrod A, Kanchanatawan W, *et al.* Short-term outcomes of subacromial injection of combined corticosteroid with low-volume compared to high-volume local anesthetic for rotator cuff impingement syndrome: A randomized controlled non-inferiority trial. Eur J Orthop Surg Traumatol 2018;28:1079-87.
19. Klontzas ME, Vassalou EE, Zibis AH, Karantanas AH. The effect of injection volume on long-term outcomes of US-guided subacromial bursa injections. Eur J Radiol 2020;129:109113.
20. Watson L, Bialocerkowski A, Dalziel R, Balster S, Burke F, Finch C. Hydrodilatation (distension arthrography): A long-term clinical outcome series. Br J Sports Med 2007;41:167-73.
21. Paruthikunnan SM, Shastry PN, Kadavigere R, Pandey V, Karegowda LH. Intra-articular steroid for adhesive capsulitis: Does hydrodilatation give any additional benefit? A randomized control trial. Skeletal Radiol 2020;49:795-803.
22. Rymaruk S, Peach C. Indications for hydrodilatation for frozen shoulder. EFORT Open Rev 2017;2:462-8.
23. Sun Y, Liu S, Chen S, Chen J. The effect of corticosteroid injection into rotator interval for early frozen shoulder: A randomized controlled trial. Am J Sports Med 2018;46:663-70.
24. Elnady B, Rageh EM, Hussein MS, Abu-Zaid MH, Desouky DE, Ekhouly T, *et al.* In shoulder adhesive capsulitis, ultrasound-guided anterior hydrodilatation in rotator interval is more effective than posterior approach: A randomized controlled study. Clin Rheumatol 2020;39:3805-14.
25. Tortora S, Messina C, Gitto S, Chianca V, Serpi F, Gambino A, *et al.* Ultrasound-guided musculoskeletal interventional procedures around the shoulder. J Ultrason 2021;21:e162-8.
26. Pourcho AM, Sellon JL, Smith J. Sonographically guided sternoclavicular joint injection: Description of technique and validation. J Ultrasound Med 2015;34:325-31.
27. Lohman M, Vasenius J, Nieminen O. Ultrasound guidance for puncture and injection in the radiocarpal joint. Acta Radiol 2007;48:744-7.
28. Smith J, Rizzo M, Sayeed YA, Finnoff JT. Sonographically guided distal radioulnar joint injection: Technique and validation in a cadaveric model. J Ultrasound Med 2011;30:1587-92.
29. Smith J, Brault JS, Rizzo M, Sayeed YA, Finnoff JT. Accuracy of sonographically guided and palpation guided scaphotrapeziotrapezoid joint injections. J Ultrasound Med 2011;30:1509-15.
30. Derian A, Amundson J, Abi-Aad K, Vasquez-Duarte R, Johnson-Greene D. Accuracy of ultrasound-guided versus palpation-based carpometacarpal joint injections: A randomized pilot study in cadavers. Ultrasound 2018;26:245-50.
31. Yildizgoren MT. Longitudinal antero-inferior approach for ultrasound-guided hip joint injection. J Ultrason 2020;20:e231-2.
32. Pourbagher MA, Ozalay M, Pourbagher A. Accuracy and outcome of sonographically guided intra-articular sodium hyaluronate injections in patients with osteoarthritis of the hip. J Ultrasound Med 2005;24:1391-5.
33. Park KD, Ahn JK, Lee SC, Lee J, Kim J, Park Y. Comparison of ultrasound-guided intra-articular injections by long axis in plane approach on three different sites of the knee. Am J Phys Med Rehabil 2013;92:990-8.
34. Wisniewski SJ, Smith J, Patterson DG, Carmichael SW, Pawlina W. Ultrasound-guided versus nonguided tibiotalar joint and sinus tarsi injections: A cadaveric study. PM R 2010;2:277-81.
35. Raza K, Lee CY, Pilling D, Heaton S, Situnayake RD, Carruthers DM, *et al.* Ultrasound guidance allows accurate needle placement and aspiration from small joints in patients with early inflammatory arthritis. Rheumatology (Oxford) 2003;42:976-9.

Review Article

Ultrasound-Guided Percutaneous Release of Pulley in Trigger Finger: A Curved Needle Technique

Dharmendra Kumar Singh, Basavaraj Chari[1]

Department of Radiodignosis, Vardhman Mahavir Medical College and Safdarjung Hospital, New Delhi, India, [1]Nuffield Orthopaedic Centre, Oxford University Hospitals NHS Foundation Trust, Oxford, UK

Abstract

Thickened A1 pulley is the most common cause of trigger finger. The patient complains of snapping and locking of finger like a trigger as the gliding of the flexor tendon become harder through the thickened pulley during flexion and superadded development of nodule on the surface of the tendon proximal to pulley. In severe cases or failed conservative/steroid injection cases, real-time percutaneous release of pulley under ultrasound (US) guidance can be considered. The percutaneous pulley release is a minimally invasive procedure compared to open surgical release and more accurate than blind percutaneous release with overall minimal complications. The US-guided percutaneous A1 pulley release has been described in the literature and done by knife, straight needles, and acutely bent needles with variable results. We describe the curved needle technique of percutaneous pulley release. The curved needle technique for US-guided A1 pulley release is novel and has the advantage of easy maneuverability over acutely bent needle and minimal chances of complications. The cutting edge of the curved needle scores through the thickened pulley with effective release and easy maneuverability.

Keywords: Fixed flexion deformity, flexion tenosynovitis, percutaneous pulley release, pulley, triggering

Introduction

Snapping and locking of the finger during flexion is known as trigger finger (TF). TF is most commonly caused by focal stenosing tenosynovitis at A1 pulley that leads to focal reduction in the volume of flexor tendon sheath, particularly in anteroposterior direction. The flexor tendon coursing underneath the thickened pulley finds it difficult to glide during flexion of finger and in severe condition gets locked. The ring finger and thumb are most often affected by TF.[1,2]

Primary or idiopathic TF is more common while secondary TF is either associated with abnormal biomechanics, for example, excessive flexion and extension of digits, sequalae to palmar skin trauma; or secondary to systemic disorder, for example, diabetes mellitus, rheumatoid arthritis, hypothyroidism, histiocytosis, amyloidosis, and gout. The incidence of TF is about 2% in the general population, more commonly in females and in patients with diabetes (7%) and rheumatoid arthritis.[3]

Mild TF is treated conservatively, with oral anti-inflammatory drugs, physical therapy, or corticosteroid injections; while severe cases are often managed by an open surgical release, which is successful in 83 ~ 98% of cases.[4]

Percutaneous pulley release in TF is a minimal invasive intervention having outcome equal to the open surgical release. Due to the advantages of outpatient procedure, shorter recovery time, avoidance of scar/fibrosis; percutaneous pulley release is nowadays accepted as a preferred management for severe/recalcitrate TF.[4-6] However, the potential risk of blind percutaneous pulley release, for example, damage to the tendon and neurovascular structures has been largely overcome by performing the release in real-time visualization under ultrasound (US). It has added advantage to confirm that the release is partial or full thickness. The TF pathologic anatomical structures identified by US are even far superior

Address for correspondence: Dr. Basavaraj Chari, Nuffield Orthopaedic Centre, Oxford University Hospitals NHS Foundation Trust, Windmill Road, Oxford OX3 7LD, UK.
E-mail: raj.chari@ouh.nhs.uk

Submitted: 05-Mar-2023 **Revised:** 31-Mar-2023
Accepted: 04-Apr-2023 **Published:** 19-Jul-2023

Access this article online

Quick Response Code:

Website: https://journals.lww.com/jajs

DOI: 10.4103/jajs.jajs_22_23

This is an open access journal, and articles are distributed under the terms of the Creative Commons Attribution-NonCommercial-ShareAlike 4.0 License, which allows others to remix, tweak, and build upon the work non-commercially, as long as appropriate credit is given and the new creations are licensed under the identical terms.

For reprints contact: WKHLRPMedknow_reprints@wolterskluwer.com

How to cite this article: Singh DK, Chari B. Ultrasound-guided percutaneous release of pulley in trigger finger: A curved needle technique. J Arthrosc Jt Surg 2023;10:125-30.

than magnetic resonance imaging (MRI), especially in the dynamic evaluation.[5,7,8] The US-guided percutaneous pulley release has been previously described and several different ways have been postulated including straight needle, needles bent in several patterns, and specially designed knives with hook shape.[2,7] The prototype knife device described in the literature is not available everywhere for routine clinical use. US-guided percutaneous A1 pulley release using a needle is usually performed with an 18-gauge or 21-gauge needle. The straight needle techniques operate between the subcutaneous tissue and the superficial surface of the pulley compared to the curved needle technique that operates between the interface of the thickened pulley and the tendon. The thickened pulley is stretched and cut by the sharp curved needle tip which causes adhesiolysis as well as cutting of the fibers of the thickened pulley. The needle usually bent at one or multiple sites at various angles to create a scalpel effect at the tip of the needle and has a variable success rate. However, it has been reported that the needles can twist or turn on themselves easily and the sharp tip inadvertently can cause injury to the surrounding structures.[5,8-10] This can potentially be avoided by converting the straight/angle bent needle into a smooth curvature. The aim of our article is to demonstrate the curved needle technique of A1 pulley release under US guidance.

Anatomy and biomechanics of pulley

The flexor tendons are long cord-like structures that pass through the tendon sheath and attach the flexor muscles to the middle and distal phalanges. The tendon glides upon the tendon sheath smoothly during flexion and extension. To prevent any bowstringing during flexion of the finger, a number of fibrous bands called "pulleys" hold the flexor tendons closely to the phalanges. The pulley at the base of the finger is called the "A1 pulley" [Figure 1] and its thickening is the most common culprit in TF.[11]

Pathogenesis of trigger finger

Inflammation and thickening of A1 pulley reduce the anteroposterior diameter of the patent tendon sheath. This increases the friction between the tendon and tendon sheath/pulley, and tenting of flexor tendon proximal or distal to the thickened pulley. Over the course of time, the flexor tendon become inflamed and develop a small nodule on its surface; thereby increasing the anteroposterior diameter of tendon and further increases the friction between tendon and sheath/pulley. On flexion of the finger, when the nodule passes through the pulley, the patient experiences pain and a catching or popping sensation. In severe cases of TF, the nodule get stuck at proximal or distal margin of the thickened pulley and the finger gets locked in a flexed position. Often the patient has to use the passive force to straighten the finger, hence giving its name of "trigger finger."[3] Most cases of TF are idiopathic, hence several factors may increase the risk for developing the condition. These include:

- Systemic disorders: TF is more common in people with diabetes, rheumatoid arthritis, hypothyroidism, histiocytosis, amyloidosis, and gout

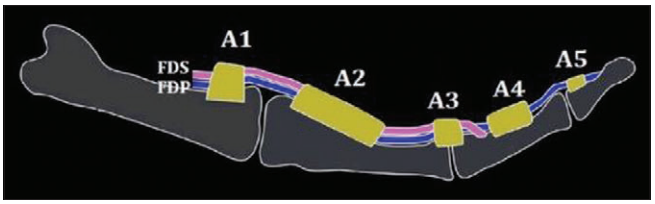

Figure 1: Illustrated diagram of flexor aspect of finger demonstrates FDS and FDP tendons passing through pulleys (A1 pulley at MCP level, A2 pulley at proximal phalanx level, A3 pulley at proximal interphalangeal joint level, A4 pulley at distal phalanx level and A5 pulley at distal interphalangeal joint level). FDS: Flexor digitorum superficialis, FDP: Flexor digitorum profundus, MCP: Metacarpophalangeal joint

- Abnormal biomechanics: The condition is known to occur after forceful use of the fingers and thumb in activities involving manual dexterity, racquet sports, etc., The other causes include the activities involving excessive flexion and extension of digits, repeated friction between the flexor tendon and tendon sheath, and secondary to palmar skin trauma.[12]

Symptoms of trigger finger

The symptoms of TF include pain and stiffness while flexion and/or extension of the finger, especially after a period of inactivity. A tender lump at the base of the finger on the palmar aspect corresponding to thickened pulley causing a catching, popping, or locking sensation with finger flexion and/extension. In a severe case, the involved finger may become locked in a bent position.[12,13]

According to the degree of entrapment between the flexor digitorum tendon and tendon sheath, TF is divided into five grades:[7,8]

- Grade 0: No triggering
- Grade 1: Intermittent, moderate triggering
- Grade 2: Continuous triggering that is eliminated with active extension
- Grade 3: Triggering with flexion contracture that requires the patient to use passive force to unlock the involved finger
- Grade 4: Active flexion of the finger is impossible i. e fixed flexion deformity.

Materials and Methods

Ultrasound imaging of A1 pulley

Fingers are best evaluated by high-frequency hockey stick probe (12-18MHz). On axial scan at MCP joint level, flexor tendon appears as hyperechoic round to oval structure superficial to volar plate. Superficial to flexor tendon, a thin hypoechoic band of A1 pulley is seen on three sides of the tendon: superficial, radial, and ulnar, while on a longitudinal scan, the tendon is demonstrated as linear fibrillar structure superficial to triangular volar plate. The thin short linear hypoechoic line of pulley is demonstrated superficial to flexor tendon. On axial scan, refraction of US beam by radial and ulnar aspects of pulley due to its oblique orientation

causes refractile shadowing and thus these should not be misinterpreted as thickening [Figure 2].

Ultrasound imaging of trigger finger

On US, fusiform thickening of the A1 pulley is the hallmark of TF and in severe cases, the development of a nodule on the surface of flexor tendon adjacent to pulley [Figures 3 and 4]. Other frequently observed features include flexor tendinosis and tenosynovitis [Figure 5]. Since the flexor tendon has a rather wavy course adhering to the adjacent phalanges, the tendon can be affected by anisotropy and to untrained eyes, this may look such as tendinosis, appropriate maneuvering of the probe is necessary to overcome anisotropy [Figure 3]. Often more than one pulley can be thickened with diffuse thickening of the tendon sheath. On dynamic imaging, there can be redundancy of the flexor tendon sliding against the thickened pulley with tenting.[14]

Patient selection for percutaneous US-guided pulley release

All our patients for percutaneous release of pulley were referred by experienced hand surgeons, plastic surgeons, exercise and sports medicine physicians or their fellows. We do not accept any patient for the procedure from the primary or secondary health-care sector unless the patients have been assessed by the relevant experts. It is important to identify the patients who would benefit from percutaneous release of pulley. There are other causes of flexion abnormality/deformity of the fingers

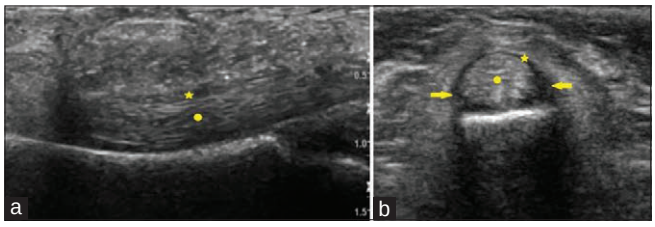

Figure 2: Longitudinal (a) and axial (b) US image of the finger demonstrating normal flexor tendon (yellow dot), and pulley (yellow asterisk). Care is taken not to misinterpret the refractile shadowing of US beam as thickening of radial and ulnar aspect of the pulley (yellow arrows in b). US: Ultrasound

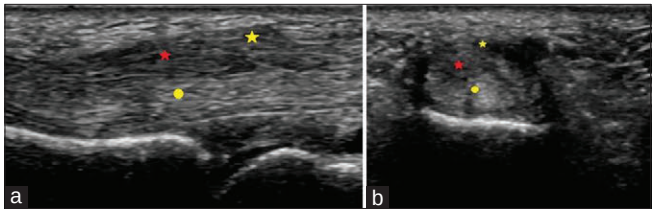

Figure 4: Longitudinal (a) and axial (b) US images of the finger demonstrating a focal hypoechogenic tendon surface nodule (red asterisk) adjacent to A1 pulley (yellow asterisk) causing triggering of flexor tendon (yellow dot). US: Ultrasound

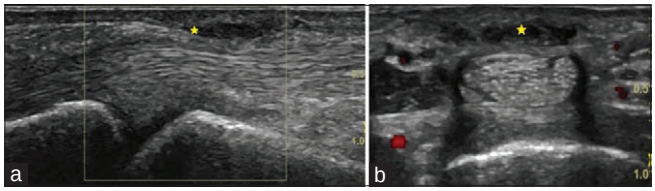

Figure 6: Longitudinal (a) and axial (b) US image of the ring finger showing a focal thickening of the palmar fascia in keeping with Dupuytren's contracture (asterisk). Note must be made that the pulley and tendon sheath appear unremarkable. US: Ultrasound

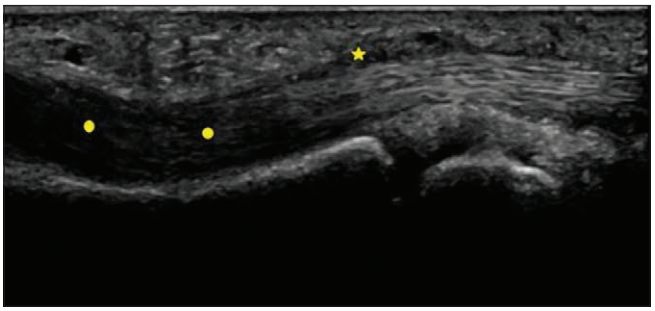

Figure 3: Longitudinal US image of the finger showing fusiform thickening of the A1 pulley (yellow asterisk) at the MCP joint level. The flexor tendon along the proximal phalanx level appears hypoechogenic due to its changed course causing anisotropy artifact (yellow dots). MCP: Metacarpophalangeal joint

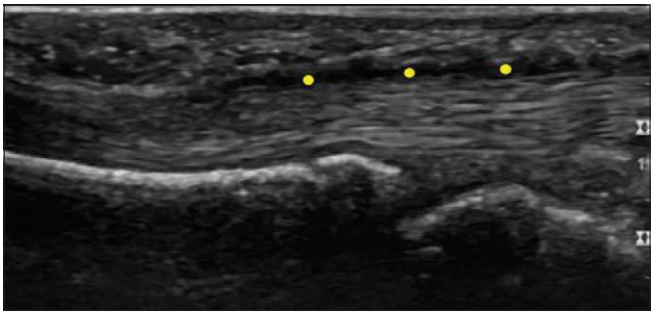

Figure 5: Longitudinal US image of the finger showing diffused thickening of the flexor tendon sheath in keeping with tenosynovitis (yellow dots). US: Ultrasound

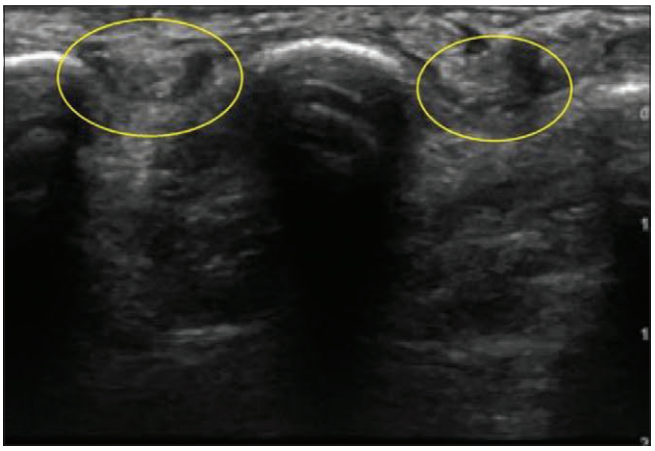

Figure 7: Transverse US image of the dorsal aspect of the hand showing radial dislocation of the extensor tendons of the middle and ring fingers (yellow rings) due to sagittal band tears causing flexion of the MCP joints mimicking fixed flexion deformity. US: Ultrasound, MCP: Metacarpophalangeal joint

such as Dupuytren's contracture, and sagittal band tear of the extensor tendons, which can mimic TF and it is important to exclude such patients from pulley intervention [Figures 6 and 7]. The clinical criterion for percutaneous pulley release sighted in the literature include triggering presence for at least 4 months and failure to respond to conservative management or steroid injections.[15]

Method of pulley release

Material necessary [Figure 8]:

- Sterile drape
- Chlorhexidine
- 25-gauge needle
- Methylprednisolone acetate 40 mg
- Bupivacaine hydrochloride (0.5%) 2 ml
- Appropriate dressing
- Lignocaine (1%) 2 ml
- 19-or 22-gauge needle.

The needle should be bent to get a diffuse curve, this can be easily achieved by threading the needle through a wider bore needle such as drawing up needle, the drawing up needles tend to have a blunt tip and also avoids inadvertent needle tip injury to the operator [Figure 9].

Procedure

Informed verbal or written consent is obtained. The procedure is performed under aseptic precautions. Following sterile draping, the target finger is fixed and kept in an extension posture. Under longitudinal US-guidance, a 25-gauge needle is used to inject 1% Lignocaine local anesthesia into the subcutaneous plane, the local anesthetic injection is helpful in more than one way, it can make the procedure more tolerable to the patient as well as the injectate can create a plane of fluid around the thickened pulley highlighting it and make it easy for the targeted release [Figure 10]. The needle insertion site can be chosen either distal or proximal to the thickened A1 pulley, it is advisable to choose the needle insertion site based on the natural inclination of the tendon desirably creating room for navigation of the bent needle (the operators prefer proximal to distal course). The prior prepared 19 or 22-gauge bent needle is inserted into the interface between the flexor tendon and the thickened pulley such that the leading end of the curve is pointed anteriorly and the cutting edge lies against the thickened pulley. Care must be taken to hold the hub of the needle firmly avoiding the turning the needle away from the targeted pulley. Once the needle tip is confirmed on the US to be located deep into the thickened pulley, the hub of the needle is gently pressed against the skin that will lift the tip of the needle and engage the cutting edge against the pulley. The needle should then be retracted from distal to proximal aspect (or proximal to distal aspect) until the needle tip snaps off the thickened pulley which is usually visible on US and also physically felt by the patient as well as the operator [Figure 11]. Transverse images should be obtained to confirm the needle position being away from the digital neurovascular bundles [Figure 12 and Video Clip 1]. The procedure should

Figure 8: Representational image of the kit necessary for the percutaneous release of the pulley including 25 g needle for local anesthetic injection, 22 g needle for cutting the pulley, red drawing up needle to aid bending of the needle, chlorhexidine skin preparation stick, gauze and sterile gloves

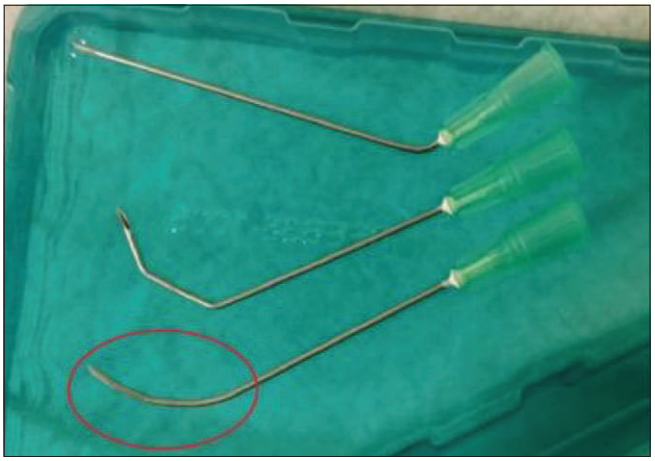

Figure 9: Image showing different kinds of needle bending including the smooth bent needle (red ring)

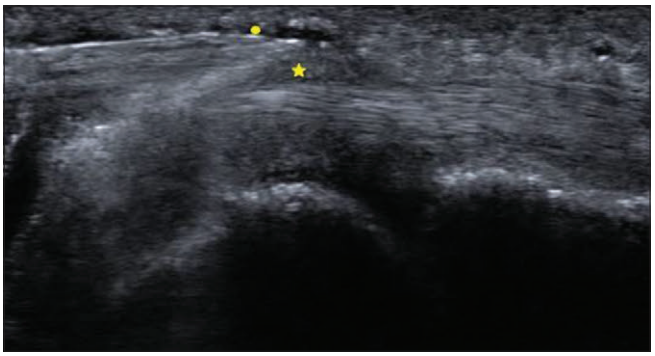

Figure 10: Longitudinal US of the finger demonstrating a plane of fluid from local aneasthetic injection (dot), highlighting the thickened pulley (asterisk). US: Ultrasound

be repeated 3–5 times until the pulley feels rather lax which confirms a successful release. The procedure is finished with an injection of methylprednisolone and bupivacaine mixture made up to around 2 ml into the tendon-pulley interface. The steroid solution can be seen as extravasating due to fenestrations created in the pulley due to successful release [Figure 13].

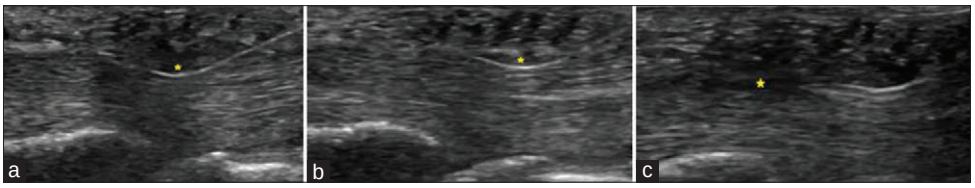

Figure 11: (a-c) Showing longitudinal ultrasound images of sequential scoring of the thickened A1 pulley (asterisk) using a curved needle

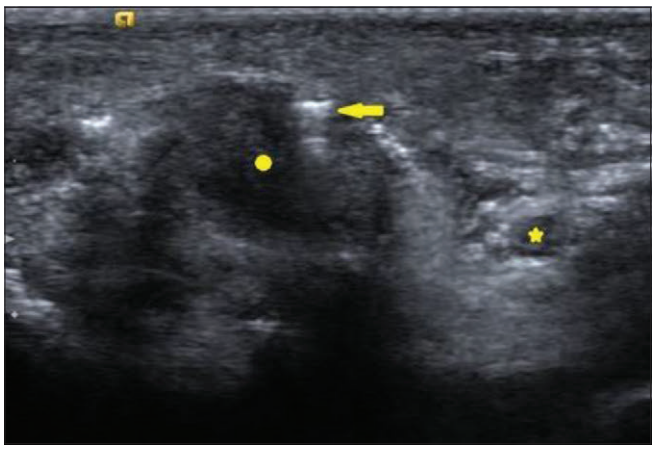

Figure 12: Transverse image demonstrating the needle (yellow arrow) under the pulley. The dot denotes the tendon and the asterisk denotes neurovascular bundle

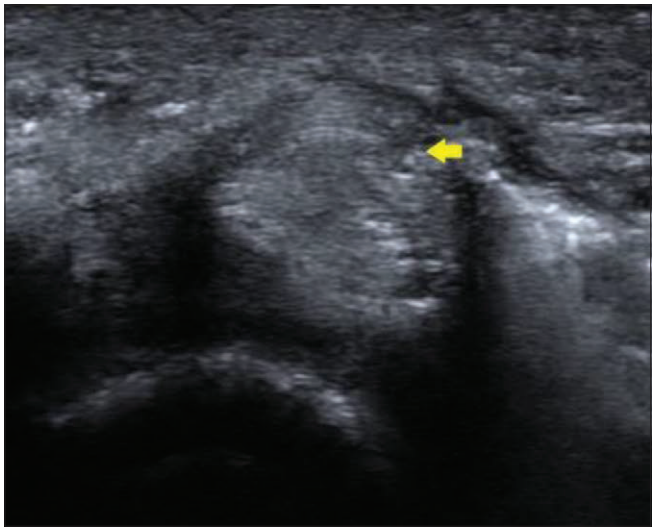

Figure 13: Transverse US image of A1 pulley demonstrate focal defect in pulley after percutaneous release (arrow) and extravasation of steroid outside pulley through the defect. US: Ultrasound

The result is usually a partial thickness scoring against the thickened pulley rather than a full thickness release, but it is sufficient as the bulk of the thickened pulley is reduced by cutting down few pulley fibers to restore the smooth gliding of tendon. The phenomenon of bowstringing due to complete pulley release does not apply to A1 pulley and rather related to A2 pulley loss. Precaution, however, is essential to avoid any injury to flexor tendon during the procedure and hence a continuous US monitoring is essential.

Technique of needle curving

A smooth curve of the needle can be obtained by threading the needle through a wider bore needle, preferably a drawing-up needle which has blunt tip to avoid inadvertent needle stick injury to the operator. The needle should be bent such that the bevel face of the needle is facing 90° to the desired cutting/scalpel end, this enhances the sharpness of the needle tip. Once the desired length of the needle is threaded into the wider needle (usually by about 1 cm), the cutting needle is gently drawn backward applying a bending force which will allow the needle to bend at the tip of the wider needle. The needle should be pulled back in regular increments till it comes out completely and a uniform needle bending is obtained [Figure 14]. Alternatively, an artery clip forceps can be used to bend the needle but often it is difficult to create a uniform/smooth bend by this technique.

Pain diary and follow up

The procedure is followed by issuing of 2-week pain/symptoms diary to assess the symptomatic relief from the procedure which includes a 0 to 10 pain scale to be tabulated before the procedure, after the procedure, first few days up to 2 weeks. The patients are also encouraged to draft free text describing their symptomatic relief up to 6 weeks. The patients are also encouraged to document the symptomatic relief separately for pain and/or triggering. The patients get an automated clinical review with the referring clinicians after 6 weeks.

Discussion

TF is a common and often debilitating ailment, which when fails conservative treatment, a percutaneous release of the offending thickened pulley has shown promising results in the previous studies. The advantage of a percutaneous procedure is, i.e., a short outpatient procedure with short recovery time and avoidance of surgical scarring and related complications. It also contributes toward offloading of already existing burden on the long surgical procedure waiting list and allows other essential surgical procedures to take priority. There are a few different techniques of release of the pulley and we describe a curved needle technique of A1 pulley release which is not novel but a modification of already existing needling techniques. The procedure is safe, effective, and minimally invasive intervention performed under US-guidance with minimal complications. A needle with a smooth curve is effective and easy to handle as compared to acutely bent needles which can turn on themselves making the procedure ineffective as well as operationally difficult and the straight needle which does

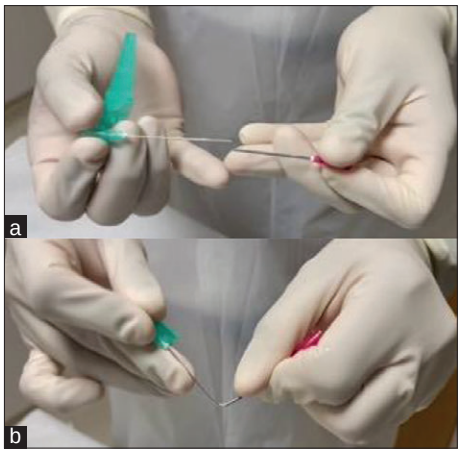

Figure 14: (a and b) Demonstrating technique of uniform needle bending for percutaneous release

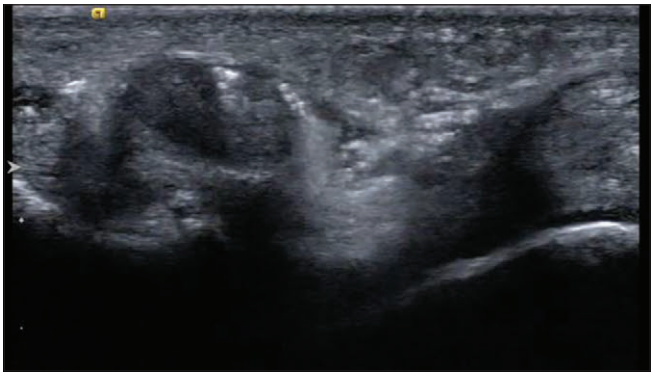

Video Clip 1: Demonstrating needle sliding between the tendon and the thickened pulley

not score the thickened pulley all the way. The procedure is outpatient based in the US suite of the radiology department, well tolerated by the patients with short recovery time and absence of surgical scarring and related complications. The initial experience based on the 2-week pain diary and feedback from the referring clinicians is excellent and promising. However, a formal audit and a case-control study is warranted to objectively analyze the short-term and long-term outcomes.

Financial support and sponsorship

Nil.

Conflicts of interest

There are no conflicts of interest.

References

1. Yin L, Guo R. Application and progress of high frequency ultrasound in trigger finger. Chin J Med Ultrasound 2016;11:87 5-80.
2. Nikolaou VS, Malahias MA, Kaseta MK, Sourlas I, Babis GC. Comparative clinical study of ultrasound-guided A1 pulley release versus open surgical intervention in the treatment of trigger finger. World J Orthop 2017;8:163-9.
3. Wainberg MC, Keith AB, Silver JK. Trigger finger: Essentials of Physical Medicine and Rehabilitation. 4th ed. Philadelphia: Elsevier; 2020.
4. Paulius KL, Maguina P. Ultrasound-assisted percutaneous trigger finger release: Is it safe? Hand (N Y) 2009;4:35-7.
5. Rajeswaran G, Healy JC, Lee JC. Percutaneous release procedures: Trigger finger and carpal tunnel. Semin Musculoskelet Radiol 2016;20:432-40.
6. Rojo-Manaute JM, Capa-Grasa A, Del Cerro-Gutiérrez M, Martínez MV, Chana-Rodríguez F, Martín JV. Sonographically guided intrasheath percutaneous release of the first annular pulley for trigger digits, part 2: Randomized comparative study of the economic impact of 3 surgical models. J Ultrasound Med 2012;31:427-38.
7. Lee SH, Choi YC, Kang HJ. Comparative study of ultrasonography-guided percutaneous A1 pulley release versus blinded percutaneous A1 pulley release. J Orthop Surg (Hong Kong) 2018;26:2309499018772368.
8. Lapègue F, André A, Meyrignac O, Pasquier-Bernachot E, Dupré P, Brun C, *et al.* US-guided percutaneous release of the trigger finger by using a 21-gauge needle: A prospective study of 60 cases. Radiology 2016;280:493-9.
9. Hoang D, Lin AC, Essilfie A, Minneti M, Kuschner S, Carey J, *et al.* Evaluation of percutaneous first annular pulley release: Efficacy and complications in a perfused cadaveric study. J Hand Surg Am 2016;41:e165-73.
10. Guo D, Guo D, Guo J, McCool LC, Tonkin B. A cadaveric study of the thread trigger finger release: The first annular pulley transection through thread transecting technique. Hand (N Y) 2018;13:170-5.
11. Fiorini HJ, Santos JB, Hirakawa CK, Sato ES, Faloppa F, Albertoni WM. Anatomical study of the A1 pulley: Length and location by means of cutaneous landmarks on the palmar surface. J Hand Surg Am 2011;36:464-8.
12. Makkouk AH, Oetgen ME, Swigart CR, Dodds SD. Trigger finger: Etiology, evaluation, and treatment. Curr Rev Musculoskelet Med 2008;1:92-6.
13. Brozovich N, Agrawal D, Reddy G. A critical appraisal of adult trigger finger: Pathophysiology, treatment, and future outlook. Plast Reconstr Surg Glob Open 2019;7:e2360.
14. Bianchi S, Gitto S, Draghi F. Ultrasound features of trigger finger: Review of the literature. J Ultrasound Med 2019;38:3141-54.
15. Rajeswaran G, Lee JC, Eckersley R, Katsarma E, Healy JC. Ultrasound-guided percutaneous release of the annular pulley in trigger digit. Eur Radiol 2009;19:2232-7.

Review Article

Bone Tumor Imaging: An Update on Modalities and Radiological Findings

Parham Shojaie[1,2], M. Afzali[1,2], Neha Nischal[1], Karthikeyan P. Iyengar[3], Mina Malak Abed Yousef[3], Rajesh Botchu[1]

[1]Department of Musculoskeletal Radiology, Royal Orthopaedic Hospital, [2]Aston Medical School, College of Health and Life Sciences, Aston University, Birmingham, [3]Department of Orthopaedics, Southport and Ormskirk Hospital NHS Trust, Southport, UK

Abstract

Radiological imaging forms an integral part in the diagnostic and management algorithm of patients with bone tumors. Although plain radiography tends to be the first line of imaging in a patient with suspected bone tumor, advances in technology, computer software, physics and techniques have expanded the modalities available to us in the form of computed tomography (CT), magnetic resonance imaging, and various scintigraphy techniques. These imaging modalities in combination with a clinician led multi-disciplinary team help in the exact diagnosis, appropriate management, and monitoring of patients for recurrence. In this narrative review, we highlight the current applications of conventional imaging, the emerging role of hybrid imaging, and explore the future directions of radiological imaging in the management of patients with bone tumors.

Keywords: ^{18}F-FDG positron emission tomography/computed tomography, bone neoplasms, computed tomography, magnetic resonance imaging, nuclear medicine, positron emission tomography/computed tomography, radiography

Introduction

The diagnostic process of bone tumors relies on various imaging modalities, ranging from conventional radiography, which can provide a two-dimensional (2-D) image of a bone lesion, structural imaging using computed tomography (CT) and magnetic resonance imaging (MRI); scintigraphy techniques, to more revolutionized hybrid techniques, such as positron emission tomography (PET), PET/CT, and PET/MRI. These can provide whole body imaging and provide simultaneous details on the morphology and anatomy of the bone tumors.[1] These imaging methods are not limited to the diagnosis; for instance, CT-guided interventions aid clinicians in performing procedures such as tumor ablation or biopsy.[2]

In the 1970s, bone tumors were mainly evaluated with radiographs and its importance as a primary imaging modality has not changed over the decades.[2] However, with technological advancement, further imaging modalities have been introduced, such as CT, MRI, and radionuclide imaging, to increase the accuracy of bone tumor evaluation.[2] Despite all the advancements, studies have shown that conventional radiographs and MRI remain the imaging modalities of choice in evaluating bone lesions.[3]

Access this article online

Quick Response Code:

Website: https://journals.lww.com/jajs

DOI: 10.4103/jajs.jajs_31_23

Furthermore, the main question remains to be the contribution level of other imaging modalities and the extent they can contribute toward diagnosing and management of bone tumors.[3]

The other is the need for a systematic approach to imaging reports, which can lead to decrease in variability and affect the accuracy of diagnosis.[4]

Artificial intelligence (AI) is an emerging area of research and debate in the delivery of patient care.[1] Some studies have found that the AI-based model can be utilized to classify bone tumors in some anatomical locations with a high performance.[5]

As bone tumor diagnosis ought to be precise and accurate, future research will focus on the new imaging techniques and

Address for correspondence: Dr. Rajesh Botchu, Department of Musculoskeletal Radiology, Royal Orthopedic Hospital, Bristol Road South, Northfield, Birmingham, UK.
E-mail: drbrajesh@yahoo.com

Submitted: 20-Mar-2023 **Revised:** 30-Mar-2023
Accepted: 30-Mar-2023 **Published:** 19-Jul-2023

This is an open access journal, and articles are distributed under the terms of the Creative Commons Attribution-NonCommercial-ShareAlike 4.0 License, which allows others to remix, tweak, and build upon the work non-commercially, as long as appropriate credit is given and the new creations are licensed under the identical terms.

For reprints contact: WKHLRPMedknow_reprints@wolterskluwer.com

How to cite this article: Shojaie P, Afzali M, Nischal N, Iyengar KP, Yousef MM, Botchu R. Bone tumor imaging: An update on modalities and radiological findings. J Arthrosc Jt Surg 2023;10:131-8.

their use in the early diagnosis, appropriate management, and effective monitoring of patients with bone neoplasms.[2]

A concerted effort needs to be undertaken to improve the diagnostic accuracy of various forms of radiological imaging in the assessment of bone tumors including the use of hybrid imaging and the evolving role of AI.[6]

This article explores the latest advancements in imaging modalities that can aid diagnosis, management, and monitoring of patients with bone neoplasms. Possible future advances will also be addressed, including the role of AI in diagnosis of bone tumors.

Radiography

Radiography remains the primary imaging modality recommended for diagnosing bone tumors.[4] Further imaging can evaluate the extension of the lesion and assist in the staging of the tumor.[7] The principles of radiography allow healthcare professionals to assess the morphology of the tumor in various aspects such as the location, margin, pattern of bone destruction, periosteal reaction (PR), matrix, soft-tissue involvement, or skip lesions.[7,8] Furthermore, this imaging allows the observation of bone tumor complications such as pathological fractures.[9]

Combining these pieces of information with the patient's age can narrow the list of differential diagnoses, and in 80%–90% of cases, this information is enough to make a diagnosis.[7,8,10]

Radiographs must be viewed systematically using the previously mentioned factors for an accurate differential diagnosis.[7]

Age of the patient

Generally, certain bone tumors occur in a specific age group. Even though some exceptions exist, it is still paramount that the patient's age be assessed first.[8] For instance, Ewing's sarcoma mainly affects patients in their teenage years. However, a similar lesion in a 40-year-old patient is more likely to be metastasis or multiple myeloma.[4] In addition, some bone tumors, such as osteosarcoma, follow a bimodal pattern with two peak ages; one is primary conventional osteosarcoma in teenagers while, the other arises from the pagetic or irradiated bone in patients over 50 years old[4] [Table 1].

Location

Reviewing the location of the bone tumor is essential. There are three crucial factors in assessing the correlation of bone tumor location with the bone, first identifying the affected bone. Second, describing the transverse and longitudinal location of the lesion.[11]

Identifying the exact location of the bone tumor is vital as some bone tumors affect specific bones and areas of the bone. For instance, while metastases can affect any bones in the body, they tend to affect bones with high red marrow content, including vertebrae, ribs, pelvis, and long bone ends.[12]

Primary bone tumors can occupy central, eccentric or a cortically based epicenter locations. These can be intramedullary, cortical, periosteal, and parosteal. Moreover, longitudinally bone tumors can be present on epiphysis, metaphysis, or diaphysis of tubular bones[12] [Figures 1 and 2].

Zone of transition and margin

The margin between the abnormal lesion and normal bone can be a determinant factor for the aggression of

Table 1: Relationship of patient's age and common bone tumors[8,10]

Age range (years)	Benign osseous tumors	Malignant osseous tumors
<5	Eosinophilic granuloma, osteofibrous dysplasia	-
5-10	Unicameral bone cyst, aneurysmal bone cyst, nonossifying fibroma, fibrous dysplasia, osteoid osteoma, osteoblastoma, eosinophilic granuloma	-
10-20	Fibrous dysplasia, osteoid osteoma, fibroma, nonossifying fibroma, aneurysmal bone cyst, chondroblastoma, osteoblastoma, giant cell tumor, osteochondroma, multiple hereditary exostosis, enchondroma, chondromyxoid fibroma	Ewing's sarcoma, osteosarcoma
20-40	Enchondroma, giant cell tumor, osteoblastoma, osteoid osteoma, chondromyxoid fibroma, fibrous dysplasia	Chondrosarcoma, periosteal osteosarcoma, pleomorphic sarcoma, osteosarcoma (parosteal), adamantinoma
>40	Fibrous dysplasia	Chondrosarcoma, chordoma, lymphoma, metastases, multiple myeloma, osteosarcoma (Paget's associated), plasmacytoma, pleomorphic sarcoma, metastatic disease

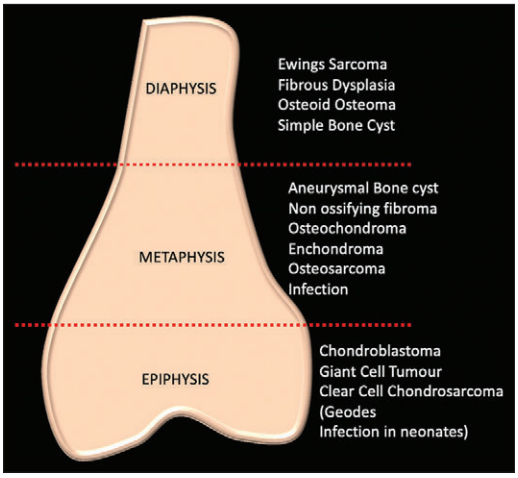

Figure 1: Schematic showing location of various bone tumors

the tumor. For instance, tumors with sclerotic margins are likely nonaggressive lesions.[7] Conversely, bone tumors with nonsclerotic margins are possibly aggressive.[7] Moreover, as the margin width between the lesion and bone structures gets bigger, the risk of malignancy increases.[7] The transition zone's width and the margin's morphology are usually correlated. For instance, malignant tumors will usually have a wide nonsclerotic margin.[7] However, it is paramount to note that benign lesions such as giant cell tumors might not follow this pattern as they usually have been found to have nonsclerotic margins with narrow transition zone[7] [Figure 3].

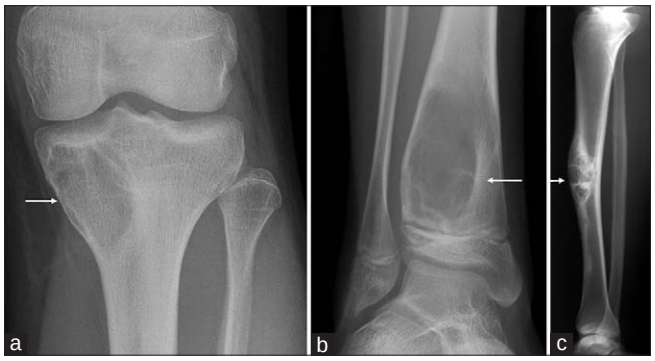

Figure 2: Figure demonstrating showing GCT (epiphyseal location-arrow) (a), ABC (metaphyseal location-arrow) (b) and adamantinoma (diaphyseal location-arrow) (c)

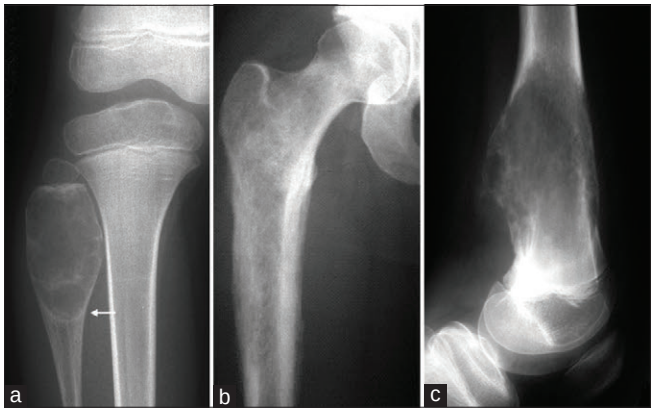

Figure 3: Anteroposterior (AP) of knee showing narrow zone of transition (arrow) (a) and AP (b) and lateral (c) of femur demonstrating wide zone of transition

Pattern of bone destruction

On radiographs, various terms are used to describe the pattern of bone destruction, such as "geographic," which indicates a well-defined and generally the least aggressive form of the lesion.[7] There are more aggressive patterns which include "moth-eaten" pattern that refers to an irregular pattern at the edges seen in malignancies such as Ewing's sarcoma or multiple myeloma.[13] The other aggressive appearance that can be confused with moth-eaten is the Permeative pattern which can be seen in lymphoma, myeloma, Ewing's sarcoma and neuroblastoma. This pattern indicates the invasion of bone tumors through the cancellous bone without destroying all the trabeculae structures.[13] The misinterpretation of these two aggressive patterns, moth-eaten and permeative, does not grossly change the management plan as both imply characteristics of malignant tumors[7] [Figure 3].

Periosteal reaction

PR is considered a nonspecific factor for tumor malignancy.[7] However, a healthcare professional should be familiar with the spectrum appearances of PR and detect its presence. These PR changes range from the lamellated pattern to solid, speculated, Codman's triangle, or expanded shell patterns[14] [Figure 4].

According to the available data, the prevalence of PR is varied between different types of bone tumors. For instance, Ewing sarcoma will always present with a form of PR and only 37% of solitary metastasis present with a degree of PR.[14]

Matrix

Some tumors comprise a unique matrix, which can be cartilage or bone-producing (osteoid).[7,15] The density of the bony matrix in bone tumors can imply their aggression level. Generally, tumors that produce less dense bony structures (amorphous osteoid) are more aggressive than bone tumors that produce

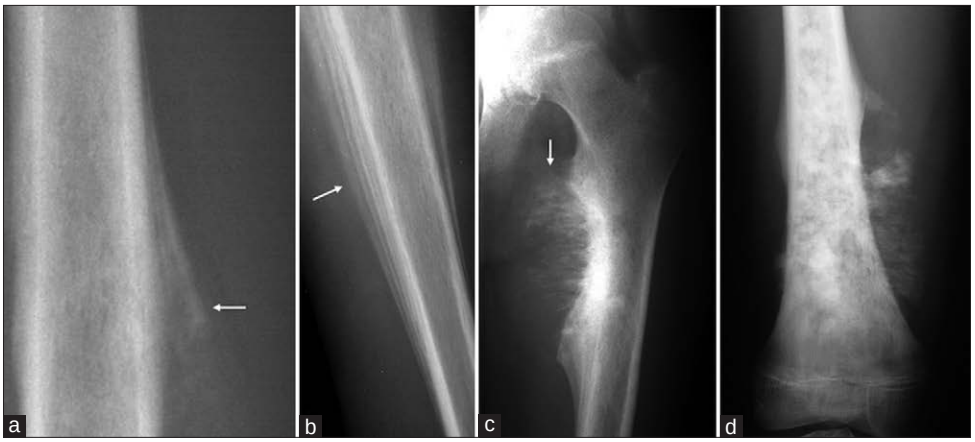

Figure 4: Figure demonstrating Codman's triangle (a), lamellated "onion skin" pattern (b), hair on end appearance (c) and mixed pattern (d) of periosteal reaction (arrow)

well-organized and denser bony matrix.[7] Furthermore, tumors that produce chondroid matrix appear stippled with popcorn or rings and arcs appearance[7,15] [Figure 5].

Soft-tissue involvement

Even though other advanced methods of imaging, such as CT and MRI, will best demonstrate any invasion of the tumor to the adjacent soft tissue and neurovascular structures. Radiographs can demonstrate bone tumor invasion into soft tissues to some extent.[16,17] Soft-tissue involvement in conventional radiography is illustrated as an obliteration of fat planes and poorly defined components.[16,17]

Pathological fracture

Fractures are a decisive factor in bone tumors. However, the pitfall of this component is the high level of radiographic similarities between pathological fractures and stress fractures.[18] It is essential to obtain patient's history to differentiate stress fractures from pathological fractures, as stress fractures usually correlate with increased activity.[18] Furthermore, pathological fractures usually occur in three locations: the subtrochanteric femur, junction between the humeral head and metaphysis and the spine. However, up to 10% of pathological fractures require further imaging for accurate diagnosis.[18]

Skip lesions

According to Enneking and Kagan., skip lesion is the presence of secondary small focus of tumor separate from the primary lesion. Radiographs might not detect these skip lesions but can be seen on MRI or bone scan[19,20] [Figure 6].

Computed Tomography

CT has similar principles as radiography. This imaging modality provides images with very thin slices (<1mm) to accurately detect the anatomical location of bone tumors.[1,2] This technique has superiority in detecting various elements of the tumors based on different densities.[21]

Moreover, it has a sensitivity of 71% to 100% and a specificity of 56% in detecting bone metastases, making it more suitable than radiography.[12,21] CT can also help to stage tumors by identifying pulmonary metastasis on CT of chest[21] [Figures 7 and 8].

CT enables to perform image guided biopsies and tumoral radiofrequency, chemical, microwave or cryo-ablation[2] [Figure 9]. Biopsy tract contamination is a significant concern, and surgical removal of the biopsy tract should be included in the surgical plan.

Magnetic Resonance Imaging

MRI is the gold standard for the detailed evaluation of bone tumors and tumour-like lesions. There are several advantages for the MRI over other imaging modalities, such as its ability to differentiate between different types of bone tumors and detect early bone marrow involvement. It can demonstrate components such as cartilage, vascular tissue, fat, liquid, and hemosiderin, which may be indistinguishable on other imaging modalities.[22] It can narrow the differential diagnosis and provide additional information to aid treatment planning.[22]

One of the significant advantages of MRI is its ability to detect bone marrow involvement. Faint lytic/sclerotic bone

Figure 5: AP radiograph of tibia showing ground-glass matrix of fibrous dysplasia (a), proximal phalanx showing chondroid matrix (b) and distal femur showing osteoid matrix (c) arrow. AP: Anteroposterior

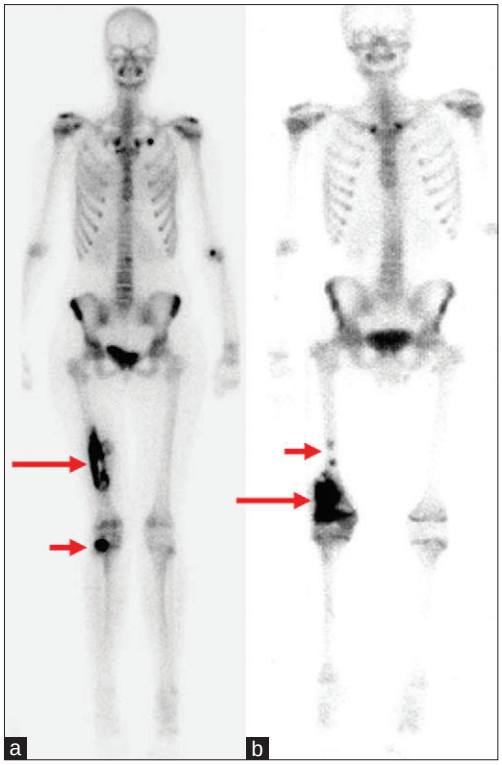

Figure 6: Bone scan showing osteosarcoma of right distal femur (long arrow) with proximal tibial skip metastasis (short arrow) (a) and osteosarcoma of right distal femur (long arrow) with femoral skip metastasis (short arrow) (b)

lesions can be difficult to visualize using only radiographs, and MRI is superior to other imaging modalities in detecting bone marrow lesions. This phenomenon is critical as early detection of bone marrow involvement can help plan the appropriate management strategy. MRI is also helpful in local staging and surgical planning because it assesses the degree of intramedullary extension and invasion of adjacent structures such as physis, joints, muscle compartments, and neurovascular bundles. Additionally, MRI can be used for restaging after neoadjuvant therapy and for follow-up.[22]

Magnetic resonance imaging protocols

Imaging protocols for bone tumors vary between institutions, but a combination of T1 imaging and fluid-sensitive sequences (e.g., T2, Proton Density Fat Saturated (PDFS), Short Tau Inversion Recovery (STIR)) in different planes are required at a minimum. Gadolinium-enhanced MRI sequences can provide additional information, particularly to distinguish between solid and necrotic/cystic components within a lesion that generally do not enhance but not essential.[23]

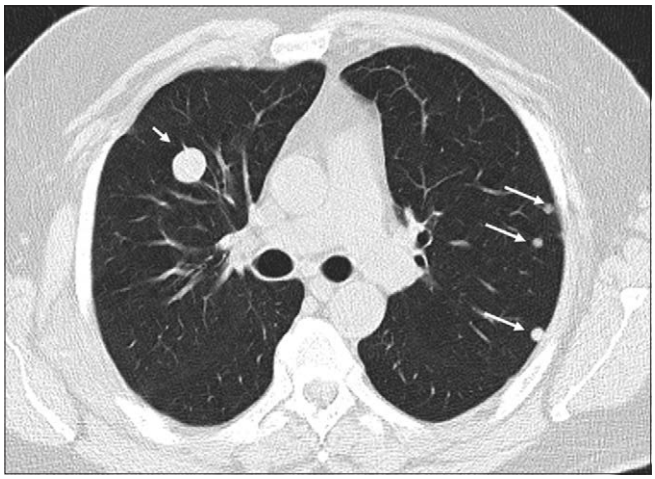

Figure 7: Axial CT of the chest showing pulmonary metastases (arrows). CT: Computed tomography

Figure 8: AP radiograph of femur (a), CT coronal (b) and axial (c) showing stress fracture with thick periosteal reaction (arrow)

Whole-body magnetic resonance imaging for oncological staging

Whole-body MRI is sometimes used for staging bone tumors, particularly childhood bone tumors such as Ewing sarcoma and osteosarcoma. This involves the acquisition of wide-field-of-view images over large body regions using limited sequences, such that the entire body from head to toe is imaged. Whole-body MRI is particularly valuable in identifying small intramedullary osseous metastasis that may be occult on CT and nuclear imaging. Additionally, it avoids ionizing radiation exposure[23] [Figures 10-12].

Radionuclide Imaging

Radionuclide imaging is a technique that uses radioactive tracers to assess and visualize the function of different organs and tissues, including bones.[12] In this technique, the radiotracers are injected into the body.[24] Subsequently, the gamma rays emitted by the radiotracers are detected by a gamma camera, generating a 2-D image to assess the biological activity of the investigated tissue.[12,24] It is worth noting that the integration of tomography allows three-dimensional imaging with a Gamma camera called single-photon emission CT (SPECT).[24,25]

The two main types of radioisotopes used to assess skeletal metastasis are osteotropic and oncotropic radioisotopes.[12] Radioisotopes that specifically target bones, known as osteotropic radioisotopes, can accumulate at the site of active bone deposition, regardless of the underlying cause. Methylene diphosphonate (99mTc-MDP), a metastable technetium 99 labeled diphosphonate, is the most used osteotropic agent in skeletal scintigraphy due to its effectiveness, low price, extensive accessibility, and advantageous radiation dosage profile.[12] PET uses an osteotropic compound called ^{18}F-labelled sodium fluoride (NaF), which has a higher extraction rate compared to 99mTc-MDP.[12] Nonetheless, its use is limited by its relatively low specificity when used alone and the need for a cyclotron to produce it.[12] Hybrid imaging techniques may be required to improve diagnostic specificity.[12]

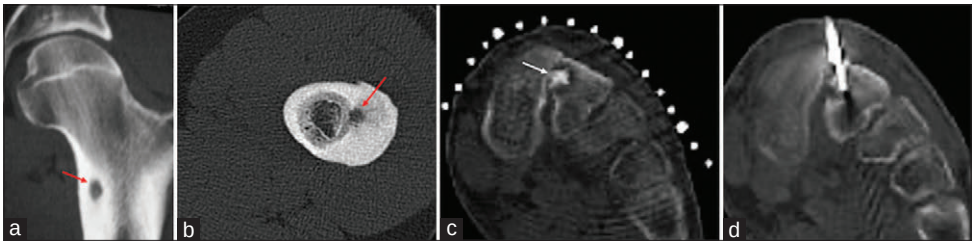

Figure 9: CT demonstrating osteoid osteoma of left proximal femur (arrows [a and b]) and left second metatarsal (c) treated with RFA (d). RFA: Radiofrequency ablation

In contrast, oncotropic radioisotopes are taken up by malignant cells and are further sub-classified into specific and nonspecific oncotropic radioisotopes.[12] There are three main types of radionuclide imaging used in the imaging of bone tumors: planar scintigraphy, SPECT imaging, and PET.[12]

Planar Bone Scintigraphy

PBS is a commonly used radionuclide technique for identifying skeletal metastasis; this is mainly a result of its widespread availability.[26] To gain a comprehensive understanding of the findings from PBS, it is imperative to acquire knowledge on the characteristic features of a normal PBS. In a healthy adult, bone activity should be symmetrical throughout the skeletal system.[27] Scant renal and soft-tissue activity is also typically observed, along with urinary bladder activity.[27] Areas of increased uptake, referred to as hotspots, correlate with osteoblastic activity and may indicate the presence of bone tumors.[28] Scintigraphy using planar imaging is advantageous as it enables the visualization of the entire skeleton, including regions that are not typically part of a skeletal survey.[12] Scintigraphy has high sensitivity, allowing for early detection of skeletal metastases, and can detect abnormal radio-tracer accumulation on a bone scan with only a slight change in the lesion-to-normal bone ratio.[12] For detecting bone metastasis, bone scintigraphy has a sensitivity of 78% and a specificity of 48%. As a result, it is a valuable tool for detecting osteoblastic bone metastases, which can be identified up to 18 months earlier on bone scintigraphy than on radiographs[12] [Figure 6].

It is vital to consider the limitations of bone scintigraphy as a diagnostic tool for detecting bone metastases. As osteotropic radioisotopes are widely used for this purpose, they are not specific to malignant lesions and can result in false positive results.[29,30] Moreover, the inadequate precision of bone scintigraphy in assessing anatomical information hinders its ability to determine benign lesions and the precise location of the lesion.[29,31] Another limitation is the lack of radio-tracer accumulation in osteolytic lesions, such as renal cell carcinoma metastasis, which limits its sensitivity in evaluating metastases with osteolytic lesions.[32] False-negative results can also occur since bone scintigraphy primarily assesses the bone deposition process rather than the tumor's proliferation.[33]

Furthermore, evaluating focal accumulation of the radioisotope in the spine often requires further imaging modalities, as it may result from degenerative disease rather than bone metastasis.[33] It is important to note that extensive bone metastases may initially appear normal on bone scans, a phenomenon known as a super scan.[34,35] A super scan is characterized by diffuse increased skeletal radioisotope uptake in relation to soft tissue, with little or no renal activity.[36] Therefore, careful renal activity and uptake inspection is crucial for excluding super scans.[12]

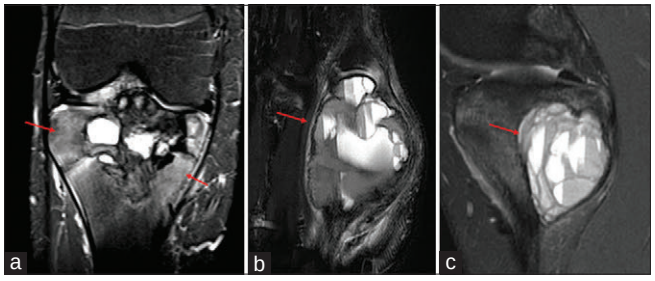

Figure 10: STIR images showing osseous edema (arrows) adjacent to chondroblastoma (a), fluid-fluid levels (arrow) in ABC (b and c)

Single Photon Emission Computed Tomography Imaging

SPECT is a technique that utilizes a gamma camera and radiotracers to generate tomography images.[37] For skeletal imaging, 99mTc-MDP is injected as the radiotracer. 2–6 h after intravenous administration of the radiotracer, the gamma camera is used, which rotates 360 degrees to reconstruct adequate images of the musculoskeletal system.[1,38] SPECT allows for better spatial resolution compared to PBS, enhancing the bone scintigraphy's sensitivity. This is especially useful when assessing anatomically complex areas like the spine and pelvis.[39,40] One of the main limitations of SPECT is its limited specificity, as it may not distinguish between benign and malignant bone tumors, which can lead to false-positive results.[39] Additionally, SPECT provides physiological information on tissues and not anatomical information, which limits its accuracy in the localization of the lesions.[41]

Positron Emission Tomography Imaging

PET imaging utilizes the tomography technique to create images of metabolically active tissues.[12] The radiopharmaceuticals used in PET imaging differ from those used in SPECT

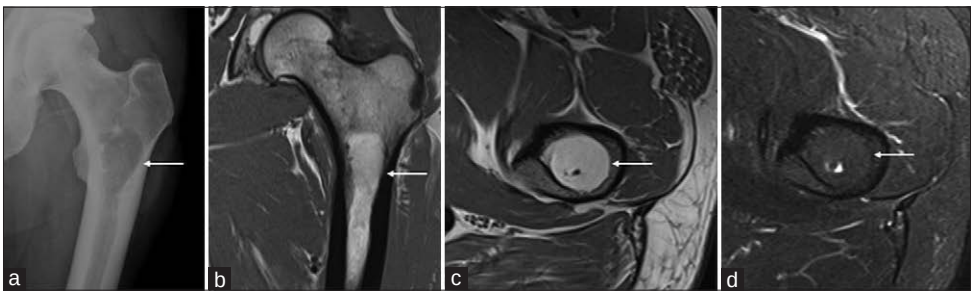

Figure 11: AP radiograph of left femur (a) T1 coronal (b), axial (c), and STIR axial (d) showing intraosseous lipoma (arrow)

Figure 12: Coronal T1 (a) and STIR (b) showing infarcts in distal femur and proximal tibia

and PBS as they undergo positron decay.[42] When the radiopharmaceutical accumulates in the tissue, it emits a positron that annihilates with an electron of the tissue, resulting in the emission of two photons in opposite directions.[43] The gamma camera detects these high-energy photons, and a computer reconstructs the information into an image.[43] The two most common radiotracers used for bone tumor imaging are ^{18}F-fluorodeoxyglucose (FDG) and ^{18}F-Sodium Fluoride (NaF).[12,44]

FDG is a glucose analogue that accumulates in cells with high glucose metabolism, such as cancer cells.[12] On the other hand, NaF is a bone-seeking radiopharmaceutical that accumulates in areas of increased bone turnover, such as bone metastases.[12] Both radiotracers effectively detect bone tumors, and their choice depends on various factors, including the type of tumor being imaged and the clinical question being asked.[12] The available literature indicates that ^{18}F-NaF PET is more sensitive and specific in detecting metastases, specifically osteolytic lesions, compared to PBS and SPECT.[12] A study conducted by Cook *et al.* concluded that ^{18}F-FDG PET is superior to PBS in identifying osteolytic lesions caused by breast cancer metastasis. However, the same research also revealed that PET could not detect osteoblastic lesions due to their lower metabolic activity.[45] It is worth noting that PET is much more expensive than SPECT and utilizes shorter-lived, harder-to-find radiotracers.[46]

Hybrid Imaging

As previously mentioned, radionuclide imaging provides molecular information on the lesions rather than anatomical information.[47] As such, combining the two imaging techniques can be helpful in the management and monitoring of patients with bone metastasis.[47] The well-established forms of hybrid imaging are SPECT/CT and PET/CT.[48] The sensitivity and specificity of PET/CT in skeletal malignancy are 100% and 97%, respectively, compared to 98% and 56% with ^{18}F FDG-PET alone.[12] It is worth mentioning that PET/MRI is a more recent technology which has been found to be more sensitive at finding clinically relevant information than PET/CT.[48] Therefore, PET/MRI has the greatest potential for the early detection of bone tumors.[12]

Future Directions in Bone Tumor Imaging

Advancements in technology and radiopharmaceutical development are expected to have a promising impact on the future of bone tumor imaging. In addition, hybrid imaging methods such as PET/MRI and SPECT/CT are gaining popularity as they provide anatomical and functional information in a single scan.[1] These developments offer exciting possibilities for the future of bone tumor imaging, potentially leading to more accurate diagnoses and targeted treatments for patients.

AI is also being integrated into imaging systems, particularly in radiography.[49] The primary purpose of this model is to minimize the misdiagnosis of bone tumors by radiologists who are not specialized in musculoskeletal oncology.[5]

Some studies have shown that AI algorithms have a 6.3% higher accuracy in detecting a bone tumor when compared to radiology residents.[50] However, the detection rate of bone tumors with AI algorithms could not be assessed as all the data sets had a lesion, and no normal radiographs were present.[50] Moreover, the main drawback of AI is that the algorithms require experts to manually check the quality of data inputs, which is time-consuming and expensive.[3]

Conclusion

There is no doubt, radiological imaging forms a crucial element in the diagnosis, management decisions, monitoring and surveillance of patients with bone tumors. Plain radiography, CT, MRI, and radionuclide imaging have their own advantages and disadvantages. However, selection of appropriate modality and application of hybrid imaging is essential in the management of such patients particularly in the complex clinical presentations. Emerging technology such as AI will have evolving role in the diagnostic algorithm of bone neoplasm management as we understand the applicability, diagnostic accuracy, and cost-benefit analysis of innovative techniques.

Financial support and sponsorship

Nil.

Conflicts of interest

There are no conflicts of interest.

References

1. Goyal N, Kalra M, Soni A, Baweja P, Ghonghe NP. Multi-modality imaging approach to bone tumors – State-of-the art. J Clin Orthop Trauma 2019;10:687-701.
2. Mintz DN, Hwang S. Bone tumor imaging, then and now: Review article. HSS J 2014;10:230-9.
3. Rajakulasingam R, Botchu R. Current progress and future trends in imaging of musculoskeletal bone tumours. J Clin Orthop Trauma 2021;23:101622.
4. Gemescu IN, Thierfelder KM, Rehnitz C, Weber MA. Imaging features of bone tumors: Conventional radiographs and MR imaging correlation. Magn Reson Imaging Clin N Am 2019;27:753-67.
5. Park CW, Oh SJ, Kim KS, Jang MC, Kim IS, Lee YK, *et al.* Artificial intelligence-based classification of bone tumors in the proximal femur

on plain radiographs: System development and validation. PLoS One 2022;17:e0264140.
6. Vogrin M, Trojner T, Kelc R. Artificial intelligence in musculoskeletal oncological radiology. Radiol Oncol 2020;55:1-6.
7. Umer M, Hasan OH, Khan D, Uddin N, Noordin S. Systematic approach to musculoskeletal benign tumors. Int J Surg Oncol (N Y) 2017;2:e46.
8. Miller TT. Bone tumors and tumorlike conditions: Analysis with conventional radiography. Radiology 2008;246:662-74.
9. Rizzo SE, Kenan S. Pathologic Fractures. [Updated 2023 Jan 15]. In: StatPearls [Internet]. Treasure Island (FL): StatPearls Publishing; 2023 Jan-. Available from: https://www.ncbi.nlm.nih.gov/books/NBK559077/. [Last accessed on 2023 Mar 18].
10. Yildiz C, Erler K, Atesalp AS, Basbozkurt M. Benign bone tumors in children. Curr Opin Pediatr 2003;15:58-67.
11. Ramachandran M, editor. Basic Orthopaedic Sciences. Boca Raton (FL): CRC Press; 2018.
12. O'Sullivan GJ, Carty FL, Cronin CG. Imaging of bone metastasis: An update. World J Radiol 2015;7:202-11.
13. Plant J, Cannon S. Diagnostic work up and recognition of primary bone tumours: A review. EFORT Open Rev 2016;1:247-53.
14. Wenaden AE, Szyszko TA, Saifuddin A. Imaging of periosteal reactions associated with focal lesions of bone. Clin Radiol 2005;60:439-56.
15. Taminiau AH, Bovée JV, van Rijswijk CS, Gelderblom HA, van de Sande MA. Cartilage tumours of bone. In: Bentley G, editors. European Surgical Orthopaedics and Traumatology. Berlin, Heidelberg: Springer. 2014. Available from: https://doi.org/10.1007/978-3-642-34746-7_206 [Last accessed on 2023 Mar 15].
16. Wyers MR. Evaluation of pediatric bone lesions. Pediatr Radiol 2010;40:468-73.
17. Priolo F, Cerase A. The current role of radiography in the assessment of skeletal tumors and tumor-like lesions. Eur J Radiol 1998;27 Suppl 1:S77-85.
18. Fayad LM, Kamel IR, Kawamoto S, Bluemke DA, Frassica FJ, Fishman EK. Distinguishing stress fractures from pathologic fractures: A multimodality approach. Skeletal Radiol 2005;34:245-59.
19. Enneking WF, Kagan A. "Skip" metastases in osteosarcoma. Cancer 1975;36:2192-205.
20. Kager L, Zoubek A, Kastner U, Kempf-Bielack B, Potratz J, Kotz R, *et al*. Skip metastases in osteosarcoma: Experience of the Cooperative Osteosarcoma Study Group. J Clin Oncol 2006;24:1535-41.
21. Choi J, Raghavan M. Diagnostic imaging and image-guided therapy of skeletal metastases. Cancer Control 2012;19:102-12.
22. Nascimento D, Suchard G, Hatem M, de Abreu A. The role of magnetic resonance imaging in the evaluation of bone tumours and tumour-like lesions. Insights Imaging 2014;5:419-40.
23. Kho J, Botchu R, James SL, Bone tumurs. Textbook of Radiology and imaging by David Sutton, 8th edition, Elsevier publishers. [In Print]. 2023, vol 1, chapter 62, pages 1-50.
24. Johansson L, Wehling M. Translational imaging research. In: Principles of Translational Science in Medicine. 2nd ed., Ch. 3.7.3. Boston, MA: Academic Press; 2015. p. 189-94.
25. Adams C, Banks KP. Bone scan. In: StatPearls. Treasure Island (FL): StatPearls Publishing; 2022. Available from: https://www.ncbi.nlm.nih.gov/books/NBK531486/. [Last updated on 2022 Aug 08].
26. Lambers FM, Kuhn G, Müller R. Advances in multimodality molecular imaging of bone structure and function. Bonekey Rep 2012;1:37.
27. Love C, Din AS, Tomas MB, Kalapparambath TP, Palestro CJ. Radionuclide bone imaging: An illustrative review. Radiographics 2003;23:341-58.
28. Chaudhuri TK, Chaudhuri TK. The "hot" spot in bone imaging. Semin Nucl Med 1983;13:75-7.
29. Agrawal K, Marafi F, Gnanasegaran G, Van der Wall H, Fogelman I. Pitfalls and limitations of radionuclide planar and hybrid bone imaging. Semin Nucl Med 2015;45:347-72.
30. Zhang Y, Zhao C, Liu H, Hou H, Zhang H. Multiple metastasis-like bone lesions in scintigraphic imaging. J Biomed Biotechnol 2012;2012:957364.
31. Cuccurullo V, Cascini GL, Tamburrini O, Rotondo A, Mansi L. Bone metastases radiopharmaceuticals: An overview. Curr Radiopharm 2013;6:41-7.
32. Bäuerle T, Semmler W. Imaging response to systemic therapy for bone metastases. Eur Radiol 2009;19:2495-507.
33. Rajarubendra N, Bolton D, Lawrentschuk N. Diagnosis of bone metastases in urological malignancies – An update. Urology 2010;76:782-90.
34. Roberts CC, Daffner RH, Weissman BN, Bancroft L, Bennett DL, Blebea JS, *et al*. ACR appropriateness criteria on metastatic bone disease. J Am Coll Radiol 2010;7:400-9.
35. Gnanasegaran G, Cook G, Adamson K, Fogelman I. Patterns, variants, artifacts, and pitfalls in conventional radionuclide bone imaging and SPECT/CT. Semin Nucl Med 2009;39:380-95.
36. Manohar PR, Rather TA, Khan SH, Malik D. Skeletal metastases presenting as superscan on technetium 99m methylene diphosphonate whole body bone scintigraphy in different type of cancers: A 5-year retro-prospective study. World J Nucl Med 2017;16:39-44.
37. Herscovitch P, Aminoff MJ, Daroff RB. Single-photon emission computed tomography (SPECT). In: Encyclopedia of the Neurological Sciences. 2nd ed. Oxford: Academic Press; 2014. p. 173-8. Available from: https://doi.org/10.1016/B978-0-12-385157-4.00204-9 [Last accessed on 2023 Mar 17].
38. Nikpoor N, Weissman BN. Scintigraphy of the musculoskeletal system. In: Weissman BN, editor. Imaging of Arthritis and Metabolic Bone Disease. Ch. 2. Philadelphia: W.B. Saunders; 2009. p. 17-33. Available from: https://www.sciencedirect.com/science/article/pii/B9780323041775000021 [Last accessed on 2023 Mar 15].
39. Ghosh P. The role of SPECT/CT in skeletal malignancies. Semin Musculoskelet Radiol 2014;18:175-93.
40. Shen G, Deng H, Hu S, Jia Z. Comparison of choline-PET/CT, MRI, SPECT, and bone scintigraphy in the diagnosis of bone metastases in patients with prostate cancer: A meta-analysis. Skeletal Radiol 2014;43:1503-13.
41. Yandrapalli S, Puckett Y. SPECT imaging. In: StatPearls. Treasure Island (FL): StatPearls Publishing; 2022. Available from: https://www.ncbi.nlm.nih.gov/books/NBK564426/. [Last updated on 2022 Oct 03].
42. Lu FM, Yuan Z. PET/SPECT molecular imaging in clinical neuroscience: Recent advances in the investigation of CNS diseases. Quant Imaging Med Surg 2015;5:433-47.
43. Shukla AK, Kumar U. Positron emission tomography: An overview. J Med Phys 2006;31:13-21.
44. Crișan G, Moldovean-Cioroianu NS, Timaru DG, Andrieș G, Căinap C, Chiș V. Radiopharmaceuticals for PET and SPECT imaging: A literature review over the last decade. Int J Mol Sci 2022;23:5023.
45. Cook GJ, Houston S, Rubens R, Maisey MN, Fogelman I. Detection of bone metastases in breast cancer by 18FDG PET: Differing metabolic activity in osteoblastic and osteolytic lesions. J Clin Oncol 1998;16:3375-9.
46. Lee MG, Burton VJ, Shapiro BK, Zigmond MJ, Rowland LP, Coyle JT. Developmental disabilities and metabolic disorders. Ch. 3. In: Neurobiology of Brain Disorders. San Diego: Academic Press; 2015. p. 18-41.
47. Cook GJ, Goh V. Functional and hybrid imaging of bone metastases. J Bone Miner Res 2018;33:961-72.
48. Heindel W, Gübitz R, Vieth V, Weckesser M, Schober O, Schäfers M. The diagnostic imaging of bone metastases. Dtsch Arztebl Int 2014;111:741-7.
49. Adams SJ, Henderson RD, Yi X, Babyn P. Artificial intelligence solutions for analysis of X-ray images. Can Assoc Radiol J 2021;72:60-72.
50. von Schacky CE, Wilhelm NJ, Schäfer VS, Leonhardt Y, Gassert FG, Foreman SC, *et al*. Multitask deep learning for segmentation and classification of primary bone tumors on radiographs. Radiology 2021;301:398-406.

BIOTEK®
we put life in metal

Super-Vim Suture Anchor

BAS-9002.50F Super-Vim Suture Anchor,
Dia. 5.0mm, Titanium (Loaded with two pc Biofiber), Sterile

- Ideal for mini-open rotator cuff repair procedures
- Anchors made of Ti 6Al-4V ELI Titanium Alloy
- Multiple Biofibers dispense load over more of the tendon
- Independent Biofiber channels reduce suture binding
- Needlepoint tip permits atraumatic hand insertion through soft tissue
- Anchor's wide threads and small core optimize bone purchase
- Fully-threaded anchor body increases resistance to pull-out
- Laser etched markings on the drivers for insertion depth and suture orientation

Vim-Fix PK Suture Anchor

BAS-9091.55F Vim-Fix PK III Suture Anchor,
Dia. 5.5mm (Loaded with three pc Biofiber), Sterile

- Clinical used for primary or medial row fixation
- Fully threaded; Cancellous and cortical threads provide exceptional fixation strength
- Broaching punch minimizes cortical stress fractures
- Double or triple loaded with Biofiber suture
- Enhanced tip thread profile for easy insertion
- Provides initial fixation strength and stability
- Technique-create hole, screw-in anchor

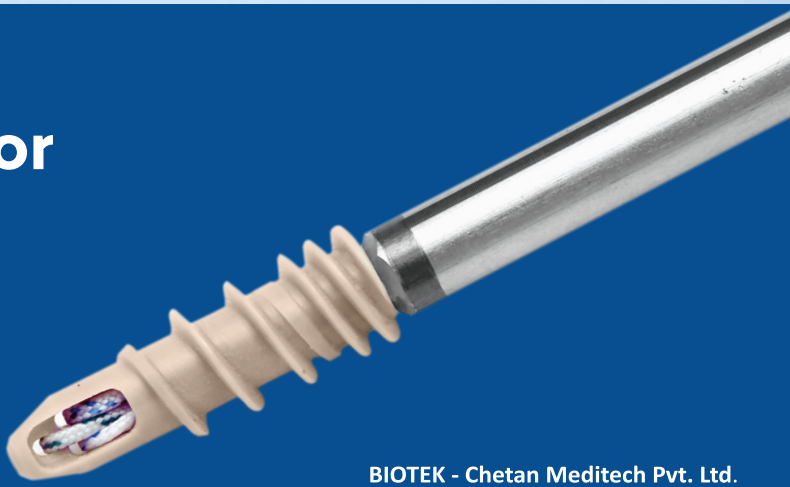

BIOTEK - Chetan Meditech Pvt. Ltd.
Opp. V. S. Hospital, Ellisbridge,
Ahmedabad-380 006. Gujarat, INDIA.
Phone: +91 79 26578092 Fax: +91 79 26577639
Email: info@biotekortho.com
www.biotekortho.com

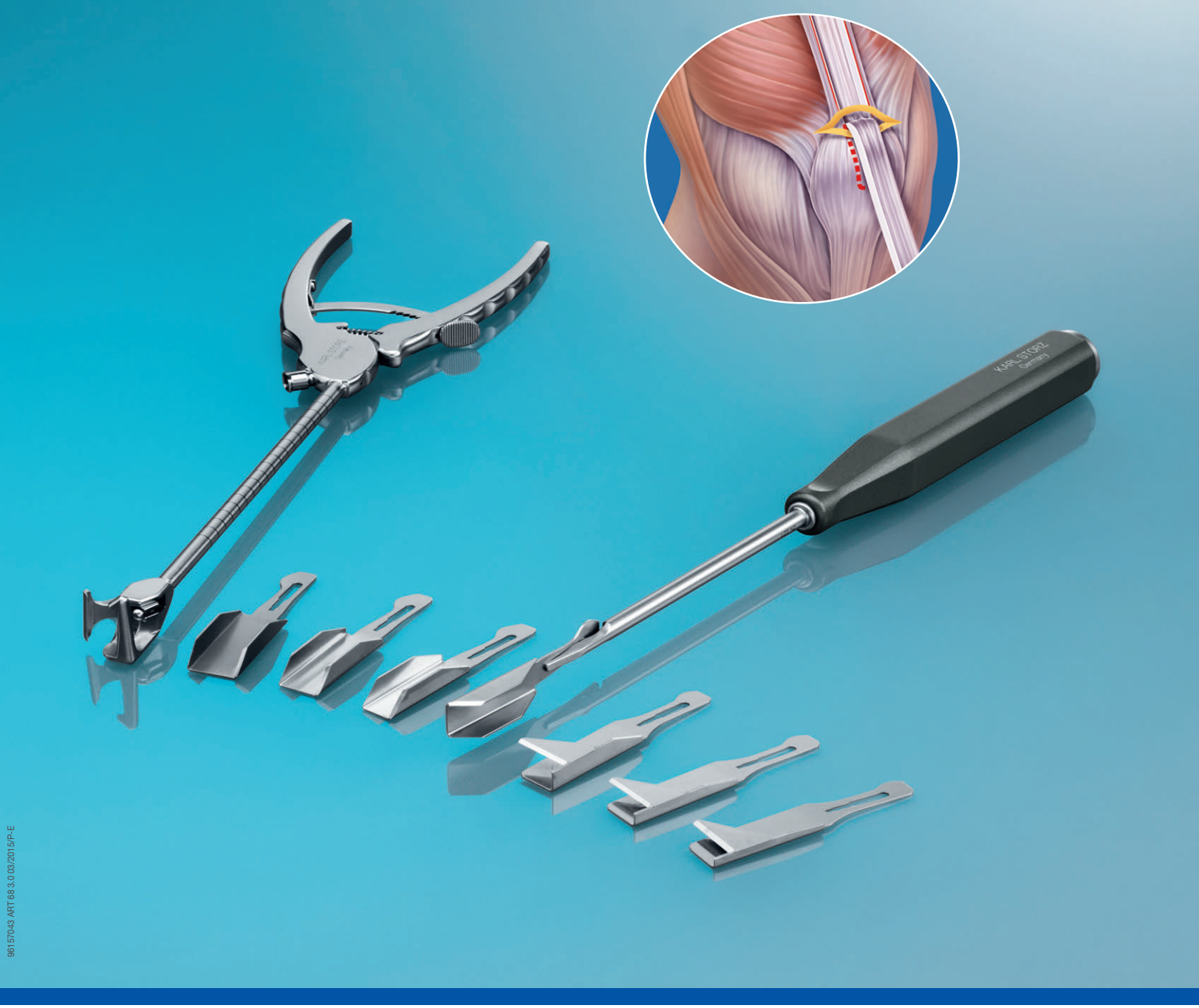

9615704 3 ART 68 3.0 03/2015/P-E

QuadCut

Minimally Invasive Quadriceps Tendon Harvesting

STORZ
KARL STORZ — ENDOSKOPE
THE DIAMOND STANDARD

www.karlstorz.com

Printed and published by Wolters Kluwer India Pvt. Ltd. on behalf of International Society for Knowledge for Surgeons on Arthroscopy and Arthroplasty and printed at Balaji Art, Bhandup (W), Mumbai, India. and published at A-202, 2nd Floor, The Qube, C.T.S. No. 1498A/2 Village Marol, Andheri (East), Mumbai - 400 059, India